



Programa de Pós Graduação em Ecologia e Conservação
Centro de Ciências Biológicas e da Saúde
Universidade Federal de Mato Grosso Do Sul

**Evaluation and Performance of Ecological Niche Models in
South America: a whip-spider case study**

João Frederico Berner



Campo Grande
Maio 2022

**Evaluation and Performance of Ecological Niche Models in South America: a
whip-spider case study**

João Frederico Berner

Dissertação apresentada como requisito para
obtenção do título de **Mestre em Ecologia**,
pelo Programa de Pós Graduação em Ecologia
e Conservação, Universidade Federal de Mato
Grosso do Sul.

Orientador: Gustavo Gracioli

Co-orientador: Gustavo Silva de Miranda

Banca avaliadora

Dr.

[endereço institucional]

Dr.

[endereço institucional]

Dr.

[endereço institucional]

Dr.

[endereço institucional]

Dr.

[endereço institucional]

Acknowledgements

I thank my advisors for their trust and patience, and for the time they spared to share their knowledge with me. I thank my family for the ongoing support over the years, and my friends for the company over the past isolated couple of years. Above all, I am grateful to the University personnel and public servants that were in any way involved in my Academic Education so far.

Index

Table of Figures.....	viii
Index of Tables.....	xi
General Abstract.....	1
Resumo Geral.....	2
General Introduction.....	3
Chapter 1.....	8
Abstract.....	8
Resumo.....	9
1.0 - Introduction.....	10
2.0 – Methods.....	11
2.1 – Taxon selection.....	12
2.2 - Study area.....	12
2.3 - <i>Species data</i>	12
2.4 - Environmental data.....	14
2.5 - <i>Model built</i>	15
2.5.1 - <i>Accessible area (M)</i>	16
2.5.2 - <i>Algorithm choice</i>	16
2.5.3 - Model evaluation.....	17
2.5.4 - Model comparison.....	18
2.5.5 - Software, codes and data.....	18
3.0 - Results.....	18
3.1 - Model outputs.....	18
3.1.1 – Environmental Datasets.....	19
3.1.2 – M size.....	20
3.1.2.1 – <i>Heterophrynus batesii</i>	20
3.1.2.2 – <i>Heterophrynus alces</i>	21
3.1.2.3 – <i>Heterophrynus cheiracanthus</i>	22
3.1.3 – Algorithm.....	22
3.2 – Model Performance and Evaluation.....	23
3.2.1 – Environmental Datasets.....	23
3.2.2 – M size.....	24
3.3.3 – Algorithm.....	25
4.0 - Discussion.....	29
4.1 – Environmental Datasets.....	29
4.2 – M size.....	30
4.3 – Algorithm.....	30
4.4 – Evaluation.....	31
5.0 - Conclusions.....	31
Acknowledgements.....	32

Chapter 2.....	33
Abstract.....	33
Resumo.....	34
1.0 – Introduction.....	35
2.0 – Methods.....	36
2.1 – Species data.....	36
2.2 – Climate Data.....	36
2.3 – Protected Areas Dataset.....	36
2.4 – M selection.....	37
2.5 – Algorithm selection.....	37
2.6 – Software, Code and Data.....	37
2.7 – Model Workflow.....	38
3.0 – Results.....	39
3.1 – Model Results.....	39
3.2 – <i>Heterophrynus alces</i> Pocock, 1902.....	42
3.3 – <i>Heterophrynus armiger</i> Pocock, 1902.....	45
3.4 – <i>Heterophrynus batesii</i> Butler, 1873.....	47
3.5 – <i>Heterophrynus boterorum</i> Giupponi & Kury, 2013.....	49
3.6 – <i>Heterophrynus cervinus</i> Pocock, 1894.....	51
3.7 – <i>Heterophrynus cheiracanthus</i> Gervais, 1842.....	53
3.8 – <i>Heterophrynus elaphus</i> Pocock, 1903.....	55
3.9 – <i>Heterophrynus longicornis</i> Butler 1873.....	57
3.10 – <i>Heterophrynus vesanicus</i> Mello-Leitão 1931.....	59
4.0 – Discussion.....	61
5.0 – Conclusions.....	63
General Conclusion.....	64
Cited Literature.....	65

Table of Figures

Fig. 1: accessible area (M) selection scheme. Three different accessible areas were defined for each species as the bounding box of different-sized radii buffers around the occurrence records. The bounding box of the smallest radius buffers defines the small M (SM) (red), and the same follows for the medium M (MM) (blue) and large M (LM) (violet). Background is an elevation map of central Brazil.....	16
Fig. 2: model workflow. For each of nine <i>Heterophrynus</i> species three sized Ms were defined, on which we constructed models for each of three climatic datasets, using ten bootstrap replications of eight algorithms of three different classes.....	17
Fig. 3: Box+violin-plot of d-stat results for Environmental Dataset comparison including all 648 models. Individual values in grey dots.....	19
Fig. 4: D-stat results for the comparison of environmental datasets under Maxent-MM models for all modeled species.....	20
Fig. 5: <i>batesii</i> -BioClim-Maxent model outputs for SM (A), MM (B) and LM (C).....	21
Fig. 6: <i>alces</i> -BioClim-Maxent model outputs for SM (A), MM (B) and LM(C).....	21
Fig. 7: <i>cheiracanthus</i> -BioClim-Maxent model outputs for SM (A), MM (B)and LM(C).....	22
Fig. 8: mean D-Stat values (below diagonal) for model output comparison between algorithms. Highest values indicate more similar outputs.....	23
Fig. 9: AOcCs for longicornis-RF (A), batesii-GLM (B) and elaphus-GLM (C) models.....	24
Fig. 10: AOcCs for <i>alces</i> -MERRA models. As M increases, the curve of low performing algorithms crosses the random counts curve in fewer cells.....	24
Fig. 11: AOcCs for <i>H.alces</i> models for GLM, GLMNet and MaxLike. The plot shows how occurrences were accumulated in each <i>H. alces</i> model for the algorithms. MERRA-SM models are not below the random counts line as in the previous Fig. because the scale of the X axis here is the LM scale. SM=50km buffer around occurrence points or 9576 cells, MM=100km or 12180 cells, LM=150km or 15072 cells. Target at 19 occurrences.....	25
Fig. 12: AOcCs for longicornis-BioClim SM (A) and LM (B) models.....	26
Fig. 13: AOcC for cervinus-Bioclim-SM model (SM = 200km radius, 10920 cells).....	28
Fig. 14: Line plot of the number of cells at AOcC-target by algorithm for <i>H. alces</i> models, under each climatic dataset, at each M size.....	28
Fig. 15: Models in Environmental Space (A, C, E, G) and in Geographical Space (B, D, F, H). <i>longicornis</i> -BioClim-LM RF (A-B) and MaxEnt (C-D), <i>cervinus</i> -BioClim-LM RF(E-F) MaxEnt (G-H) for comparison of the overfitting under RF models.....	29
Fig. 16: Model Workflow.....	39
Fig. 17: AOcCs for the first round of models (10 bootstrap replications), with all tested algorithms. These Figures are the same as the BioClim columns in Figs. S1 A-J.....	40
Fig. 18: <i>H. alces</i> model and ensemble outputs for the three climate scenarios. Purple dots represent occurrence records.....	43
Fig. 19: <i>H. alces</i> Ensembled Presence/Absence maps for the three climatic scenarios and their overlap with the Protected Areas Datasets. A: occurrence records. B: present-day presence/absence ensembled projections. C: presence/absence ensembled projections under SSP2-4.5 scenario. D: presence/absence ensembled projections under SSP5-8.5 scenario. E: A-C overlaid in a single map. F: Full protected areas dataset overlaid with occurrence records. G: Full protected areas dataset overlaid with B. H: Full protected areas dataset overlaid with C. I: Full protected areas dataset overlaid with D. J: Integral Protection Areas dataset overlaid with occurrence records. K: Integral	

Protection Areas dataset overlaid with B. L: Integral Protection Areas dataset overlaid with C. M: Integral Protection Areas dataset overlaid with D. N: Indigenous Areas dataset overlaid with occurrence records. O: Indigenous Areas dataset overlaid with B. P: Indigenous Areas dataset overlaid with C. Q: Indigenous Areas dataset overlaid with D.....	44
Fig. 20: <i>H. armiger</i> model and ensemble outputs for the three climate scenarios. Purple dots represent occurrence records.....	45
Fig. 21: <i>H. armiger</i> Ensembled Presence/Absence maps for the three climatic scenarios and their overlap with the Protected Areas Datasets. A: occurrence records. B: present-day presence/absence ensembled projections. C: presence/absence ensembled projections under SSP2-4.5 scenario. D: presence/absence ensembled projections under SSP5-8.5 scenario. E: A-C overlaid in a single map. F: Full protected areas dataset overlaid with occurrence records. G: Full protected areas dataset overlaid with B. H: Full protected areas dataset overlaid with C. I: Full protected areas dataset overlaid with D. J: Integral Protection Areas dataset overlaid with occurrence records. K: Integral Protection Areas dataset overlaid with B. L: Integral Protection Areas dataset overlaid with C. M: Integral Protection Areas dataset overlaid with D. N: Indigenous Areas dataset overlaid with occurrence records. O: Indigenous Areas dataset overlaid with B. P: Indigenous Areas dataset overlaid with C. Q: Indigenous Areas dataset overlaid with D.....	46
Fig. 22: <i>H. batesii</i> model and ensemble outputs for the three climate scenarios. Purple dots represent occurrence records.....	47
Fig. 23: <i>H. batesii</i> Ensembled Presence/Absence maps for the three climatic scenarios and their overlap with the Protected Areas Datasets. A: occurrence records. B: present-day presence/absence ensembled projections. C: presence/absence ensembled projections under SSP2-4.5 scenario. D: presence/absence ensembled projections under SSP5-8.5 scenario. E: A-C overlaid in a single map. F: Full protected areas dataset overlaid with occurrence records. G: Full protected areas dataset overlaid with B. H: Full protected areas dataset overlaid with C. I: Full protected areas dataset overlaid with D. J: Integral Protection Areas dataset overlaid with occurrence records. K: Integral Protection Areas dataset overlaid with B. L: Integral Protection Areas dataset overlaid with C. M: Integral Protection Areas dataset overlaid with D. N: Indigenous Areas dataset overlaid with occurrence records. O: Indigenous Areas dataset overlaid with B. P: Indigenous Areas dataset overlaid with C. Q: Indigenous Areas dataset overlaid with D.....	48
Fig. 24: <i>H. boterorum</i> model and ensemble outputs for the three climate scenarios. Purple dots represent occurrence records.....	49
Fig. 25: <i>H. boterorum</i> Ensembled Presence/Absence maps for the three climatic scenarios and their overlap with the Protected Areas Datasets. A: occurrence records. B: present-day presence/absence ensembled projections. C: presence/absence ensembled projections under SSP2-4.5 scenario. D: presence/absence ensembled projections under SSP5-8.5 scenario. E: A-C overlaid in a single map. F: Full protected areas dataset overlaid with occurrence records. G: Full protected areas dataset overlaid with B. H: Full protected areas dataset overlaid with C. I: Full protected areas dataset overlaid with D. J: Integral Protection Areas dataset overlaid with occurrence records. K: Integral Protection Areas dataset overlaid with B. L: Integral Protection Areas dataset overlaid with C. M: Integral Protection Areas dataset overlaid with D. N: Indigenous Areas dataset overlaid with occurrence records. O: Indigenous Areas dataset overlaid with B. P: Indigenous Areas dataset overlaid with C. Q: Indigenous Areas dataset overlaid with D.....	50
Fig. 26: <i>H. cervinus</i> model and ensemble outputs for the three climate scenarios. Purple dots represent occurrence records.....	51
Fig. 27: <i>H. cervinus</i> Ensembled Presence/Absence maps for the three climatic scenarios and their overlap with the Protected Areas Datasets. A: occurrence records. B: present-day presence/absence	

ensembled projections. C: presence/absence ensembled projections under SSP2-4.5 scenario. D: presence/absence ensembled projections under SSP5-8.5 scenario. E: A-C overlaid in a single map. F: Full protected areas dataset overlaid with occurrence records. G: Full protected areas dataset overlaid with B. H: Full protected areas dataset overlaid with C. I: Full protected areas dataset overlaid with D. J: Integral Protection Areas dataset overlaid with occurrence records. K: Integral Protection Areas dataset overlaid with B. L: Integral Protection Areas dataset overlaid with C. M: Integral Protection Areas dataset overlaid with D. N: Indigenous Areas dataset overlaid with occurrence records. O: Indigenous Areas dataset overlaid with B. P: Indigenous Areas dataset overlaid with C. Q: Indigenous Areas dataset overlaid with D.....52

Fig. 28: *H. cheiracanthus* model and ensemble outputs for the three climate scenarios. Purple dots represent occurrence records.....53

Fig. 29: *H. cheiracanthus* Ensembled Presence/Absence maps for the three climatic scenarios and their overlap with the Protected Areas Datasets. A: occurrence records. B: present-day presence/absence ensembled projections. C: presence/absence ensembled projections under SSP2-4.5 scenario. D: presence/absence ensembled projections under SSP5-8.5 scenario. E: A-C overlaid in a single map. F: Full protected areas dataset overlaid with occurrence records. G: Full protected areas dataset overlaid with B. H: Full protected areas dataset overlaid with C. I: Full protected areas dataset overlaid with D. J: Integral Protection Areas dataset overlaid with occurrence records. K: Integral Protection Areas dataset overlaid with B. L: Integral Protection Areas dataset overlaid with C. M: Integral Protection Areas dataset overlaid with D. N: Indigenous Areas dataset overlaid with occurrence records. O: Indigenous Areas dataset overlaid with B. P: Indigenous Areas dataset overlaid with C. Q: Indigenous Areas dataset overlaid with D.....54

Fig. 30: *H. elaphus* model and ensemble outputs for the three climate scenarios. Purple dots represent occurrence records.....55

Fig. 31: *H. elaphus* Ensembled Presence/Absence maps for the three climatic scenarios and their overlap with the Protected Areas Datasets. A: occurrence records. B: present-day presence/absence ensembled projections. C: presence/absence ensembled projections under SSP2-4.5 scenario. D: presence/absence ensembled projections under SSP5-8.5 scenario. E: A-C overlaid in a single map. F: Full protected areas dataset overlaid with occurrence records. G: Full protected areas dataset overlaid with B. H: Full protected areas dataset overlaid with C. I: Full protected areas dataset overlaid with D. J: Integral Protection Areas dataset overlaid with occurrence records. K: Integral Protection Areas dataset overlaid with B. L: Integral Protection Areas dataset overlaid with C. M: Integral Protection Areas dataset overlaid with D. N: Indigenous Areas dataset overlaid with occurrence records. O: Indigenous Areas dataset overlaid with B. P: Indigenous Areas dataset overlaid with C. Q: Indigenous Areas dataset overlaid with D.....56

Fig. 32: *H. longicornis* model and ensemble outputs for the three climate scenarios. Purple dots represent occurrence records.....57

Fig. 33: *H. longicornis* Ensembled Presence/Absence maps for the three climatic scenarios and their overlap with the Protected Areas Datasets. A: occurrence records. B: present-day presence/absence ensembled projections. C: presence/absence ensembled projections under SSP2-4.5 scenario. D: presence/absence ensembled projections under SSP5-8.5 scenario. E: A-C overlaid in a single map. F: Full protected areas dataset overlaid with occurrence records. G: Full protected areas dataset overlaid with B. H: Full protected areas dataset overlaid with C. I: Full protected areas dataset overlaid with D. J: Integral Protection Areas dataset overlaid with occurrence records. K: Integral Protection Areas dataset overlaid with B. L: Integral Protection Areas dataset overlaid with C. M: Integral Protection Areas dataset overlaid with D. N: Indigenous Areas dataset overlaid with

occurrence records. O: Indigenous Areas dataset overlaid with B. P: Indigenous Areas dataset overlaid with C. Q: Indigenous Areas dataset overlaid with D.....	58
Fig. 34: <i>H. vesanicus</i> model and ensemble outputs for the three climate scenarios. Purple dots represent occurrence records.....	59
Fig. 35: <i>H. vesanicus</i> Ensembled Presence/Absence maps for the three climatic scenarios and their overlap with the Protected Areas Datasets. A: occurrence records. B: present-day presence/absence ensembled projections. C: presence/absence ensembled projections under SSP2-4.5 scenario. D: presence/absence ensembled projections under SSP5-8.5 scenario. E: A-C overlaid in a single map. F: Full protected areas dataset overlaid with occurrence records. G: Full protected areas dataset overlaid with B. H: Full protected areas dataset overlaid with C. I: Full protected areas dataset overlaid with D. J: Integral Protection Areas dataset overlaid with occurrence records. K: Integral Protection Areas dataset overlaid with B. L: Integral Protection Areas dataset overlaid with C. M: Integral Protection Areas dataset overlaid with D. N: Indigenous Areas dataset overlaid with occurrence records. O: Indigenous Areas dataset overlaid with B. P: Indigenous Areas dataset overlaid with C. Q: Indigenous Areas dataset overlaid with D.....	60

Index of Tables

Table 1: Heterophrynus species and the locality they have been recorded.....	14
Table 2: response variables chosen from environmental datasets.....	15
Table 3: Table of accumulation of occurrences for cervinus-Bioclim-SM models (10920 cells in total) of three algorithms: RF, MaxEnt and MARS. Occurrence target = 15 (88.24%) in bold. Bottom row is the raw output of each model with occurrence records for reference.....	27
Table 4: Retained M and respective buffer sizes, and retained algorithms.....	38
Table 5: Predicted Ensembled Suitable Area in million hectares, and the corresponding overlap percentage with the three Protected Area Datasets.....	41

General Abstract

1 In this work Ecological Niche Models were built using the occurrence records of nine species of the
2 endemic South American whip-spider genus *Heterophrynus*. With this dataset, we tested the use and
3 compared performance and output similarity of three climatic datasets (BioClim, MERRAclim and
4 ENVIREM) and eight algorithms (RF, BRT, SVM, MaxEnt, MaxLike, GLM, GLMNet and MARS)
5 under three M sizes for each of the nine species. Furthermore, we used one of the climatic datasets,
6 BioClim, to build and project models for two end-of-century SSP scenarios and quantify suitable area
7 lying inside Protected Areas (National Parks and Indigenous Land) in each scenario. Our results
8 suggest MERRAclim is the most dissimilar from other climatic datasets, and that the interpolation
9 artifacts in both BioClim and ENVIREM dictate model output in the Amazon Basin. In our analyses,
10 the algorithms RF and MARS overfitted models, while GLM, GLMNet and MaxLike underfitted
11 models given tested settings. We further illustrate how AUC and TSS statistics are uninformative as
12 evaluation methods for presence-background or presence-pseudoabsence models. We found that
13 Indigenous Land or Territories cover as much suitable area as Integral Protection Areas on average.
14 Some species are estimated to lose over two thirds of their current suitable area by the end of the
15 century, while others to have their suitable area more than doubled. From our conclusions, we
16 emphasize that the use of a single climatic dataset, GCM and/or algorithm should be avoided.
17 Furthermore, we suggest that defining M should be based on building a few models *a priori* with
18 different M sizes and selecting the one with the best performance and best fit for intended model use.

Resumo Geral

1 Construimos Modelos de Nicho Ecológico utilizando os dados de ocorrência de nove espécies do
2 amblipígeo *Heterophrynus*, endêmico da América do Sul. Testamos e comparamos a performance a a
3 similaridade do *output* de três conjuntos de dados climáticos e nove algoritmos sob três tamanhos de
4 M para cada espécie. Além disso, utilizamos um dos conjuntos de dados climáticos, BioClim, para
5 construir e projetar modelos para dois cenários SSP ao final do século, e quantificamos a área com
6 adequabilidade climática dentro de Áreas de Conservação em cada cenário. Nossos resultados
7 sugerem que MERRAclim é o conjunto de dados climático mais dessemelhante dos outros testados, e
8 que artefatos de interpolação em ambos os conjuntos BioClim e ENVIREM ditam o *output* dos
9 modelos na bacia amazônica. Em nossas análises, os algoritmos RF e MARS sobreajustaram os
10 modelos, enquanto GLM, GLMNet e MaxLike subajustaram os modelos dadas as configurações
11 testadas. Nós demonstramos como as estatísticas AUC e TSS são pouco informativas como método de
12 avaliação de modelos presença-fundo ou presença-pseudoausência. Encontramos que Terras Indígenas
13 cobrem em média tanta área climaticamente adequada quanto Áreas de Proteção Integral. Algumas
14 espécies perderão mais de dois terços da sua área de adequabilidade climática atual, enquanto outras
15 terão essa área mais do que duplicada até o final do século. De nossas conclusões, enfatizamos que o
16 uso de um único conjunto de dados climático, modelo de circulação global e/ou algoritmo deve ser
17 evitado. Além disso, sugerimos que a definição de M deve ser baseada na construção de alguns
18 modelos *a priori* com diferentes tamanhos de M e selecionando o com melhor performance e que
19 melhor se ajusta ao uso pretendido do modelo.

General Introduction

1 The factors that shape species distributions have long been debated, and multiple efforts to
2 elucidate this problem have been done since the first works on biogeography by Wallace (1858).
3 Grinnell (1914, 1917) developed some of what are now considered the fundamental concepts of
4 distributional species areas, such as the early niche concept, which was based solely on species'
5 habitat requirements. Others such as Elton, Gause and Hutchinson developed central ideas to the
6 ecological niche theory and its relationship with distribution areas (Elton 1927, Gause 1934,
7 Hutchinson 1957, Hutchinson 1978). It was not until the late twentieth century, however, that tools
8 emerged to explore the ramifications and implications of these ideas, as well as standardized data to
9 test them. As highlights are geographic information systems (GIS) software and GPS devices, and
10 advances in computational capacity and programming languages. Major improvements regarding data
11 acquisition are remote sensing technologies (e.g. satellite imaging), which are a source of climate data
12 at global scales (Farrell et al. 2013, Hijmans et al. 2005, Waltari et al. 2014), and online open access to
13 biodiversity data publishers (e.g. museums, herbaria).

14 The wide range of correlative (as opposed to mechanistic, Merow et al. 2011) methods for
15 modeling species distributions are collectively called ecological niche modeling (ENMs). ENMs use
16 environmental data and species' occurrence records to infer species distribution based on ecological
17 niche characteristics derived from these data. ENMs are sometimes interchangeably referred to as
18 species distribution models (SDMs), yet these are not the same as SDMs focus solely on present
19 species range, and not necessarily on the characterization of species' niche limits and requirements,
20 the potential range, and the range's responses to different factors. Deep semantic and theoretic
21 discussions are presented by Sillero (2011), Peterson & Sobefón (2012) and Warren (2012), but for
22 simplicity, the methods will be collectively referred to as ENMs hereafter. ENMs have been used for a
23 wide variety of applications, e.g. predicting the range and impact of invasive species, predicting
24 suitable sites for searching for new populations, predict the impact of climate change on species'
25 distributions, predicting past distributions and assessing niche similarity between species (Guisan &
26 Thuiller 2005).

27 Environmental data is central to the ENM process, and there are several datasets available in
28 the literature. These datasets are built from real-world data, and they can be classified by their data
29 source. Most ENM literature uses the so-called bioclimatic variables, a dataset that contains global
30 temperature and precipitation data in 19 variables, first developed by WorldClim (BioClim, Hijmans
31 et al. 2005), built from interpolated weather-station data. Other datasets have been built from
32 interpolated remote-sensing data (e.g. MOD11C3 v.6 and CHIRPS v.2, Deblauwe et al. 2016,
33 MERRAclim, Vega et al. 2018), from complex Global Climate Models (e.g. CHELSA, Karger et al.
34 2017), or from complex simulations spanning several time periods both past and future (e.g.
35 ecoClimate, Lima-Ribeiro et al. 2015, PaleoClim, Brown et al. 2018). Most of these datasets represent
36 the 19 bioclimatic variables and differ by their source type. Yet, these are not the only data that can be
37 predictors in ENMs as topography, landscape variables, other types of temperature and precipitation
38 data, soil characteristics, geomorphology and hydrology data can and should be incorporated into
39 models when relevant and available. Climate datasets that simulate past or future climates are built on
40 Global Circulation Models (GCMs), and the ones that represent future climate are representative of
41 the Shared Socioeconomic Pathways (SSPs, Riahi et al. 2017) coupled with the Representative
42 Concentration Pathways (RCPs, Van Vuuren et al. 2011). These pathways aim to represent possible

43 future scenarios of carbon concentration in the atmosphere. The latest version of these simulations is
44 CMIP6 (Coupled Model Intercomparison Project Phase 6, Eyring et al. 2016).

45 ENMs consist of using occurrence records to define the environmental characteristics of
46 species' niche, and project similar environments back into geographic space. It is a convoluted
47 process, and recent literature have been published proposing sets of standards and guidelines to make
48 it more robust and reproducible (Araújo et al. 2019, Feng et al. 2019, Fitzpatrick et al. 2017, Jiménez
49 & Soberón 2020, Regos et al. 2019, Sillero & Barbosa 2021, Sofaer et al. 2019). Ecological niche
50 modelling relies on key ecological concepts about species' niches components and dimensions, as
51 Hutchinson's duality (Colwell & Rangel 2009), the different types of niches (Arckerly 2003, Guisan
52 & Zimmerman 2000, Jackson & Overpeck 2000, Pulliam 2000, Silvertown 2004, Soberón & Peterson
53 2011), the BAM diagram theoretical framework (Barve et al. 2011, Saupe et al. 2012, Soberón &
54 Peterson 2005), Hutchinson's inequalities (Soberón & Arroyo-Peña 2017) and niche adaptation and
55 conservatism (Liu et al. 2020, Pili et al. 2020, Pulliam 2000, Zhu et al. 2020). The output of an ENM
56 depends on the input data and the algorithm used. Algorithms can be classified by their input
57 requirements, some requiring presence-only data (e.g. BioClim, Euclidian Distance, Mahalanobis
58 Distance, Gower Distance or Ecological Niche Factor Analysis – ENFA), others presence-background
59 data (e.g. Genetic Algorithm for Rule-Set Production – GARP, Maximum Entropy – MaxEnt, Support
60 Vector Machine -SVM) or presence-absence data (e.g. Generalized Linear Models – GLMs,
61 Generalized Additive Models – GAMs, Flexible Discriminant Analysis – FDA, Multivariate Adaptive
62 Regression Splines – MARS, Boosted Regression Trees – BRT, Gradient Boosting Machine – GBM,
63 Classification and Regression Trees – CART, Random Forest – RF, Neural Networks – NNET,
64 Artificial Neural Networks – ANN), and each represents niche properties differently. A model and
65 output terminology based on algorithm input requirement was proposed by Sillero (2011), the central
66 conclusion being that correlative methods can only model species' realized niche, not the fundamental
67 nor potential niches, and different inputs result in different portions of the realized niche: presence-
68 absence and presence-pseudoabsence methods are the most informative and accurate, and they model
69 the suitability of those habitats strictly occupied by the species, as presence-only methods are the least
70 informative, and model all suitable habitat for the species.

71 The technique has been popularized and improved over the past 20 years, with hundreds of
72 papers being published every year (Lobo et al. 2010). Applications of ENMs have mostly been used to
73 terrestrial systems (Araújo et al. 2019), especially with vertebrate species (Titley et al. 2017), but
74 rarely on marine environments (Melo-Merino et al. 2020), tree canopies (Burns et al. 2020)
75 (environments in which three-dimensionality is a factor), and invertebrates (Mammola et al. 2021,
76 Taucare-Ríos et al. 2018). This bias towards terrestrial vertebrates seems to be a trend in biodiversity
77 research in general and has been reported by several authors (Leandro et al. 2017, Mammides 2019,
78 Mammola et al. 2020). Evidence suggests this bias is partly derived from cognitive bias in terms of
79 researchers' subjective preferences for certain taxa over others (Clark & May 2002), also known as
80 'taxonomic chauvinism' (Leather 2009).

81 On top of the taxonomic bias towards vertebrates, several other barriers hamper the application
82 of ENMs to invertebrates, because of their immense diversity, small size, short and complex life
83 cycles and lack of information about most species' biology, ecology, phylogeny and physiology. This
84 scarcity of knowledge turns decision-making about model inputs and methodological variables
85 difficult, and greatly influences model performance (Peterson & Soberón 2012). Among arthropods,
86 there is taxonomic bias towards certain megadiverse groups, e.g. bees and butterflies (Cardoso 2012,
87 Leandro et al. 2017). A recent systematic literature review regarding terrestrial arthropods ENMs

88 (Mammola et al. 2021) showed that the most well represented invertebrates in ENM studies are
89 butterflies (which may be due to a greater amount of information available, as well as their diversity),
90 and species of economic interest such as flies and mosquitoes (vectors of diseases), beetles (crop
91 pests), and pollinators.

92 Arachnids have 110.615 described species, and the estimated number is predicted to be far
93 greater (Stork 2018). However, that diversity is not equally spread among the 16 Orders, most of it
94 being represented by spiders (Araneae – 42,473 species) and mites (Acariformes and Parasitiformes –
95 54.473 species collectively in 6 Orders), the remaining orders collectively accounting for circa of 12%
96 of the diversity within Arachnida (Harvey 2002, Stork 2018). The so-called Smaller Orders of
97 Arachnida are not only less diverse, presenting 671 species collectively in 5 Orders, a little over one
98 percent of the number of spider species (Stork 2018), but also have been historically less studied, and
99 the early taxonomic works on the group have made it difficult to diagnose species and genera then
100 described.

101 Whip spiders (Amblypygi) are no exception, but recent advances have been made in assigning
102 new and relevant characters (e.g. Giupponi & Kury 2013) and several new species have been
103 described over the last two decades. Amblypygids are poorly known and can be difficult to find in
104 nature due to their nocturnal behavior, their tendency to live between rocks, cracks and caves, and
105 inconspicuous colors (Harvey 2002). The first species described for the Order was *Phalantium*
106 *reniforme* Linnaeus 1758, and the number of described species today is over 220 (Miranda et al.
107 2018). Recent genetic evidence showed the presence of cryptic diversity in amblypygids (Reveillon et
108 al. 2020, Seifer et al. 2020), as has been suggested on taxonomic publications (Chiriví-Joya et al.
109 2020), which is specially accentuated by these organisms' conservative morphology. They have a
110 dorsoventrally flattened body divided into prosoma and opisthosoma, connected by a pedicel, have
111 eight eyes and four pair of legs, the first of which are sensorial and not used for walking. Amblypygi
112 are mainly recognized by their pair of spine-covered pedipalps which are used for catching prey, in
113 courtship and in territory defense (Chapin & Hebets 2016). Special attention has been given to their
114 neuroanatomy, because they present the largest mushroom bodies known in any arthropod, a structure
115 that has been shown to be associated with locomotion and navigation (Chapin & Hebets 2016), and is
116 responsible for receiving olfactory and tactile inputs (Sinakevitch & Gronenberg 1989), which are the
117 main components of whip spiders homing (i.e. the behavior of leaving to forage, mate or patrol
118 territory, and returning to the original nest or refuge) (Ortega-Escobar 2020) followed by visual cues.
119 The fragmented knowledge on homing in whip spiders was recently revised by Ortega-Escobar
120 (2020). Individual recognition appears to be present, at least in one African species (Walsh & Rayor
121 2008).

122 The oldest known whip spiders date to the Carboniferous circa 312 mya, known today as
123 *Weygoldtina scudderi* Pocock 1911 and *Weygoldtina anglicus* Pocock 1911 (Dunlop 2018). The Order
124 has a pantropical distribution, with a few genera in temperate zones (Weygoldt 2000). With the
125 exception of one cosmopolitan genus, *Charinus* Simon 1892, most families or genera are restricted to
126 certain parts of the world (Miranda et al. 2020). In the Neotropics, aside from *Charinus*, the families
127 Phrynichidae and Phrynidae are present, the first represented by a single species *Trichodamon*
128 *princeps* Mello-Leitão 1935 in this region, and the latter by 75 species (Chiriví-Joya 2018, Chiriví-
129 Joya et al 2020, Chiriví-Joya 2021) divided into two sub-families: i) Phryninae, which is further
130 divided into 8 genera and ii) Heterophryninae which is represented by a single genus *Heterophrynus*
131 Pocock 1894 and 18 species (Chiriví-Joya et al. 2020, Seiter & Gredler 2020).

132 *Heterophrynus* was traditionally considered restricted to the Amazon (Weygoldt 2000), but
133 recent work have shown the genus to be present from the North and West of Colombia to the South of
134 Pantanal, in Brazil, to the Western edge of the Amazon and even in refugia in the arid Brazilian
135 Caatinga (Armas et al. 2015, Carvalho et al. 2011, Cordeiro et al. 2014, García et al. 2015, Viquez et
136 al. 2014). Despite recent efforts (Armas et al. 2015, Armas et al. 2015, Chiriví-Joya et al. 2020,
137 Chiriví-Joya 2018, Giupponi & Kury 2013, Giupponi 2002, Seiter & Gredler 2020), taxonomic
138 problems in the group remain, and they are presented and discussed by Chiriví et al. (2020).

139 *Heterophrynus* species are all carnivorous, seemingly opportunist generalists, that have been
140 recorded preying on spiders, orthopterans, moths, frogs, anole lizards (Chapin & Hebets 2016), bat
141 carcasses (Prous et al. 2017), and have even been recorded fishing for freshwater prawn (Ladle &
142 Velandar 2003). On the other hand, species of *Heterophrynus* have been seen being preyed upon by
143 lycosid spiders (*H. batesii*), and confamiliar species also by a wide range of other arachnids and small
144 vertebrates (Chapin & Hebets 2016). These interactions characterize symmetrical intraguild predation
145 (Polis et al. 1989) happening in the ecosystems in which *Heterophrynus* occurs. Cannibalism has also
146 been recorded, although it is apparently more common in adults as a resolution of conflicts (e.g.
147 defending territory, fighting for partner). These territorial contests can often occur for most species,
148 but some are notably more tolerant to conspecifics (Chapin 2014) and/or congeners (Weygoldt 1977),
149 while others are even somewhat social (Carvalho et al. 2012). This tolerance is suggested to be
150 microhabitat specific, as reported by Chapin (2015). They reproduce once to twice a year, displaying
151 complex courtship patterns, and the females care for the young until their first molt (Weygoldt 2000).
152 They are most commonly found on large, buttressing trees, or in trees with either burrows at their
153 bases (Chapin 2014) or some other form of refuge, in trees with termite nests at their bases (Carvalho
154 et al. 2012), crevices or caves. For *H. longicornis* the presence of a burrow has been showed to be
155 more important than tree diameter (Porto & Peixoto 2013). Furthermore, Lehmann and Friedrich
156 (2018) reported collecting *H. elaphus* on three different species of tree, namely *Ceiba pentandra*
157 (Malvaceae), *Dipteryx* sp. (Fabaceae) and *Ficus* sp. (Moraceae), the latter being an exotic species,
158 suggesting that at least *H. elaphus* is not dependent on any specific host plant. This reliance on large,
159 old grown trees makes these large-tree-dwelling species especially vulnerable to selective logging
160 (Bloch & Weiss 2002).

161 We argue that these ecological features, along with their wide distribution on different regions
162 of South America, characterize *Heterophrynus* species as a reasonable choice to test different ENM
163 approaches, as no strong biotic interactions appear to be significantly impacting species' distribution.
164 Instead, abiotic conditions and accessibility are probably more important in shaping these species'
165 distributions at present, following the Eltonian noise hypothesis (Saupe et al. 2012) which states that
166 although local ecological processes define local presence they are diluted in larger scales, an
167 information that increases model reliability (Qiao et al. 2015) and can seldom be assumed for
168 arthropods (Mammola et al. 2021). This does not regard present Neotropical biogeographical
169 hypotheses, which aim to explain the patterns that shaped biodiversity distribution in the continent
170 especially in the Pleistocene (e.g. Rangel et al. 2008, Sacek 2014, Sobral-Souza et al. 2015, Werneck
171 2011), which are ultimately one of the main drivers of species distributions. Rather, it is about the role
172 of biotic interactions in shaping species distributions, which we argue is smaller for the taxon than
173 abiotic conditions or accessibility. Moreover, each species of the genus has its own caveats and
174 considerations in modeling, for example two closely related species *H. boterorum* and *H. silviae*
175 (Giupponi & Kury 2013), which occur in transandean areas of Colombia, have few occurrence
176 records, but the records can be combined as their niche can be assumed to be similar (Qiao et al.

177 2017), an extreme opposite example would be *H. longicornis*, for which there are relatively many
178 occurrence records.

179 This document is divided into two chapters. In the first chapter, we aimed to test a relatively
180 new approach on evaluating Ecological Niche Models, and compare the output and performance of
181 eight algorithms, under three climatic datasets, at three M sizes, for each of nine *Heterophrynus*
182 species. In the second chapter, we use the findings of our first chapter and build models to assess
183 Protected Areas coverage of the suitability maps for present-day climate and two end-of-century
184 climate scenarios on projected models.

Chapter 1

1 **Abstract**

2 Here ecological niche models for nine species of the South American whip-spider genus
3 *Heterophrynus* are built. Performance and output similarity between climatic datasets and algorithmic
4 output under different M sizes for each species are evaluated. The Accumulation of Occurrences
5 Curve approach recently proposed in the literature is used as a metric in evaluation. Our results imply
6 that RF and MARS overfit models, and GLM, GLMNet and MaxLike underfit models given tested
7 settings. MERRAclim is the most dissimilar climatic dataset from the other two tested. Models that
8 span most of the Amazon Basin are influenced by interpolation artifacts in BioClim and ENVIREM
9 models. We illustrate how AUC and TSS are uninformative in presence-background or presence-
10 pseudoabsence models.

11 **Key-words: Accumulation of Occurrences Curve; Amblypygi; Algorithm selection; Ecological**
12 **Niche Models; South America**

13 **Resumo**

14 Aqui modelos de nicho ecológico para nove espécies do gênero de amblipígeo sul-americano
15 *Heterophrynus* são construídos. A performance e a similaridade do *output* entre conjuntos de dados
16 climáticos e do *output* de algoritmos sob diferentes tamanhos de M para cada espécie são avaliadas. A
17 abordagem da Curva de Acumulação de Ocorrências recentemente proposta na literatura como
18 método de avaliação de modelos é utilizada como métrica de avaliação. Nossos resultados sugerem
19 que os algoritmos RF e MARS sobreajustam modelos, e que os algoritmos GLM, GLMNet e
20 MaxLike subajustam modelos, dadas as configurações testadas. MERRAclim é o conjunto de dados
21 climáticos mais diferente dos demais testados. Modelos que abrangem a maior parte da bacia
22 Amazônica são influenciados por artefatos de interpolação em modelos que utilizam BioClim ou
23 ENVIREM como preditores. Demonstramos como AUC e TSS são estatísticas pouco informativas
24 em modelos de presença-fundo ou presença-pseudoausência.

25 **Palavras-chave: Amblypygi; América do Sul; Curva de Acumulação de Ocorrências; Modelos**
26 **de Nicho Ecológico; Seleção de algoritmos**

27

28 1.0 - Introduction

29 Ecological Niche Modeling (ENM) are a suite of techniques that aim to predict species distributions
 30 or their niches based on characteristics of the environment in which they are found. It is a convoluted
 31 process, and literature have been published proposing sets of standards and guidelines to make it
 32 robust and reproducible (Araújo et al. 2019, Farrel et al. 2013, Ficetola et al. 2019, Jackson and
 33 Overpeck 2000, Qiao et al. 2017, Seiter et al. 2020, Soberón & Peterson 2011). The technique has
 34 been popularized and improved over the past 20 years, with hundreds of papers being published
 35 every year (Liu et al. 2020). Applications of ENMs have mostly been used on terrestrial systems
 36 (Araújo et al. 2019), especially with vertebrate species (Taucare-Ríos et al. 2018), but rarely on
 37 invertebrates (Mammides 2019, Mammola et al. 2021). Moreover, ENM literature is produced and
 38 tested on the Global North, while new techniques, GCMs, datasets and methods are seldomly tested
 39 outside of North America and Eurasia (Titley et al. 2017). A recent review of ENM literature in Latin
 40 America clearly shows that researchers from the region take part in few of the advances of the field,
 41 and also that there is great room for improvement in collaboration of research in the region (Urbina-
 42 Cardona et al. 2019).

43 In order to build an ENM, researchers must go through a plethora of decisions, all of which
 44 influence what is actually being modeled, and what can be interpreted from model outputs (Guillera-
 45 Arroita et al. 2015). These decisions include: 1) careful choice of occurrence data, and how to split it,
 46 as different types of datasets can result on starkly different models (Konowalik & Nosol 2021); 2)
 47 choosing one or more environmental datasets, as they usually differ and its not well defined which
 48 one represent environmental conditions better (Morales-Barbero & Vega-Álvarez 2018); 3) defining
 49 the area in which the model will be calibrated is of utmost importance (hereafter M, Barve et al.
 50 2011); 4) selecting the algorithms used in building the models as they seldom have similar outputs
 51 (Konowalik & Nosol 2021); and 5) defining how to assess model performance and evaluate their
 52 results, one of the most debated and active topics of discussion in ENM literature (Jiménez &
 53 Soberón 2020, Sillero & Barbosa 2021). All of these decisions introduce uncertainty to models, and
 54 the path of least uncertainty is anyone's guess. Still, there are steps that can be taken in order to
 55 minimize or at least assess and quantify uncertainty: checking occurrence data quality (both presence
 56 and absence; Lobo et al. 2010, Oliveira et al. 2016), ensembling models (Breiner et al. 2015, 2018),
 57 accounting for predictor's uncertainty or inconsistency (Morales-Barbero & Vega-Álvarez 2018),
 58 selecting algorithms suitable for the intended application and for the input data (Lobo et al. 2010),
 59 selecting a reasonable accessible area in order to minimize evaluation metrics inflation (Barve et al.
 60 2011), and avoiding common mistakes (see Sillero & Barbosa 2021).

61 The set of decisions in building ENMs comes with even larger set of available options. One
 62 can choose from several Environmental Datasets (or predictors) widely available online. These
 63 datasets are all built from different sources (e.g. weather station data in BioClim, Fick & Hijmas
 64 2017, remote sensing data in MERRAclim, Vega et al. 2018) using different methods (most
 65 commonly interpolation), that represent many distinct features of the geographic space (as opposed to
 66 environmental space, hereafter **G** and **E** respectively, *sensu* Peterson & Soberón 2012). These
 67 variables range from temperature and precipitation data, through soil moisture and composition,
 68 potential evapotranspiration and up to topographic and geomorphological variables. The most
 69 commonly used variables in the literature are the nineteen WorldClim bioclimatic variables, that
 70 represent annual, seasonal, quarterly and monthly temperature and precipitation data (Fick and
 71 Hijmans 2017), and other datasets have been derived therefrom (e.g. ENVIREM, Title & Bemmels

72 2018). Another decision with many available options is selecting from a wide range of methods (or
 73 algorithms) that come from other fields and have been adapted to ENM use, and that have each their
 74 own assumptions, biases and requirements regarding input data (Sillero & Barbosa 2021). Some
 75 algorithms require presence-only data (e.g. BioClim, Euclidian Distance, Mahalanobis Distance,
 76 Gower Distance or Ecological Niche Factor Analysis – ENFA), others presence-background data (e.g.
 77 Genetic Algorithm for Rule-Set Production – GARP, Maximum Entropy – MaxEnt, Support Vector
 78 Machine -SVM) or presence-absence data (e.g. Generalized Linear Models – GLMs, Generalized
 79 Additive Models – GAMs, Flexible Discriminant Analysis – FDA, Multivariate Adaptive Regression
 80 Splines – MARS, Boosted Regression Trees – BRT, Gradient Boosting Machine – GBM,
 81 Classification and Regression Trees – CART, Random Forest – RF, Neural Networks – NNET,
 82 Artificial Neural Networks – ANN), and each represents niche properties differently. Traditionally,
 83 the most common method of evaluation of ENMs, regardless of their input data, are statistics that
 84 assess how different from random models are. Notably, the Area Under the Receiver Operating
 85 Characteristic (ROC) Curve (AUC) and True Skills Statistics (TSS) have been used to assess model
 86 performance. These statistics are well known from other scientific fields, but their use in ENMs are
 87 problematic when having no absence data, as both rely on sensitivity and specificity, which is
 88 unknown in presence-only, presence-background or presence-pseudoabsence models.

89 It has been stated in the literature that there is no simple solution or formula for decision
 90 making, and each decision should be taken according to the data and the intended use of ENMs (Qiao
 91 et al. 2015). Yet, there are still recurring examples of papers that suggest one method (e.g. Mi et al.
 92 2017, Zhang et al. 2019) to be superior to others. This is especially problematic when the conclusions
 93 are based on the AUC and/or TSS values, which: i) are highly correlated (Jiménez & Soberón 2020),
 94 ii) are inflated by the M size (Lobo et al. 2008) and the number of occurrence records (Konowalik &
 95 Nosol 2021), iii) ignores the predicted probability values and the goodness-of-fit of the model (Lobo
 96 et al. 2008) and iv) using AUC as a metric for presence-pseudoabsence models violating AUC theory
 97 (Jiménez & Soberón 2020). Instead of using AUC and TSS, recent literature has pointed towards at
 98 least two possible solutions. The first is analyzing how models perform at each range of its suitability
 99 or probability predictions; examples are the Boyce Index and its corresponding P/E plots, which
 100 correlates sample predictions over study space with predictions coinciding with presence points;
 101 (Hirzel et al. 2006, Di Cola et al., 2017) and the Accumulation of Occurrences Curve (Jiménez &
 102 Soberón 2020). The second consists of having experts systematically evaluating and scoring the
 103 output of the models (Gastón et al. 2014, Konowalik & Nosol 2021, Sarquis et al. 2018). This last
 104 concept was discouraged in early ENM literature (e.g. Soberón & Peterson 2005) but seems to be
 105 taking the spotlight, specially with initiatives like BioModelos (Velásquez-Tibatá et al. 2019).

106 In this study, we assess model output similarity between BioClim, MERRAClim and
 107 ENVIREM datasets separately for nine species of South American whip spiders. We also analyze
 108 model performance for eight different algorithms (RF, BRT, GLM, MARS, GLMNet, MaxEnt,
 109 MaxLike and SVM) by analyzing the Accumulation of Occurrences Curve recently proposed by
 110 Jiménez & Soberón (2020). Besides, we test three different M sizes for each model/environmental
 111 dataset/algorithm, to understand the influence of accessible area size on each method. We present
 112 AUC and TSS results as an argument that they do not reflect model performance in any informative
 113 way.

114 **2.0 – Methods**

115 2.1 – Taxon selection

116 For the purposes of this study, we chose to use species of the genus *Heterophrynus* Pocock 1894,
 117 which currently has 18 recognized species, to build our models. The reason we chose this taxa is that
 118 they are present in a wide area of South America. The genus used to be considered endemic to the
 119 Amazon Basin (Weygold 2000), but recent literature have shown it is present from the North and
 120 West of Colombia (de Armas 2015; de Armas, Contreras & García 2015) to the South of Pantanal in
 121 Brazil (Cordeiro et al. 2014), to the western edge of the Amazon and even in refugia in the semi-arid
 122 Brazilian Caatinga (Porto & Peixoto 2013). Despite that, all species live mostly on similar humid
 123 habitats, be it a humid forest, an altitude marsh, in caves or karstic areas, inhabiting burrows in trees
 124 and crevices or on rocky outcrops beside streams. These areas are known to have relatively higher
 125 uncertainty in predictors datasets because of relatively few weather stations monitoring the region
 126 (e.g. Fick and Hijmans 2017).

127 The second reason is that some species occur over wide areas and have many occurrence
 128 records available, while others (most species) do not and are more restricted. This allowed us to test
 129 the methods under different occurrence dataset sizes and areas, as well as exploring the effects of M
 130 size on each of them, and comparing the predictor datasets on different contexts.

131 The third reason we chose these taxa is that there is no current knowledge on these species
 132 distribution ranges, or even a compilation of occurrence records, which makes this study a valuable
 133 contribution to the knowledge of this poorly-known whip-spider group. Moreover, the Amazon
 134 Rainforest where most species occur is also under great threats from mining, logging and intense
 135 deforestation under the current Brazilian administration, despite international efforts to stop it
 136 (Carvalho et al. 2019, Rapozo 2021). For this reason, we deem studying and gaining knowledge on
 137 the lesser known taxa of the region all the more urgent and important.

138 2.2 - Study area

139 Most *Heterophrynus* species occur in Northern South America, and their records are summarized in
 140 Fig. S11 and Table 1. As other whip spiders, individuals usually remain in or close to a resourceful
 141 territory and seldom wander away (Weygoldt 2000).

142 2.3 - Species data

143 We obtained occurrence records for all *Heterophrynus* species from four sources: i) from the Global
 144 Biodiversity Information Facility (GBIF); ii) the literature (e.g. Giupponi & Kury 2013, Palacios et al.
 145 2019, Seiter & Gredler 2020); iii) from natural history museums and university collections (Instituto
 146 de Ciencias Naturales **ICN-MHN**; State Museum of Natural History Stuttgart **SMNS**; Universidade
 147 Federal de Minas Gerais **UFMG**; Universidade Federal da Paraíba **UFPA**; Universidade Federal de
 148 Mato Grosso do Sul **ZUFMS**; Museo Javeriano de Historia Natural **MPUJ**); and iv) directly from
 149 experts' personal databases, namely A.P.L. Giupponi and G.S. de Miranda. As no single source had
 150 abundance of records for any single species, all records were merged in a single dataset, totaling 1036
 151 occurrence records for the 18 *Heterophrynus* species.

152 After gathering the data, records were geo-referenced in the GEOLocate Web Client (Rios &
153 Bart 2010), following the guidelines in Chapman & Wiczorek (2020) in order to obtain latitude and
154 longitude, and uncertainty radius for each occurrence, which we later used to filter records with
155 uncertainty >10km to match climatic variables' resolution (uncertainty of coordinates by species
156 summarized in Fig. S6). Other data cleaning was executed using the coordinateCleaner R package
157 (Zizka et al. 2019) using the following parameters: records in capitals, centroids of countries and
158 provinces, duplicates, equal records, records around GBIF facilities, records on water, zeros and
159 records outside of the coordinate system. Records in or around biodiversity institutions and in urban
160 areas were intentionally not removed, because *Heterophrynus* are known to be synantropic, given that
161 any dark and humid environment can be occupied, as some are found in or close to cities, or suburban
162 areas. Species with less than 10 occurrence records were dropped from the study, resulting in nine
163 *Heterophrynus* species being kept in the study (Table S1). Finally, records were screened by G.S. de
164 Miranda for possible dubious identifications, which were also removed. We intentionally did not
165 perform records thinning (or spatial filtering; Sillero & Barbosa 2021, Steen et al. 2021) as it allowed
166 us to assess record clustering effect on different methods and to follow cells with more than one
167 occurrence record in the Accumulation Tables (from Jiménez & Soberón 2020).

168 The nine studied species of *Heterophrynus* are not evenly sampled, and most species have
169 relatively few occurrence records (e.g. *H. cervinus*, n=17) and only two have over 50 records, not
170 coincidentally the most widespread species *H. batesii* (n=117) and *H. longicornis* (n=238).

171 *Table 1: Heterophrynus species and the locality they have been recorded.*

Species	Recorded Area
<i>H. alces</i> Pocock 1902	Guyana, Suriname, French Guiana and in the Brazilian states of Amapá and Roraima
<i>H. armiger</i> Pocock 1902	Colombia and Ecuador
<i>H. batesii</i> Butler 1873	Ecuador, Colombia, Peru and Brazilian states of Acre, Amazonas, Rondônia, Roraima and Pará
<i>H. boterorum</i> Giupponi & Kury 2013	Colombia
<i>H. caribensis</i> Armas, Torres-Contreras & Álvarez García, 2015	Colombia, with some dubious records available in Ecuador and Peru
<i>H. cervinus</i> Pocock 1894	Colombia and Ecuador
<i>H. cheiracanthus</i> Gervais 1842	Northern half of Venezuela
<i>H. elaphus</i> Pocock 1903	Peru, scarce records in Bolivia and Brazilian states of Acre and Amazonas
<i>H. gorgo</i> Wood 1869	Amazonian Peru
<i>H. guacharo</i> de Armas 2015	Colombian caves
<i>H. javieri</i> Seiter & Gredler 2020	Colombia
<i>H. longicornis</i> Butler 1873	Northern Bolivia, spanning the entire Amazon Basin, also in the Brazilian Caatinga and Cerrado domains in refugia
<i>H. origamii</i> Chirivi-Joya, Moreno-González & Fagua 2020	Brazilian state of Rondônia
<i>H. seriatus</i> Mello-Leitão 1939	Mid-Western Brazilian state of Goiás
<i>H. silviae</i> Giuppony & Kury 2013	Colombia
<i>H. vesanicus</i> Mello-Leitão 1931	Mid-Western Brazil in caves and forest patches of the Cerrado domain
<i>H. yarigui</i> Álvarez García, Armas & Díaz Pérez, 2015	Northern Colombia

172 *2.4 - Environmental data*

173 In order to compare different environmental data, we obtained three sets of climatic predictors. The
174 first dataset **BioClim** (WorldClim v2.1, Fick & Hijmans 2017; available at <www.worldclim.org>),
175 which is by far the most widely used dataset of bioclimatic variables in the literature. Bioclim was
176 generated using interpolated data of climate stations all over the globe (Hijmans et al. 2005). This
177 dataset is known to present artifacts from interpolation, specially in areas where few weather stations
178 are present such as the Amazon Basin (Fick & Hijmans 2017, Campbell et al. 2015), which directly
179 impacts model output.

180 The second dataset is **MERRAClim** (Vega, Pertierra & Olalla-Tárraga 2018; obtained from
181 <<https://datadryad.org/stash/dataset/doi:10.5061/dryad.s2v81>>), generated using hourly data of

182 temperature and humidity from 1981 to 2010, from satellite data provided by NASA's Modern-Era
183 Retrospective Analysis for Research and Applications (MERRA).

184 Finally, the third dataset tested is the Environmental Rasters for Ecological Modelling dataset
185 (**ENVIREM**, Title & Bemmels 2018, obtained from <<https://doi.org/10.7302/Z2BR8Q40>>), a dataset
186 of mixed interpolated climate variables derived from WorldClim, and elevation-derived topographic
187 variables. This last dataset was originally intended to be used as a complementary dataset to BioClim
188 (Title & Bemmels 2018), but we wanted to test if the dataset could be used by itself to model non-
189 plant species. All datasets were downloaded on August 19th, 2021.

190 We selected four variables from each dataset (Table 2) that we judged important to the species'
191 biology and that were uncorrelated (correlation values in Table S2) within datasets. Correlation among
192 datasets' selected layers can be found in Table S3 and Fig. S7. Layers were cropped at the different M
193 sizes for each model of each species. All climatic layers were obtained in a standard 5' resolution
194 (~10km), as finer grain would invalidate most occurrence records.

195 *Table 2: response variables chosen from environmental datasets*

BioClim		MERRAclim		ENVIREM	
Bio 2	Mean diurnal range temperature	Bio 2	Mean diurnal range temperature	Annual PET	Annual potential evapotranspiration: a measure of the ability of the atmosphere to remove water through evapotranspiration processes, given unlimited moisture
Bio 3	Isothermality	Bio 3	Isothermality	Aridity Index	Thornthwaite aridity index: index of the degree of water deficit below water need
Bio 5	Max temperature of warmest month	Bio 5	Max temperature of warmest month	Climatic Moisture Index	A metric of relative wetness and aridity
Bio 15	Precipitation seasonality	Bio 8	Mean temperature of the most humid quarter	Thermicity Index	Compensated thermicity index: sum of mean annual temp., min. temp. of coldest month, max. temp. of the coldest month, ffj 10, with compensations for better comparability across the globe

196 2.5 - Model built

197 We built 6480 models in total, one set of ten bootstrap replications for each of the eight algorithms,
198 under three climatic datasets, at three different M sizes for each of nine species (Fig. 1). When we
199 refer to any model, we refer to the mean of these bootstrap replications.

200 2.5.1 - Accessible area (*M*)

201 To tackle the accessible area issue (Barve et al. 2011), separate models were calibrated within three
 202 different accessible areas (or **M**s; Fig. 2), hereafter called **SM**, **MM** and **LM** (referring to small,
 203 medium and large **M**s, respectively), that were defined as the bounding box of buffers created around
 204 the occurrence records at different sized radii for each species (Table S1). The values of buffer radius
 205 were arbitrarily defined based on how widespread were the occurrence records, ranging from 50km in
 206 the **SM**s of the most localized species (e.g. *H. alces*), to up to 800km in the **LM**s in more widespread
 207 species (e.g. *H. longicornis*).

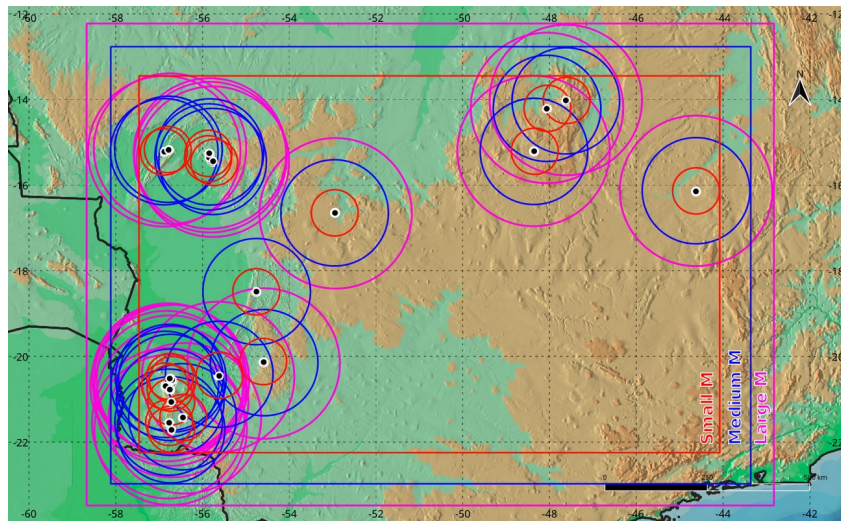


Fig. 1: accessible area (*M*) selection scheme. Three different accessible areas were defined for each species as the bounding box of different-sized radii buffers around the occurrence records. The bounding box of the smallest radius buffers defines the small *M* (**SM**) (red), and the same follows for the medium *M* (**MM**) (blue) and large *M* (**LM**) (violet). Background is an elevation map of central Brazil.

208 2.5.2 - Algorithm choice

209 We built our models for each species, *M* size and climatic dataset using eight different algorithms, as
 210 no single method can be blindly followed (Qiao et al. 2015). The different statistical methods can be
 211 segregated in three classes: i) tree-based methods, ii) machine-learning methods and iii) regression-
 212 based methods. From the first class, we tested the Random Forest (**RF**) and the Boosted Regression
 213 Trees (**BRT**) algorithms. The main difference between these two is that **RF** generates independent
 214 trees, and **BRT** dependent trees that make decisions informed by the former trees. From the second
 215 class of algorithms (machine learning), we selected three algorithms: **MaxEnt**, a Maximum Entropy
 216 machine learning algorithm, widely used in ENMs; **MaxLike**, a Maximum Likelihood algorithm like
 217 the former; and Support Vector Machine (**SVM**), a machine learning algorithm based on classifiers to
 218 separate data. And from the third class of algorithms, we chose: a Generalized Linear Model (**GLM**),
 219 a well known statistical approach based on linear regressions; Multivariate Adaptive Regression
 220 Splines (**MARS**), a method that fits several regression lines to parts of the data and builds the model

221 from them; and **GLMNet**, an algorithm based on custom linear models and elastic net regression via
 222 penalized maximum likelihood. All of these methods are available in the *sdm* package (Naimi &
 223 Araújo 2021), and were used in the standard settings of the *sdm* function.

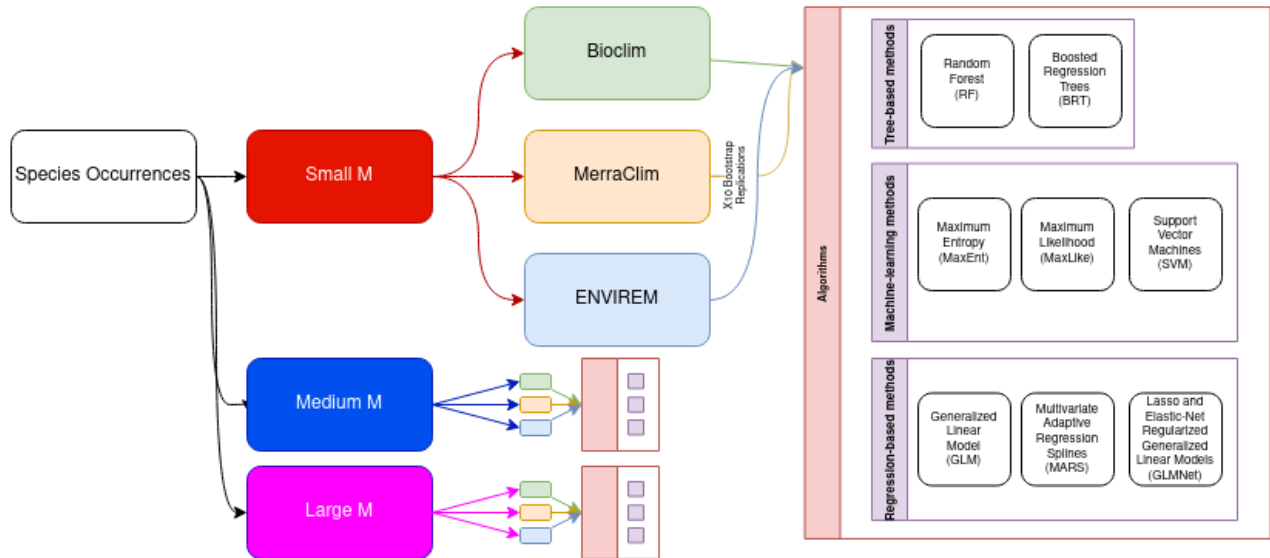


Fig. 2: model workflow. For each of nine *Heterophrynus* species three sized Ms were defined, on which we constructed models for each of three climatic datasets, using ten bootstrap replications of eight algorithms of three different classes

224 Most of these algorithms require absence data, and in the lack thereof we randomly generated a
 225 standard number of 200 pseudoabsences (Barbet-Massin et al. 2012) in geographic space for all
 226 models. From the methods listed above, only MaxEnt and SVM are meant to be used with pseudo-
 227 absence data, and others treat pseudoabsences as proper absences, yet good results have been achieved
 228 using pseudoabsences with them (Konowalik & Nosol 2021). We tested and compared the algorithms'
 229 responses against the different climate datasets, Ms, and in the different scales and regions where
 230 *Heterophrynus* species occur.

231 2.5.3 - Model evaluation

232 We then compared algorithm performance under three evaluation metrics: i) the Area Under the ROC
 233 Curve (**AUC**), ii) true skill statistic (**TSS**); and iii) the accumulation of occurrences curve (hereafter
 234 **AOcC**), an evaluation method recently presented by Jiménez & Soberón (2020). The AUC is a
 235 threshold-independent evaluation method that quantifies the relationship of specificity and sensitivity
 236 under different thresholds compared to random, that should not be used with pseudo-absences, yet it is
 237 the most used evaluation metric in ENMs to date despite its unrestricted use having been recently
 238 questioned by several authors (Jiménez-Valverde & Lobo 2007, Jiménez & Soberón 2020, Konowalik
 239 & Nosol 2021). TSS is a threshold-dependent metric that calculates the values of sensitivity minus
 240 specificity of a model.

241 The AOcCs take into account the accumulation of occurrences and number of cells predicted as
 242 suitable needed to find them. The authors propose that the algorithm which correctly finds most

243 occurrences (target) in the least number of high suitability prediction cells should be used, considering
 244 Occam's razor. In this study, we define a new metric and set the **AOcC-target** at the number of cells
 245 in which 90% of occurrences were found. We built AOcCs for all models to compare algorithm
 246 performance as their original intended use, and also built the same plots by algorithms to compare
 247 each algorithm's performance on the different M sizes and Environmental Datasets for each species.

248 2.5.4 - Model comparison

249 For quantifying the similarity of predictions based on the three climatic datasets, we used Schoener's
 250 D statistic to compare the model output prediction of each climatic dataset under each algorithm. We
 251 also performed this analysis to compare each algorithm's output to its pairs. For this purpose, the
 252 output of some of the models (particularly models for MERRAclim and/or under the GLMNet
 253 algorithm) had to be transformed not to include negative values, and this was done by adding the
 254 lowest negative value to all values, i.e. shifting the results to zero as the minimum.

255 2.5.5 - Software, codes and data

256 All analyses were performed in R (version 4.0.4). Models were built and projected using the *sdm*
 257 package version 1.1-3 (Naimi & Araújo 2021), spatial data was manipulated using the *raster* package
 258 version 3.5-2 (Hijmans 2022) to match extent and cell sizes of the three climatic datasets, the
 259 accumulation of occurrences curve and comparison were constructed using the *accum.occ* and
 260 *comp.accplot* functions presented by Jiménez & Soberón (2020) and obtained from
 261 <<https://github.com/LauraJim/SDM-hyperTest>>. Schoener's D statistic was calculated using the
 262 *nicheOverlap* function in the *dismo* package version 1.3-5 (Hijmans et al. 2021), and plotted using the
 263 *ggplot2* package version 3.3.5 (Wickham 2016). Some maps were post-processed in QGIS version
 264 3.16.9-Hannover for aesthetics. We provide an R script in <github.com/jfberner/ENMs> as a sample
 265 for the modeling process of *H. alces*, as the same process was repeated for all species.

266 To easily refer to a specific model, we hereafter refer to them by their composition of Climatic
 267 Data, M size, Algorithm and Species: for example the MERRAclim model, built under the large M
 268 (LM), using MARS as method, for the occurrence records of *H. batesii* will be referred to as the
 269 ***batesii*-MERRA-LM-MARS** model. Moreover, when we use this codification with missing
 270 information, we mean all models that are grouped by the same characteristics: the *batesii*-GLM
 271 models are the nine models built using GLM for *H. batesii*, three for each M size for each of three
 272 environmental datasets; and MaxEnt-MM models are the 27 models for the nine species times the
 273 three environmental datasets built only with this algorithm and M size.

274 3.0 - Results

275 3.1 - Model outputs

276 All models performed better than random regardless of M size, algorithm, predictors, sample size,
 277 species or geographic area of occurrence. All model outputs are presented in Figs. S3A-I.

278 3.1.1 – Environmental Datasets

279 To assess output similarity between datasets, we analyzed Schoener’s D statistics for niche similarity
 280 (Table S5). We expected to find that BioClim and ENVIREM model outputs to be more similar to
 281 each other than to MERRAClim, as both were generated using the same method and original dataset,
 282 yet represent different climatic variables. This appears to be mostly true (Fig. 3), with exceptions (Fig.
 283 4). As we used different layers representing different climatic variables in each dataset, we also
 284 expected outputs to have overall low similarity, but this was not the case. We present in Fig. S10 a plot
 285 similar to Fig. 3, but the data was split by each species and M size, and in Fig. S8 split by each
 286 algorithm and M size.

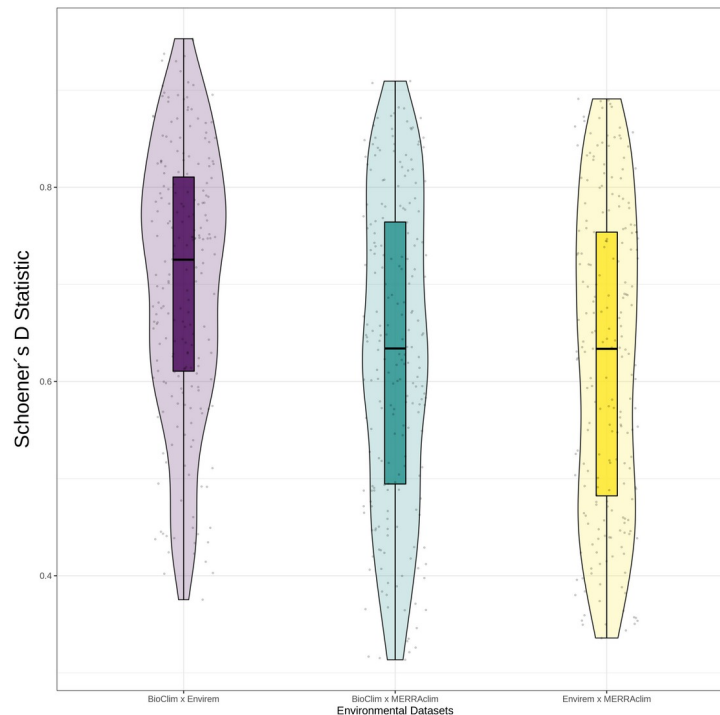


Fig. 3: Box+violin-plot of d-stat results for Environmental Dataset comparison including all 648 models. Individual values in grey dots.

287 The mean of all similarity tests between climate datasets were equal (BioClim x ENVIREM,
 288 $d=0.6515$; BioClim x MERRAcLim, $d=0.6519$; ENVIREM x MERRAcLim, $d=0.6525$), but these
 289 varied greatly among methods, M sizes and species. As the mean value is not informative of how
 290 similar individual models are, we present in Fig. 3 a box-and-violin-plot to better visualize the
 291 distribution of d-stat values when comparing the outputs of environmental datasets.

292 Fig. 3 suggests that although not significantly, BioClim and ENVIREM had more similar
 293 results in general, but this varied greatly in different geographical areas. For simplicity, we present the
 294 d-stat results by species for MaxEnt-MM models in Fig. 4 (the complete Fig. for all methods and M
 295 sizes can be found on Fig. S8).

296 As shown in Fig. 4 similarity varied greatly between species, as model outputs for some
 297 species were very similar (e.g. *H. elaphus*) while others were not (e.g. *H. boterorum*). Some

298 algorithms retained the same similarity curves, or at least the same trends, between M sizes (e.g.
 299 MaxEnt column in Fig. S8), others have no clear trends (e.g. MaxLike column in Fig. S8).

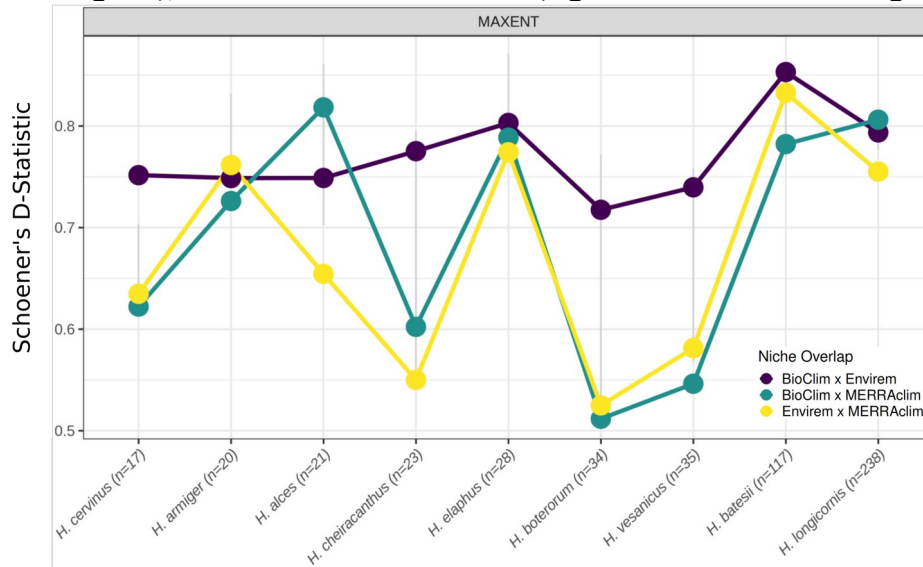


Fig. 4: D-stat results for the comparison of environmental datasets under Maxent-MM models for all modeled species.

301 What can be interpreted from these plots is that some species had more similar models than
 302 others (regarding the datasets' response comparison), namely *H. armiger*, *H. elaphus*, *H. batesii* and
 303 *H. longicornis*. The first is present in a narrow region West of the Andes in Ecuador and Colombia.
 304 The second species, *H. elaphus*, occurs East of the Andes mainly in the Peruvian Amazon, and as both
 305 these regions are areas of low uncertainty in the weather datasets that generated both BioClim and
 306 ENVIREM, the similarity was to be expected. The latter two species are the most widespread, *H.*
 307 *batesii* is present mainly in the Western Amazon Basin (Fig. 5, Fig. S11), while *H. longicornis* mainly
 308 in the Eastern half (Fig. S3-H), and their distributions overlap in the middle of the Amazon, which is
 309 the area with greatest amount of uncertainty in the BioClim and ENVIREM datasets.

310 3.1.2 – M size

311 Model output (suitability maps) varied considerably among algorithms (section 3.1.3), but very little
 312 among M sizes (Fig. S3). Considering occurrence location of each species is crucial to model
 313 interpretation: species *H. longicornis*, *H. batesii*, *H. alces* and *H. cheiracanthus* all occur in areas of
 314 high uncertainty for the BioClim dataset (and therefore, ENVIREM as well), given that few weather
 315 stations exist in Central and West Amazon (Fick & Hijmans 2017). For this reason, we will look
 316 closely at the outputs of the models for three of these species: *H. batesii*, *H. alces*, and *H.*
 317 *cheiracanthus*. In this section we briefly mention evaluation for context, but present M size impact on
 318 model performance and evaluation in detail in section 3.2.2.

319 3.1.2.1 – *Heterophrynus batesii*

320 This is a widespread species with 117 records which SM, MM and LM sizes are 127395, 155043 and
 321 185283 cells in size respectively. We increased M size in steps of 150 km, starting at a 400 km buffer
 322 around occurrence points for SM. The LM models spanned over most of South America. Increasing
 323 M did not greatly change predicted areas of suitability for any given method or predictors (Fig. S3-
 324 C), meaning that algorithms retained mostly the same prediction regardless of M size. For example,
 325 the Bioclim-MaxEnt SM, MM and LM models for this species look very similar (Fig. 5), and the
 326 same is true for any other combination of same method/predictors.

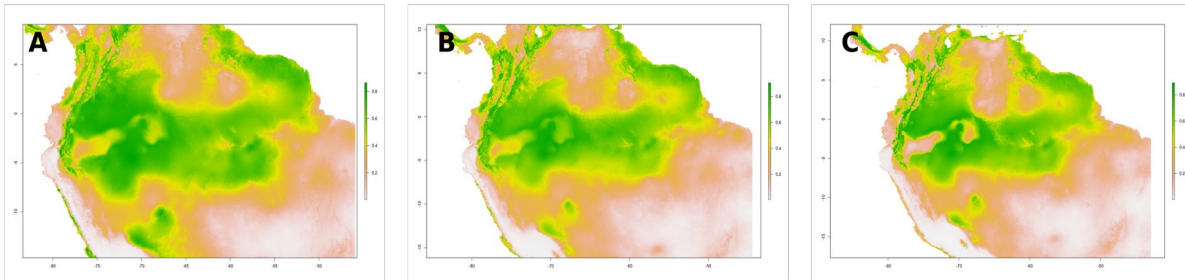


Fig. 5: batesii-BioClim-Maxent model outputs for SM (A), MM (B) and LM (C).

327 AUC values increased very slightly (0.83 SM, 0.83 MM and 0.84 LM), and the same is true
 328 for TSS values (0.57, 0.57 and 0.58 for SM, MM and LM respectively). The number of cells at
 329 AOcC-target occurrences for this example remained relatively stable at 45072 (35.38% of SM area),
 330 51557 (33.25% of MM area) and 50935 cells (27.49% of LM area), indicating that increasing M in
 331 this case did nothing to enhance the model or predictions. This is true for all models of this species
 332 (Table S1, Fig. S3), but that's not the case for other species we modeled.

333 3.1.2.2 – *Heterophrynus alces*

334 For this species we had 21 records narrowly distributed in N-Western South America (in Guyana,
 335 Suriname, French Guiana and parts of Brazil), with M sizes spanning 9576, 12180 and 15072 cells.
 336 For this species, we increased M size in steps of 50 km, starting at a 50 km buffer around occurrence
 337 points for SM. To allow some comparability to the former example, we'll look at the BioClim-
 338 MaxEnt models for the species (Fig. 6).

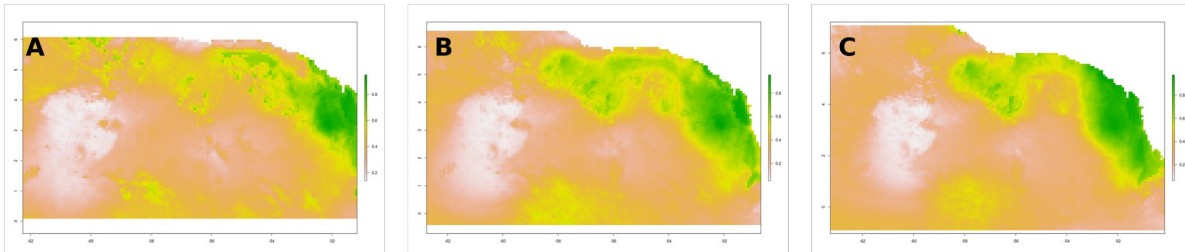


Fig. 6: alces-BioClim-Maxent model outputs for SM (A), MM (B) and LM(C).

339 The number of cells at AOcC-target occurrences in this case are 4261 (44.5% of total area) in
 340 the SM, 4122 (33.84%) in the MM model, and 4600 (30.52%) in the LM model. AUC values
 341 decreased slightly as M was increased (0.79 in SM, 0.76 in MM and 0.77 in LM), as well as TSS
 342 values (0.58 in SM model, 0.54 in MM and 0.56 in LM). In this example, although SM has the “best”
 343 AUC and TSS scores, only in MM and LM models a definite suitable range for the species can be
 344 seen, something that may be desirable in most ENM applications. Moreover, increasing M led the

345 model to discard the western areas of the map as suitable, and concentrate suitable cells in mostly a
 346 single range.

347 3.1.2.3 – *Heterophrynus cheiracanthus*

348 This species occurs mostly in the northern half of Venezuela and in Tobago, with 23 records spread
 349 over this area, which SM, MM and LM sizes are 15036, 29964 and 73644 cells in size respectively.
 350 We doubled M size at each step starting at a 200 km buffer around the occurrence records for SM.
 351 Again, we present the BioClim-MaxEnt models for the species (Fig. 7), to allow some degree of
 352 comparability with the last two examples.

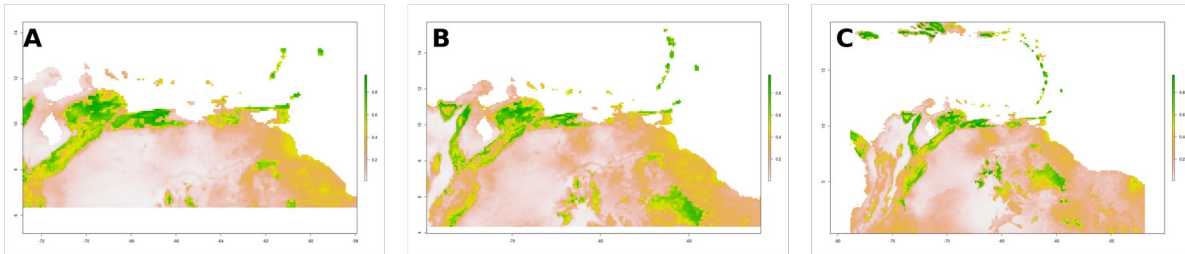


Fig. 7: cheiracanthus-BioClim-Maxent model outputs for SM (A), MM (B) and LM (C).

353 The number of cells at AOcC-target occurrences for these models are 2221 in SM (14.77% of
 354 area), 3502 in MM (11.69%) and 6423 in LM (8.72%). As the species' suitability range is very small
 355 compared to the whole area, AUC and TSS scores are significantly greater than the previous two
 356 examples (0.9 AUC and 0.74 TSS in SM; 0.93 AUC and 0.80 TSS in MM; 0.88 AUC and 0.74 TSS
 357 in LM). The case of *H. cheiracanthus* is an example that mixes the former two: i) as with *H. batesii*
 358 the entirety of the suitable range predicted in the SM model is fully present in MM and LM models,
 359 and only new areas were added as M increased; ii) as was the case in *H. alces*, increasing M revealed
 360 a somewhat continuous distribution westward that was unrepresented in SM.

361 3.1.3 – Algorithm

362 To assess the similarity between algorithms' output, we present the mean of all models Schoener's D-
 363 Stat in Fig. 8 (for the results of any particular model please refer to Fig. S5). The highest output
 364 similarity is between BRT and MaxEnt (d=0.86), and the lowest is between BRT and MARS
 365 (d=0.49).

366 Other highly similar outputs are between GLM with both MaxEnt and GLMNet, and GLMNet
 367 with MaxEnt, BRT and GLM. Although the final output is somewhat similar according to d-stat
 368 results, the AOcCs clearly suggest that neither GLM or GLMNet perform satisfactorily in high-
 369 suitability cells (further discussed in section 3.3.3; Fig. 10), which suggests that for similar output and
 370 better performance, both BRT or MaxEnt should be preferred over GLM or GLMNet.

371 Moreover, analyzing outputs for each model, we observed that GLMNet and MaxLike tend to
 372 overpredict suitability ranges when compared to other algorithms, sometimes predicting almost the
 373 entire given area as suitable for the species (e.g. the *cheiracanthus*-BioClim-SM-GLMNet model
 374 output in Fig. S3-F). This can be the reason why GLMNet's output appears to be similar to the
 375 algorithms previously mentioned in this paragraph. Moreover, this high GLMNet similarity with
 376 other model outputs could be influenced by the transformation we did in order to apply the

377 nicheOverlap function from the dismo package, which does not accept negative values, but it remains
 378 unclear whether this is the case.

379 3.2 – Model Performance and Evaluation

380 3.2.1 – Environmental Datasets

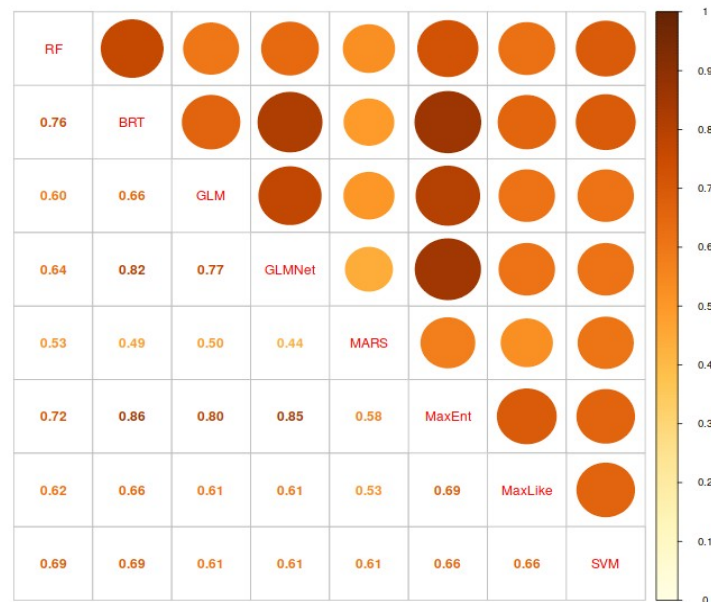


Fig. 8: mean *D*-Stat values (below diagonal) for model output comparison between algorithms. Highest values indicate more similar outputs.

381 To compare environmental dataset by their performance, we built AOcCs for each species by
 382 algorithm (Fig. S2). In Fig. 9 we present three examples of the most common patterns we found. In
 383 Fig. 9-A, the AOcC for the *longicornis*-RF models, in which there is no clear distinction on
 384 performance of the three environmental datasets or M sizes, all reaching target occurrences in ~40
 385 thousand cells. This was the case in all RF and MARS models, and most BRT, MaxEnt and SVM
 386 models. In Fig. 9-B we present the AOcC for the *batesii*-GLM models, in which a clear distinction is
 387 made between the three environmental datasets, where BioClim (shades of yellow) reached target
 388 occurrences first, followed by ENVIREM (shades of blue) and lastly MERRAclim (shades of brown).
 389 In Fig. 9-C we present the third type of trend we observed in these AOcCs using the *elaphus*-GLM as
 390 an example of an AOcC in which no clear distinction can be made between the best performing
 391 environmental dataset or M size.

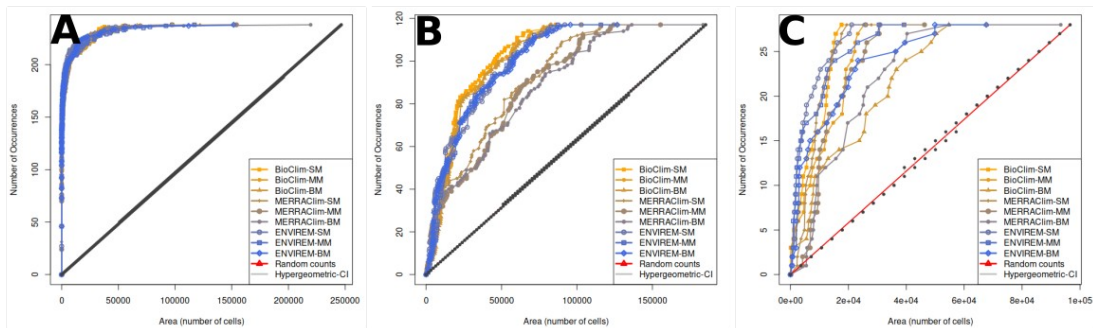


Fig. 9: AOCs for longicornis-RF (A), batesii-GLM (B) and elaphus-GLM (C) models.

392 Overall, MERRAClim tended to reach target occurrences in more cells than its counterparts,
 393 and its outputs were also less similar to other datasets as shown in section 3.1.1.

394 3.2.2 – M size

395 We expected to find increasing AUC and TSS values as M size increased, and although this happened
 396 in several cases it is not a definite pattern. AUC and TSS scores for all models are summarized in Fig.
 397 S12A-B.

398 M size did have an impact on the performance of some algorithms. To illustrate it, we present
 399 the example of *alces*-MERRA models SM through LM (Fig. 10): GLM, MaxLike and GLMNet
 400 performed close to or worse than random up until 4~5 thousand cells in the SM model. The curves
 401 shifted above random in fewer cells in larger M models (under 2000 cells in MM and under 1600
 402 cells in LM). This means that increasing M size can increase model performance using these
 403 algorithms. Still, it had little to no effect on initial performance of the other tested algorithms (e.g. the
 404 MARS or SVM AOCs in Fig.S2 for all species). Understandably, all methods reached target in more
 405 cells in the LM models than in their respective SM models (Figs. 9, 10 and 11), simply because more
 406 suitable cells were included.

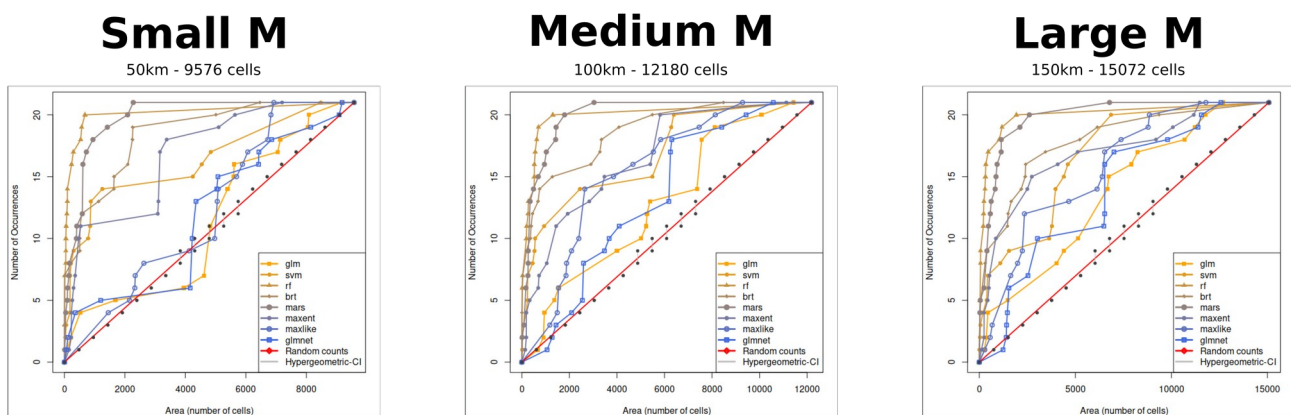


Fig. 10: AOCs for *alces*-MERRA models. As M increases, the curve of low performing algorithms crosses the random counts curve in fewer cells

407 Moreover, focusing on how each algorithm performed under any given M size and predictors,
 408 we analyzed the AOCc for the three algorithms above-mentioned as low-performing (GLM, GLMNet

409 and MaxLike; Fig. 11). We found that it is not as simple as increasing M: the left plot on Fig. 11
 410 (GLM) shows that although MERRA-BM performed better than its SM and MM counterparts
 411 initially, it had the worst performance at AOcC-target (11208 cells at 19 occurrences). The same
 412 happened for MERRA-BM on MaxLike models (right plot, Fig. 11). Still at the left plot, even though
 413 the MERRA-SM and MERRA-MM (the worst initial performance) lines do not follow the same path,
 414 they reach target at roughly the same number of cells (SM: 8050 and MM: 8104; Table S1), which
 415 indicates that increasing M had little effect on both performance and output (Fig. S3-A), at least for
 416 the MERRA models for this species. We found this same pattern for GLMNet models outputs for this
 417 species (middle plot, Fig. 11).

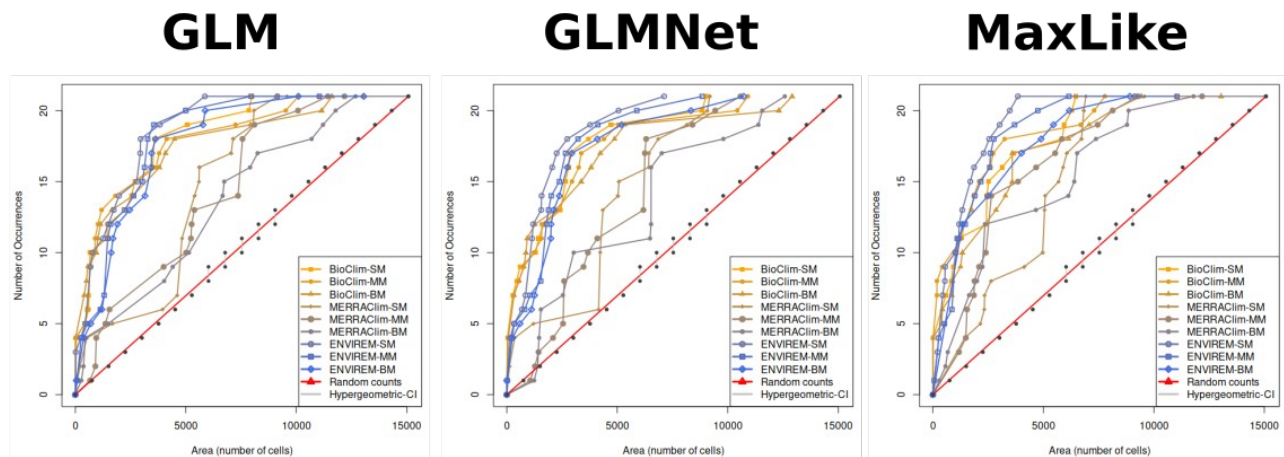


Fig. 11: AOcCs for *H.alces* models for GLM, GLMNet and MaxLike. The plot shows how occurrences were accumulated in each *H.alces* model for the algorithms. MERRA-SM models are not below the random counts line as in the previous Fig. because the scale of the X axis here is the LM scale. SM=50km buffer around occurrence points or 9576 cells, MM=100km or 12180 cells, LM=150km or 15072 cells. Target at 19 occurrences.

418 3.3.3 – Algorithm

419 In general, algorithms performed well for all tested settings, but some tended to overfit models (RF
 420 and MARS) and others underfit them (GLMNet and MaxLike) regardless of species, predictors or M
 421 size (see Figs. S3A-I for an output comparison by species). AUC and TSS scores indicate that all
 422 models performed better than random (Table S1), and AOcCs suggest that most do too, but not at the
 423 entire range of predictions.

424 First, we focus on the “worst performing” algorithms. Fig. 12 the AOcC shows an example of
 425 the algorithms that perform overall better than random, but do not do so for the highest ranked 40~50
 426 thousand cells, performing poorly when compared to the other tested algorithms (MaxLike, GLMNet
 427 and GLM specifically).

428 This is an extreme case where there is a clear distinction between the best performing
 429 algorithms (generally RF, MARS, MaxEnt, SVM and BRT) from their worst performing counterparts
 430 cited above, but this segregation is not always clear (e.g. Fig. 10).

431 Shifting the focus to the “best performing” algorithms, RF and MARS are the algorithms that
 432 invariably reached AocC-target in the least number of cells. To illustrate this, we present in Table 3 a

433 table of accumulation of occurrences for RF, MaxEnt and MARS, for the species with the least
 434 number of occurrences for simplicity (*H. cervinus*, $n=17$), under the widely used BioClim climatic
 435 dataset, and under the smallest M tested for the species. We also present the AOcC that corresponds to
 436 Table 3 in Fig. 13, which further illustrates this repeating pattern: RF identifies all occurrences with
 437 very few cells, and is followed by MARS.

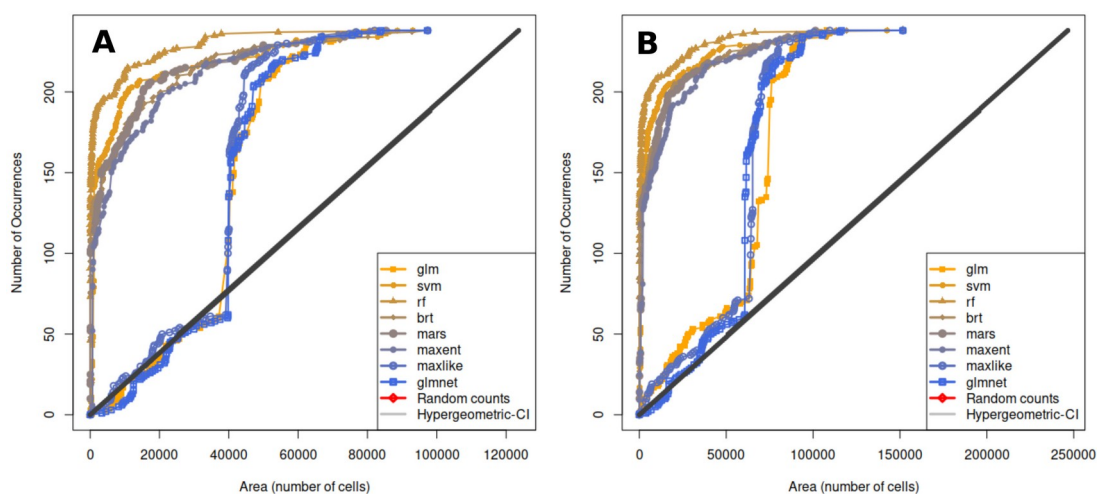
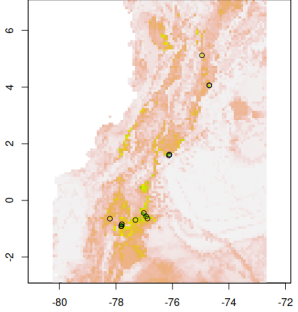
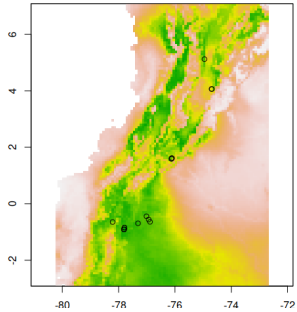
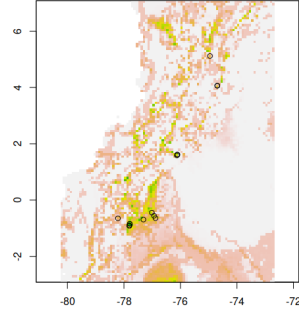


Fig. 12: AOcCs for longicornis-BioClim SM (A) and LM (B) models.

438 *Table 3: Table of accumulation of occurrences for cervinus-Bioclim-SM models (10920 cells*
 439 *in total) of three algorithms: RF, MaxEnt and MARS. Occurrence target = 15 (88.24%) in*
 440 *bold. Bottom row is the raw output of each model with occurrence records for reference.*

RF				MaxEnt				MARS			
No.occurrences	No.cells	%Gained Occ	%Area	No.occurrences	No.cells	%Gained Occ	%Area	No.occurrences	No.cells	%Gained Occ	%Area
0	0	0	0	0	0	0	0	0	0	0	0
6	1	35.29	0.01	6	10	35.29	0.09	6	52	35.29	0.48
7	2	41.18	0.02	7	216	41.18	1.98	9	74	52.94	0.68
8	3	47.06	0.03	8	401	47.06	3.67	10	77	58.82	0.71
11	5	64.71	0.05	9	787	52.94	7.21	11	256	64.71	2.34
13	12	76.47	0.11	10	898	58.82	8.22	12	288	70.59	2.64
14	32	82.35	0.29	11	984	64.71	9.01	14	326	82.35	2.99
15	66	88.24	0.6	12	1092	70.59	10	15	337	88.24	3.09
16	82	94.12	0.75	15	1306	88.24	11.96	16	407	94.12	3.73
17	8593	100	78.69	17	3058	100	28	17	8820	100	80.77

		
---	---	---

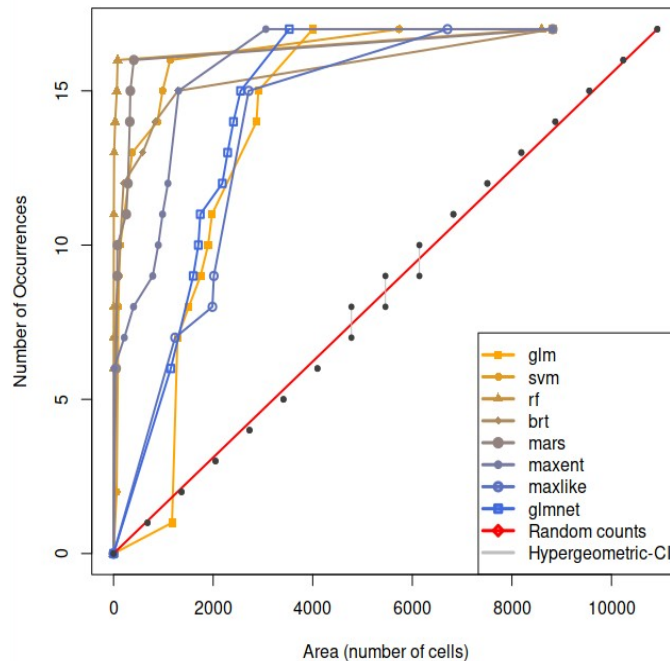


Fig. 13: AOCc for cervinus-Bioclim-SM model (SM = 200km radius, 10920 cells)

442 To further explore the extent of this trend, Fig. 14 presents a chart that shows the number of
 443 cells at target occurrence for each algorithm, for all *H. alces* models. We chose this as a clear example,
 444 for similar plots for the other species and models in our study please refer to Fig. S4.

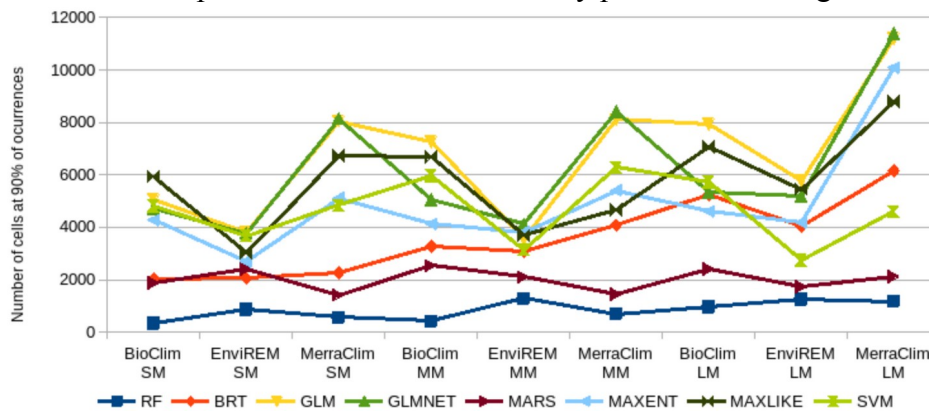


Fig. 14: Line plot of the number of cells at AOCc-target by algorithm for *H. alces* models, under each climatic dataset, at each *M* size.

445 Moreover, RF seems to have overfitted all models we generated, which is best observed in the
 446 suitability regions plotted in Environmental Space (Figs. S9A-I). We expected this to perhaps be the
 447 case in the species with the least number of records (*H. cervinus*, $n=17$, Fig. 15C-D), because we
 448 generated more pseudo-absences than the number of occurrences, but we observed overfitting even in
 449 the species where occurrence records outnumbered pseudo-absences (*H. longicornis*, $n=238$, Fig.
 450 15A-B).

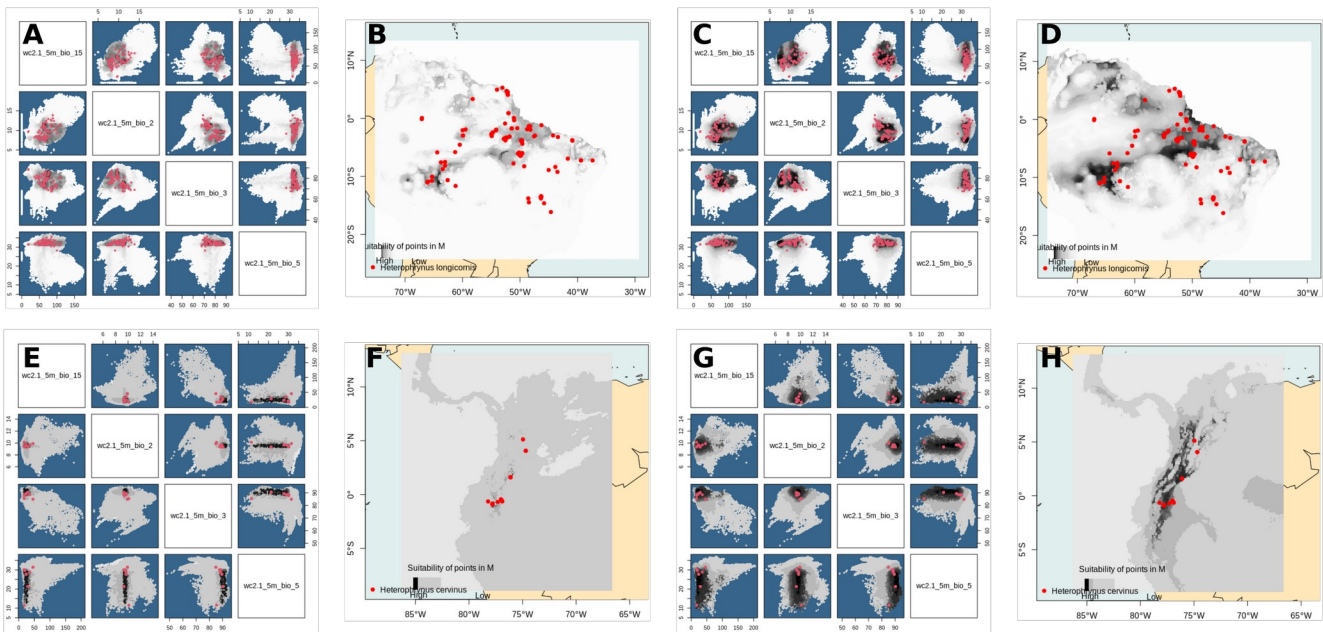


Fig. 15: Models in Environmental Space (A, C, E, G) and in Geographical Space (B, D, F, H). longicornis-BioClim-LM RF (A-B) and MaxEnt (C-D), cervinus-BioClim-LM RF (E-F) MaxEnt (G-H) for comparison of the overfitting under RF models.

451 There are seven exceptions (out of 648 models) to this: models *armiger*-BioClim-LM,
 452 *boterorum*-BioClim-MM, *boterorum*-MERRAclim-MM, *boterorum*-MERRAclim-LM, *cervinus* -
 453 MERRAclim-SM, *cervinus* -MERRAclim-MM, and *elaphus*-MERRAclim-LM had MARS reach
 454 target in fewer cells than RF (Table S1; Figures S1 and S2). All AOCs are presented in Figures S1
 455 by climatic dataset and S2 by algorithm, Table S1 contains the number of cells at target for all models
 456 and Tables S4 A-I presents every individual accumulation table.

457 4.0 - Discussion

458 4.1 – Environmental Datasets

459 This study showed that all three environmental datasets produced reasonable, useful and informative
 460 models. However, for some species (and therefore some regions of South America), the three
 461 datasets' outputs were more dissimilar than in others (Fig. S10). This conclusion comes with a grain
 462 of salt, as each predictors' similarity was also influenced by the algorithms we tested (Fig. S11), and
 463 different algorithms responded very differently. The algorithms BRT, RF and GLMNet notably
 464 retained more similar model outputs among predictor datasets than other algorithms, even though the
 465 latter two algorithm's outputs are barely useful or informative for under- and overpredicting,
 466 respectively.

467 Knowing how much each predictor dataset differs from the other two could allow us to use this
 468 information as a proxy for model uncertainty, as we expected that model similarity would not be low
 469 among predictors for two reasons. The first reason is that the ENVIREM dataset was generated using
 470 the same layers as BioClim. The second is that MERRAclim (satellite data) and BioClim (weather

471 station data) models had three layers out of the four representing the same variables. Our results
 472 suggest that the first of these reasons is true, while the other is not, as the MERRAclim models were
 473 the least similar to their BioClim and ENVIREM counterparts. This finding is in accordance, from
 474 completely different evaluation methods, with the results in Morales-Barbero & Vega-Álvarez (2018),
 475 in which they find MERRAclim to be the least congruent with other tested datasets. Unfortunately,
 476 they tested only RF as a method, which can be problematic for reasons discussed in this study, and
 477 further research could better explore this congruence under different methods.

478 4.2 – *M size*

479 Our findings indicate that there is no simple rule to define *M* size, and we defend that fitting a few
 480 models and trying different *M* sizes before defining *M* should be standard practice. Comparing
 481 models with different *M* sizes both in **G** and in **E** can clarify what type of environment is being
 482 introduced with larger *M*s and what impacts that has on the model in **G**, and it can help modelers to
 483 choose the most suitable *M* size for their applications. For simple suitability maps to project species'
 484 distribution (a standard SDM), the best *M* size could be the one that encompasses one or more clearly
 485 defined ranges. As for modelers interested in niche models and projecting in any region in space or
 486 time different from the one the model was trained in (ENMs), the best *M* size may be the one that
 487 most clearly defines suitability in **E**, rather than **G**, meaning the *M* size that has sufficient
 488 heterogeneity in **E** for a model to be useful when projected to a new environment (Peterson &
 489 Soberón 2012).

490 4.3 – *Algorithm*

491 The same is true for algorithm choice: selecting what algorithm to use is crucial, as our results show.
 492 Three out of the eight algorithms we chose, all easily accessible in the sdm package, performed
 493 poorly in all regions, under any predictors. Ease of access and of reproducibility is what made
 494 MaxEnt ubiquitous in ENMs (Liu et al. 2020), and with these new tools freely and easily available in
 495 CRAN we expect their use to become more popular. That's why knowing each of these algorithms'
 496 bias and limitations is so important.

497 Algorithms GLM, GLMNet and MaxLike under-fitted nearly all models, regardless of
 498 geographical context, occurrence sample size, *M* size or predictors dataset. Moreover, these
 499 algorithms worked very close to or under the AOcCs' random baseline in many cases for the first
 500 third or half of the highest-ranking suitable cells. We argue that if an algorithm is under-performing in
 501 the highest ranking cells under any given input, it should be avoided in ENMs, as these are the cells
 502 that are usually retained when selecting a threshold for presence/absence maps.

503 Algorithms RF and MARS typically overfitted models, but were the "best" at correctly
 504 identifying occurrence records in the AOcCs, meaning they did so in the least number of cells. From
 505 our study design, we cannot infer whether these two algorithms are being influenced more by spatial
 506 clustering or to the number of pseudo-absences, but these two factors are certainly causing overfitting
 507 on these two algorithms' performance. We can state however, that they are the most sensible to these
 508 factors from the eight algorithms we tested. Jiménez & Soberón (2020) propose when presenting their
 509 method that when comparing algorithms using the AOcCs, the one that finds "target" occurrences (in
 510 our case, ~90%) in the least number of cells should be used. Our analyses suggest that this should not

511 always be the case, as it would favor overfitting models and retained models would invariably be the
512 most overfit.

513 We therefore argue that algorithms should be chosen based on the characteristics of what is to
514 be modeled on top of reasonable AOcC performance: RF and MARS could potentially be used with
515 excellency for fitting models of endemic species narrowly distributed in **G**, and with relatively few
516 numbers of records. For example, the *cheiracanthus*-BioClim-SM-RF model output is reasonable, but
517 its MM and LM counterparts are not (Fig. S3-F).

518 Our findings of RF being suitable for localized species modeling is in accordance with the
519 literature in Mi et al. (2017), but for starkly different reasons. We highly disagree with the authors'
520 conclusions, especially because they drew their conclusions mainly from RF having the highest AUC
521 and TSS scores, and we've shown with our results that this is almost certainly because of a
522 combination of RF overfitting models and the statistics being inflated by M and sample sizes.

523 Of all the tested algorithms, MaxEnt, BRT and SVM had the most reasonable outputs and
524 performance, and delivered informative models under all tested circumstances without over- or
525 under-fitting models.

526 4.4 – Evaluation

527 We intentionally disregarded AUC and TSS scores in our evaluation of models, and presented them
528 precisely to show that they have little to no meaning in evaluating models. The first reason we chose
529 to do so is that these statistics, the most widely used in ENMs literature, have been shown to be
530 heavily influenced and inflated by M size (Barve et al. 2011, Castellanos et al. 2019), an
531 unquantifiable effect that was not clear in our results. The second reason is that these two statistics are
532 correlated (Konowalik & Nosol 2021). Third and foremost, these evaluation metrics should not be
533 used with pseudoabsences, as it violates their underlying theory (Jiménez & Soberón 2020). Several
534 authors have pointed towards the misuse of the AUC as an evaluation metric, and it has been
535 suggested more than once in the literature that it should at least be used alongside another metric
536 (Lobo et al. 2008, Konowalik & Nosol 2021).

537 We instead chose to solely use the interpretation of the AOcCs as a performance measure, and
538 we advocate for its use instead of these metrics. They allow clear and intuitive interpretation of how
539 models are ranking suitability cells, and how well that defines a truly suitable environment as it finds
540 occurrences. The original intended use of AUC and TSS statistics (and most other metrics) is to define
541 how different from random a model is, not the quality of the model, especially not at each step of the
542 model. The P/E plots and Boyce index (Hirzel et al. 2006, Di Cola et al. 2017) were a first step a
543 tackling the performance of a model across different sections of suitability outputs. We argue that
544 Jiménez & Soberón's AOcCs are the next step in the interpretation of models built using pseudo-
545 absences, for they are simple, straightforward and flexible, yet accurate and powerful.

546 5.0 - Conclusions

547 The main conclusions drawn from this study are: i) that MERRAclim models are the most dissimilar
548 to BioClim and ENVIREM; ii) M size should be tested during model design in accordance to the
549 intended model use; iii) RF and MARS algorithms are very sensible to spatial clustering and overfit

550 models and their use should be constrained to endemic or locally restricted species; iv) GLM,
 551 GLMNet and MaxLike overpredict models regardless of predictors or geographic region; v) AUC and
 552 TSS do not inform on model performance, and AOcCs should be used to evaluate presence-only or
 553 presence-background models instead.

554 The main limitations of our study are firstly that we only had presence data for the species.
 555 Secondly, that our design did not allow us to isolate what factors drove RF and MARS to overfit
 556 models. We propose that future work should build on Jiménez & Soberón's (2020) AOcC use
 557 combined with Morales-Barbero & Vega-Álvarez's (2018) Consistency Maps, and that their
 558 combined use, along with testing different M sizes *a priori* should become standard in ecological
 559 niche modeling.

560 **Acknowledgements**

561 We would like to thank the curators and technicians from the institutions that supplied the occurrence
 562 records, who even without access to their respective collections in 2020 and 2021 due to the covid-19
 563 pandemic still managed to retrieve the data in the short windows of time they had there. We gathered
 564 occurrence data from Proyecto Colombia BIO, California Academy of Sciences (CAS), Centro de
 565 Biodiversidade da UFMG (CCT/UFMG), Coleção de Invertebrados PPBIO MPEG, Coleção
 566 Entomologica da UFPE (CEUFPE), Coleção Entomologica dos Campos Gerais do Parana (CECGP),
 567 Coleção Entomologica Pe. Jesus Santiago Moure (MZUFPR), Coleção Zoologica de Artropodes
 568 terrestres da UFMT, Coleção Zoologica de Referencia da UFMS (ZUFMS), Colección de Artropodos
 569 del Museo de Historia Natural de la Pontificia Universidad Javeriana (PUJ), Colección de Artropodos
 570 del PNN Gorgona - Museo de Entomología de la Universidad del Valle (MUSENUV), Colección de
 571 Entomologia del Instituto de Ciencias Naturales (ICN-MHN-Em), Colección de Ictiologia
 572 Universidade de Quindío (IUQ), Colección de Insectos de la Universidade del Quindío (CIUQ),
 573 Colección Zoologica Universidad del Tolima – Arácnidos (CZUT), Senckenberg Museum –
 574 Collection Arachnology (SMF), Collection of Forest Zoology and Entomology from the University of
 575 Freiburg, Denver Museum of Nature & Science, Field Museum Chicago, Instituto Nacional de
 576 Pesquisas da Amazonia (INPA), Museo La Salle (MLS), Museu de Biologia da Universidade Federal
 577 da Paraíba (MZUFPB), Museu de Ciências Naturais da Fundacao Zoobotanica do Rio Grande do Sul
 578 (MCNRS), Museu de História Natural Capão da Imbuia / Colecao de Invertebrados Nao-Insetos
 579 (MHNCI), Museu de História Natural da Universidade Estadual de Campinas (ZUEC), Museu de
 580 Zoologia da Universidade Federal da Bahia (MZUFBA), Museu de Zoologia João Moojen
 581 (MZUFV), Museu de Zoologia de São Paulo (MZSP), Museu Nacional do Rio de Janeiro (MNRJ-
 582 ARAC), Museu Paraense Emilio Goeldi (MPEG), Museum of Comparative Zoology at Harvard
 583 University (MCZ), Pontificia Universidade Católica do Rio Grande do Sul (PUCRS), The British
 584 Museum of Natural History (BMNH), Frankfurt Museum, Stuttgart Rosenbaum Museum, American
 585 Museum of Natural History (AMNH). This study was financed by CAPES (Coordenação de
 586 Aperfeiçoamento de Pessoal de Nivel Superior) in process 88887.480942/2020-00 and by the Federal
 587 University of Mato Grosso do Sul.
 588

Chapter 2

1 **Abstract**

2 In this work, ecological niche models for nine species of the South American whip-spider
3 *Heterophrynus* (Phrynidae) are built, present in most of the northern half of the continent. We project
4 models on present-day climate, and on two end-of-century SSP scenarios, and assess protection area
5 overlap based on the suitability maps from projections. In building our models, we test three M sizes
6 and eight algorithms for each species *a priori*, and select the best performing ones to build the final
7 models, based on the Accumulation of Occurrences Curve. This analysis resonates with the last
8 chapter in indicating that RF and MARS overfit models. Our results show that Indigenous Land or
9 Territories cover overall the same area as Integral Protection (IUCN Categories Ia, Ib and II) areas.
10 We show that while some species have up to three quarters of their predicted suitable area inside
11 Protected Areas, others have less than 10% of their suitable area protected. Moreover, even for
12 species with high coverage of suitable area protection, only a small fraction of this protection falls
13 within Indigenous Land or Integral Protection areas.

14 **Resumo**

15 Neste trabalho, modelos de nicho ecológico para nove espécies do amblipígeo sul-americano
16 *Heterophrynus* (Phrynidae) são construídos, que ocorre na maior parte da porção norte do continente.
17 Projetamos os modelos para o clima presente, e para dois cenários SSP ao fim do século, e avaliamos
18 a sobreposição de áreas de proteção com as projeções dos mapas de adequabilidade climática. Ao
19 construir nossos modelos, nós testamos três tamanhos de M e nove algoritmos para cada espécie *a*
20 *priori*, e selecionamos os que performaram melhor para construir os modelos finais, com base na
21 Curva de Acumulação de Ocorrências. Esta análise ressoa com o último capítulo ao mostrar que os
22 algoritmos RF e MARS sobreajustam os modelos. Nossos resultados mostram que Terras Indígenas
23 cobrem no geral a mesma área que Áreas de Proteção Integral (Categorias IUCN Ia, Ib e II).
24 Demonstramos que enquanto algumas espécies têm até três quartos da sua área adequada dentro de
25 Áreas de Proteção, outras têm menos de 10% desta área protegida. Além disso, mesmo para as
26 espécies com maior cobertura de Áreas de Proteção, apenas uma pequena fração desta proteção é
27 dentro de Terras Indígenas ou Áreas de Proteção Integral.

28 1.0 – Introduction

29 The climate is changing due to human release of greenhouse gases in the atmosphere, and the weather
30 patterns that have mostly held for the last ten millennia are rapidly changing. The latest version of the
31 Coupled Model Intercomparison Project (Phase 6, CMIP6) suggests considerable disruption in both
32 precipitation and temperatures patterns over South America, according to ensembled Global Climate
33 Models (GCMs, Almazroui et al. 2021). The models indicate that under any given Shared
34 Socioeconomic Pathway (SSP, Riahi et al. 2017) scenario, current annual precipitation and
35 temperature patterns will change, though to a different degree in different regions of the continent
36 (Almazroui et al. 2021). Mean annual South American temperature is suggested to increase by a
37 minimum of 1.7°C in a best case scenario under SSP1-2.6 by the end of the century, up to over 5°C in
38 a worst case scenario under SSP5-8.5. The strongest warming across all future scenarios is over the
39 Amazon. Precipitation changes however, stay mostly within baseline (i.e. present-day) variability and
40 only start becoming greater than it in the late century under SSP3-7.0 and SSP5-8.5 scenarios,
41 showing significant decrease in central-southern Chile, parts of the Amazon and the central tropical
42 belt (Almazroui et al. 2021).

43 The Amazon biome notoriously hosts a great portion of the world's biodiversity (WWF 2016).
44 It also hosts circa 47 GtC (gigatons of carbon) in Brazil alone (Nepstad et al. 2009). Area-based
45 conservation measures are by far the larger portion of conservation efforts in the region, although
46 others stand out (see Tollefson 2015). Of these areas, Indigenous Land or Territories (hereafter ITs),
47 which cover approximately 25% of the biome (RAISG 2019), contribute far more to Reducing
48 Emissions from Deforestation and Degradation (REDD) than other types of nature reserves (Ricklefs
49 et al. 2010). This is relevant because Amazon deforestation rates have been increasing over the last
50 few years (Silva Junior et al. 2021). Indeed, ITs are not only an effective measure to curb
51 deforestation, it has also been estimated that these areas host most of the world's Intact Forest
52 Landscapes (Fa et al. 2020), having been actively shaped and managed by Indigenous Peoples over
53 millennia (Barlow et al. 2012), and still presenting ecological intactness (Schleicher et al. 2017, Prada
54 & Xavante 2021, Sanabria & Achuri 2021).

55 Our purpose in this study was to assess how relevant are current ITs for a given taxon
56 preservation under different SSP scenarios through the use Ecological Niche Models (ENMs). Given
57 the uneven and disproportionate impacts of Climate Change over South America, with special
58 concerns lying over the Amazon regarding rising temperature and decreasing precipitation, and over
59 North-Western South America regarding decreasing precipitation anomalies (Almazroui et al. 2021),
60 we selected a taxon that spans both of these areas. The whip-spider genus *Heterophrynus* was once
61 deemed to be restricted to the Amazon (Weygoldt 2000), but recent work have shown the genus to be
62 present from the north and west of Colombia to the south of Pantanal, in Brazil, to the western edge
63 of the Amazon and even in refugia in the arid Brazilian Caatinga (de Armas et al. 2015, Carvalho et
64 al. 2011, Cordeiro et al. 2014, García et al. 2015, Viquez et al. 2014).

65 In this study, we use ENMs to build habitat suitability maps for nine species of the South
66 American whip-spider genus *Heterophrynus* for present-day and two future emission scenarios
67 (SSP2-4.5 and SSP5-8.5) for the 2081-2100 period. We also analyze the species' suitability areas
68 intersection with the World Database on Protected Areas (WDPA, UNEP-WCMC & IUCN 2017). We
69 further quantify how much of this area falls under IUCN types Ia, Ib and II Protected Areas (hereafter
70 IPs, for Integral Protection) and under currently recognized ITs from the same dataset.

71 **2.0 – Methods**

72 *2.1 – Species data*

73 We used the same dataset with the same acquisition and record cleaning as Chapter 1 (see page 9 for
74 more details). Species kept in the study after occurrence data cleaning and filtering are: *H. alces* (21
75 occurrence records), *H. armiger* (20), *H. batesii* (117), *H. boterorum* (34), *H. cervinus* (17), *H.*
76 *cheiracanthus* (23), *H. elaphus* (28), *H. longicornis* (238) and *H. vesanicus* (35).

77 We purposefully decided to not include records, distributions or suitable area in detail in the
78 text in fear of poachers using our work for the Pet Trade in North America, Europe and Asia, as whip-
79 spiders are commonly found in the invertebrate black market. These results will only be shared with
80 South American researchers directly to hopefully guide field expeditions, such as the one that resulted
81 in the discovery of two new *Heterophrynus* species in 2011 (Giupponi & Kury 2013).

82 *2.2 – Climate Data*

83 We acquired the 19 bioclimatic variables from WorldClim v2.1 (Fick & Hijmans 2017) to construct
84 the model for the present-day projections, and the same bioclimatic variables for the 2070 period
85 under two emission CMIP6 scenarios under the MIROC6 GCM for future projections. The first
86 scenario, **SSP2-4.5**, reflects the impacts of warming if societies rapidly reduce emissions, but fail to
87 mitigate fast enough to limit warming to below 2°C. The second scenario, **SSP5-8.5**, marks the upper
88 edge of the SSP scenario spectrum with a high reference scenario in a high fossil-fuel development
89 world throughout the 21st century. All layers were obtained in a standardized 5 arc min resolution
90 (~10km), under the WGS84 geographic projection, from <www.worldclim.org>. Variables retained
91 after considering the species' biology and checking for collinearity (Table S2) were Bio2, Bio3, Bio5
92 and Bio15 (mean diurnal range temperature, isothermality, max temperature of the warmest month
93 and precipitation seasonality, respectively).

94 *2.3 – Protected Areas Dataset*

95 For assessing the species' placement under protected areas, we obtained the World Database on
96 Protected Areas (WDPA 2021) and measured the area in km² that overlaps with the predicted species
97 climatic suitability on the three climatic scenarios. For this, we subsetted the WDPA dataset in three
98 based on the IUCN categories of protected areas (Dudley 2008). First, we retained the entire WDPA
99 dataset (hereafter **PA-Full**). Second, we selected a dataset that only contains the strictest categories of
100 protected areas, IUCN Ia, Ib and II (hereafter **PA-Integral**). And third, we isolated one dataset
101 containing the territories marked as Indigenous Land or Territory, a type of protected area strictly
102 reserved for indigenous peoples living in traditional lifestyles, which are not categorized in IUCN
103 standards (hereafter **PA-Indigenous**).

104 2.4 – *M selection*

105 We used the same M selection method and criteria as in Chapter 1 (see page 12 for more details).

106 To select an M size, we then analyzed the performance of algorithms under each M size (see
107 below), to see if M size increased algorithm performance. We further analyzed model outputs to
108 distinguish under and over-fitted models. The last step in selecting M consisted in analyzing if the
109 output maps represented a well-defined suitable area, as opposed to an incomplete suitable area.

110 2.5 – *Algorithm selection*

111 As there is no single best algorithm to be chosen *a priori* for ecological niche modelling, eight
112 algorithms (GLM, SVM, RF, BRT, MARS, MaxEnt, MaxLike and GLMNet) commonly used in
113 ENMs were tested in the same manner as **M** using the `accum.occ` function in Jiménez & Soberón
114 (2020). This method of using the Accumulation Tables and corresponding Accumulation of
115 Occurrences Curves are hereafter referred to as **AOcT** and **AOcC**, respectively.

116 To avoid using under- or overfitting algorithms, we selected the two algorithms to reach a
117 target (the smallest number of cells that retains ~90% of records, hereafter **AocC-target**; Jiménez &
118 Soberón 2020) in the smallest number of cells. For this reason, MARS and RF models were discarded
119 (overfit), as well as GLM, MaxLike and GLMNet (underfit). Algorithms retained and used in
120 ensembling for each species are summarized in Table 2. Ensemble was built by the PA (presence-
121 absence) method, that uses the mean of predicted presence-absence values (predicted probability of
122 occurrences are first converted to presence-absence using a threshold, then they are averaged),
123 available in the ensemble function in the R-package `sdm` (Naimi & Araujo 2021), which was used in
124 default settings.

125 2.6 – *Software, Code and Data*

126 All analyses and steps were performed in R version 4.0.4, except the spatial overlap analysis and
127 some maps' post-processing for aesthetics, both done in QGIS version 3.16.9-Hannover. A script for
128 the steps in creating and analyzing *H. alces* models is provided in <github.com/jfberner/ENMs> as a
129 sample, as the same process was repeated for each species. The occurrence dataset is intentionally not
130 provided in this paper due to the interest of poachers in the animals for the pet trade in the northern
131 hemisphere (particularly the U.S., E.U and Asia). Interested researchers can contact the authors for the
132 data for research purposes.

133 *Table 4: Retained M and respective buffer sizes, and retained algorithms*

Species	<i>H. alces</i>	<i>H. armiger</i>	<i>H. batesii</i>	<i>H. boterorum</i>	<i>H. cervinus</i>	<i>H. cheiracanthus</i>	<i>H. elaphus</i>	<i>H. longicornis</i>	<i>H. vesanicus</i>
M size	SM	LM	SM	SM	SM	SM	SM	SM	SM
Buffer Size – Number of cells	50km - 9576 cells	200km - 8470 cells	400km - 127395 cells	200km - 4800 cells	200km - 10920 cells	200km - 15036 cells	200km - 27745 cells	200km - 123624 cells	200km - 27495 cells
1st Algorithm	BRT	MaxEnt	BRT	BRT	SVM	BRT	BRT	BRT	SVM
2nd Algorithm	MaxEnt	BRT	MaxEnt	MaxEnt	BRT	SVM	SVM	SVM	BRT

134

135 *2.7 – Model Workflow*

136 With each species' predictors cropped at their different M sizes, background (n=200) data was
 137 generated, and we constructed the three models for each species, with 10 bootstrap replications for
 138 each. The best deemed M sizes (further explained below) and their respective two best performing
 139 algorithms were retained.

140 Then, another model was built from retained algorithms and M size with 100 bootstrap
 141 replications for each algorithm, which were then ensembled by the previously mentioned PA-method.
 142 Models were then projected back into geographic space in the three climatic scenarios (Present, SSP2-
 143 4.5 and SSP5-8.5 for 2070 period) using the same variables used in model construction, and turned
 144 into presence/absence maps by applying a standardized 0.4 threshold. The presence/absence maps
 145 were then projected with the three protected areas datasets (PA-full, PA-integral and PA-indigenous),
 146 and the area of overlap was analyzed. This entire process is summarized in Fig. 16.

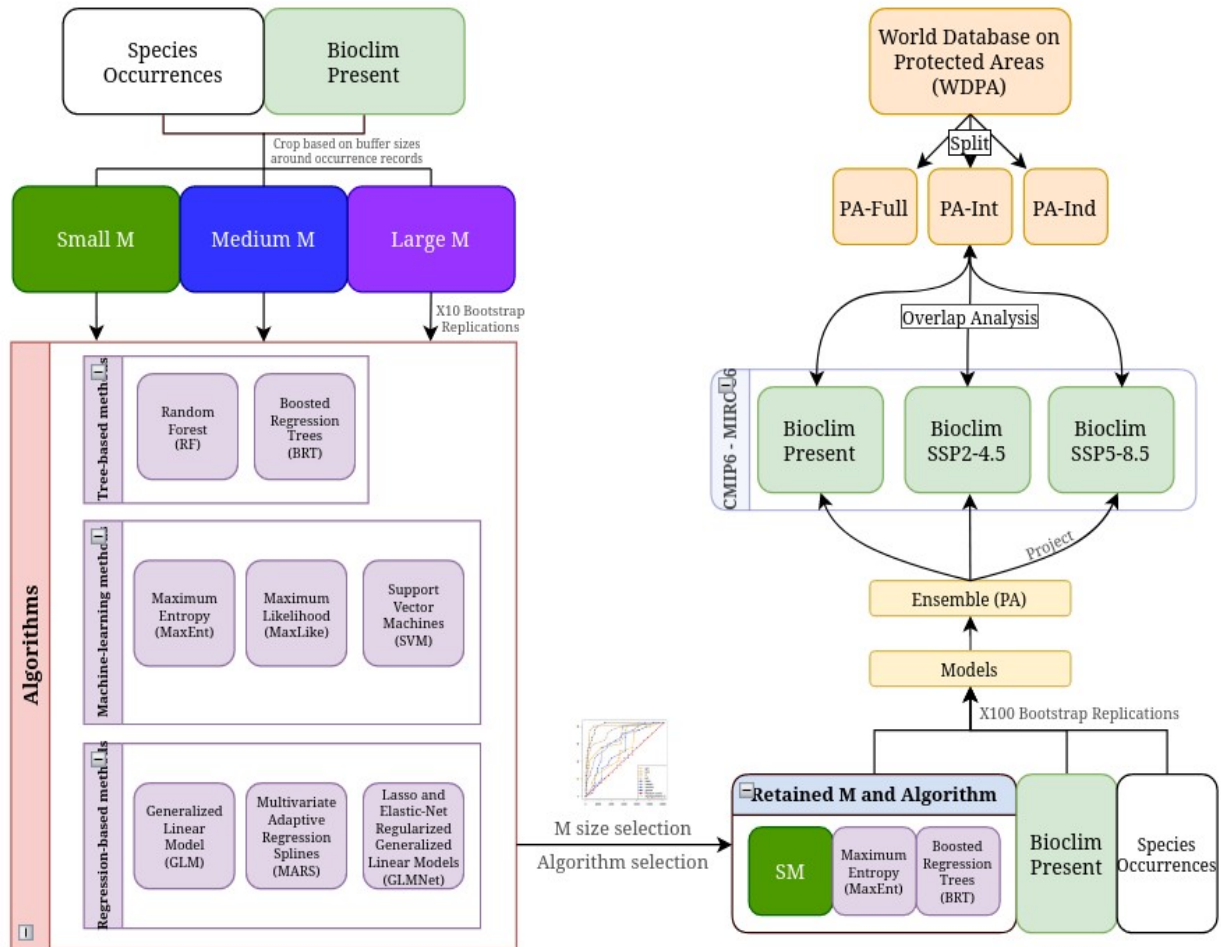


Fig. 16: Model Workflow

147 3.0 – Results

148 3.1 – Model Results

149 Species' target for model evaluation, and results of algorithm performance (number of cells at
 150 AoOc-target) are presented in Table S1. Algorithms and M sizes retained for each species are
 151 summarized in Table 4. The accumulation of occurrences curve for each model and algorithm is
 152 presented in Fig. 17.

153 All algorithms performed better than random, at all M sizes, and we kept the smallest M for
 154 all species with one exception. We selected LM for *H. armiger*, as SM and MM left out a contiguous
 155 suitable area of the Colombian coast where there are no clear geographical barriers. Total protection
 156 area and protection percentage under the three climatic scenarios, for each protected areas dataset and
 157 for each species is presented in Table 5.

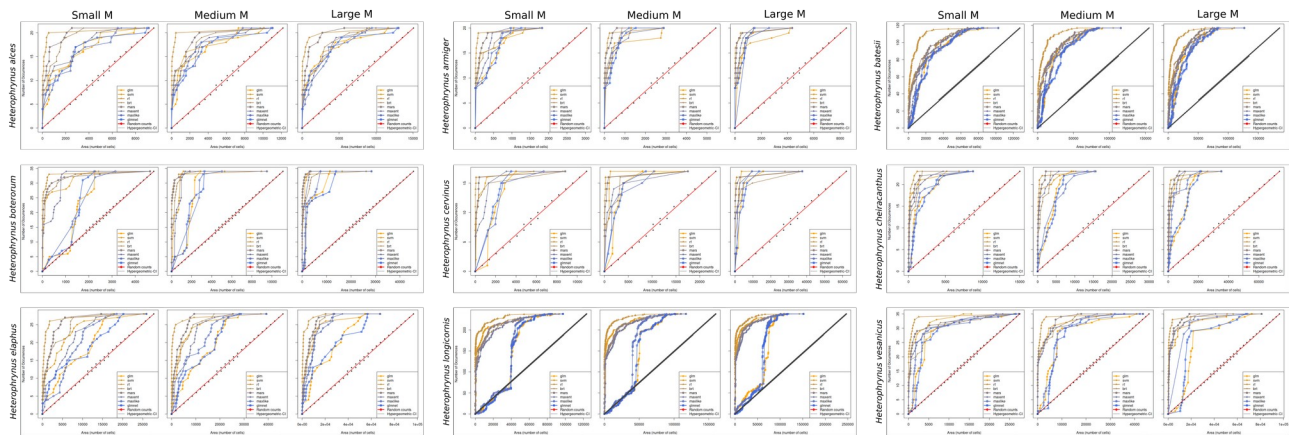


Fig. 17: AOCs for the first round of models (10 bootstrap replications), with all tested algorithms. These Figures are the same as the BioClim columns in Figs. S1 A-J.

158 Our projections show that suitable area will increase in size for some species under both of the
 159 tested SSP scenarios. Namely: *H. alces* (doubling suitable area under SSP2-4.5 and increasing it by
 160 148% under SSP5-8.5), *H. armiger* (+28% under SSP2-4.5 and +35% under SSP5-8.5) and *H. batesii*
 161 (+28% under SSP2-4.5 and +33% under SSP5-8.5). For other species however, projections show a
 162 dramatic decrease in suitable area: *H. boterorum* (-34% under SSP2-4.5 and -13% under SSP5-8.5),
 163 *H. cervinus* (-43% under SSP2-4.5 and -66% under SSP5-8.5), *H. cheiracanthus* (-41% under SSP2-
 164 4.5 and -65% under SSP5-8.5), *H. longicornis* (-72% under SSP2-4.5 and -94% under SSP5-8.5) and
 165 *H. vesanicus* (-10% under both scenarios). One of the nine species, *H. elaphus*, showed mixed results
 166 in the projections (-0.81% area under SSP2-4.5 and +35% under SSP5-8.5).

167 It is worth noting that our approach to ensembling models by presence/absence has its
 168 downside. We chose this method of ensembling for we deem it to be one of the most straightforward
 169 ways to do so. Ensembling worked perfectly well for some species where model outputs presented
 170 similar outputs (e.g. *H. batesii* on Fig. 22 or *H. armiger* on Fig. 18).

171 For other species however, most notably *H. longicornis*, the selected algorithms had highly
 172 dissimilar outputs and the P/A ensembling method resulted in a minimal, scattered distribution (Fig.
 173 33). This also happened to some extent to *H. cervinus* and *H. cheiracanthus* ensembled models (Figs.
 174 25 and 29 respectively). Both *H. longicornis* and *H. cheiracanthus* occur in the Amazon Basin, and *H.*
 175 *cervinus* occurs in the Western portion of the Andean Valleys in Ecuador and Colombia, with some
 176 occurrences down the far Eastern Amazon. These two regions have relatively few weather stations
 177 collecting data and BioClim, which uses this type of data to generate its layers, has known uncertainty
 178 and artifacts from interpolation in these areas (Fick & Hijmans 2017). This could be the reason
 179 algorithm outputs are so dissimilar, but it doesn't solely explain the dissimilarity as other species in
 180 this study occur in relatively close or even overlapping areas but did not present such problems.
 181 Whatever the reason, *H. longicornis* ensembled models are useless, and no conclusions can be made
 182 from them. Regardless, we present the results of model build and ensemble, and protected area
 183 datasets overlap for all species.

184 *Table 5: Predicted Ensembled Suitable Area in million hectares, and the corresponding*
 185 *overlap percentage with the three Protected Area Datasets.*

Species	Projection	Predicted Area (Mha)	PA-Full Overlap (Mha)	PA-Integral Overlap (Mha)	PA-Indigenous Overlap (Mha)
<i>H. alces</i>	Present	20.47	9.76 (47.68%)	1.10 (5.37%)	0.47 (2.30%)
	SSP2-45	40.85	19.98 (48.92%)	0.97 (2.37%)	1.47 (3.60%)
	SSP5-85	50.74	26.73 (52.68%)	1.85 (3.65%)	1.99 (3.92%)
<i>H. armiger</i>	Present	5.68	0.70 (12.26%)	0.01 (0.13%)	0.00
	SSP2-45	7.29	0.87 (11.99%)	0.02 (0.34%)	0.00
	SSP5-85	7.69	0.97 (12.56%)	0.05 (0.60%)	0.00
<i>H. batesii</i>	Present	278.92	138.15 (49.53%)	9.92 (3.56%)	14.1 (5.06%)
	SSP2-45	359.18	180.76 (50.33%)	12.43 (3.46%)	16.32 (4.54%)
	SSP5-85	372.67	200.53 (53.81%)	15.67 (4.20%)	16.8 (4.51%)
<i>H. boterorum</i>	Present	6.38	0.55 (8.57%)	0.09 (1.49%)	0.00
	SSP2-45	4.24	0.33 (7.70%)	0.07 (1.74%)	0.00
	SSP5-85	5.55	0.55 (9.98%)	0.18 (3.20%)	0.00
<i>H. cervinus</i>	Present	7.32	1.52 (20.74%)	0.26 (3.48%)	0.00
	SSP2-45	4.15	1.06 (25.55%)	0.15 (3.52%)	0.00
	SSP5-85	2.52	0.64 (25.56%)	0.26 (10.34%)	0.00
<i>H. cheiracanthus</i>	Present	10.00	6.85 (68.50%)	0.56 (5.60%)	0.00
	SSP2-45	5.89	4.47 (75.86%)	0.58 (9.87%)	0.00
	SSP5-85	3.49	2.69 (77.17%)	0.44 (12.65%)	0.00

Species	Projection	Predicted Area (Mha)	PA-Full Overlap (Mha)	PA-Integral Overlap (Mha)	PA-Indigenous Overlap (Mha)
<i>H. elaphus</i>	Present	36.61	11.88 (32.46%)	0.22 (0.60%)	0.00
<i>H. elaphus</i>	SSP2-45	36.31	9.37 (25.81%)	0.25 (0.70%)	0.01 (0.02%)
	SSP5-85	49.56	10.09 (20.36%)	0.53 (1.07%)	0.11 (0.22%)
<i>H. longicornis</i>	Present	96.48	51.21 (53.07%)	3.91 (4.05%)	4.82 (4.99%)
	SSP2-45	27.22	15.94 (58.55%)	0.60 (2.21%)	1.43 (5.25%)
	SSP5-85	5.58	2.22 (39.79%)	0.05 (0.86%)	0.32 (5.75%)
<i>H. vesanicus</i>	Present	31.72	4.03 (12.72%)	0.34 (1.07%)	0.09 (0.29%)
	SSP2-45	28.50	2.99 (10.47%)	0.29 (1.01%)	0.08 (0.28%)
	SSP5-85	28.58	3.76 (13.17%)	0.28 (0.99%)	0.08 (0.30%)

186 3.2 – *Heterophrynus alces* Pocock, 1902

187 The final *H. alces* model was constructed using an M built from a 50km radius around the
 188 occurrence records (amounting to 9576 cells), and BRT and MaxEnt algorithms were used in
 189 ensembling. Suitability projections are presented in Fig. 18. Ensembled P/A projections and their
 190 overlap with the PA-datasets are presented in Fig. 19.

191 Present day ensembled projections indicate a highly suitable climate close to the coast in
 192 French Guiana, Suriname and Guyana, as well as in the eastern half of the Brazilian state of Amapá.
 193 Ensembled projections under SSP2-4.5 scenario show a shrinking of suitable area where Present
 194 projections were appointed, specially along the coast of Suriname, but it also shows the appearance of
 195 a suitable climate corridor with the interior of the Amazon Basin through French Guiana and
 196 Suriname. SSP5-8.5 projections further expand this connection and the suitable area towards the
 197 interior of the continent, yet the suitable area close to the coast is further diminished. This indicates a
 198 shift in suitable climate conditions, that may or may not be followed by the species, as dispersal is
 199 limited and theorized only to occur by juvenile propagules as adults are, in theory, committed to their
 200 territories (Weygoldt 2000).

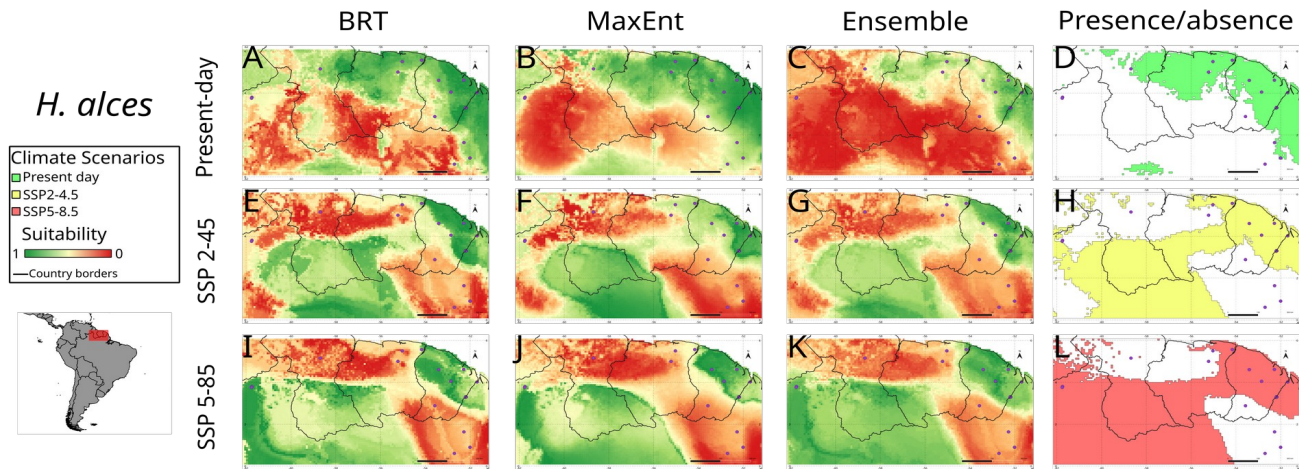


Fig. 18: *H. alces* model and ensemble outputs for the three climate scenarios. Purple dots represent occurrence records.

201 Despite having almost half of its projected suitable area inside Protected Areas, only a small
 202 part of it is under strict Protection (IUCN categories IA, IB and II). For this species, PA-Indigenous
 203 covers more area than PA-Integral under both SSP2-4.5 and SSP5-8.5, still collectively these two
 204 datasets cover less than 8% of predicted suitable area under any scenario. This means that despite
 205 having almost half its projected suitable area under protection (Fig. 19 F-I), most of it can still suffer
 206 from anthropogenic pressures over time.

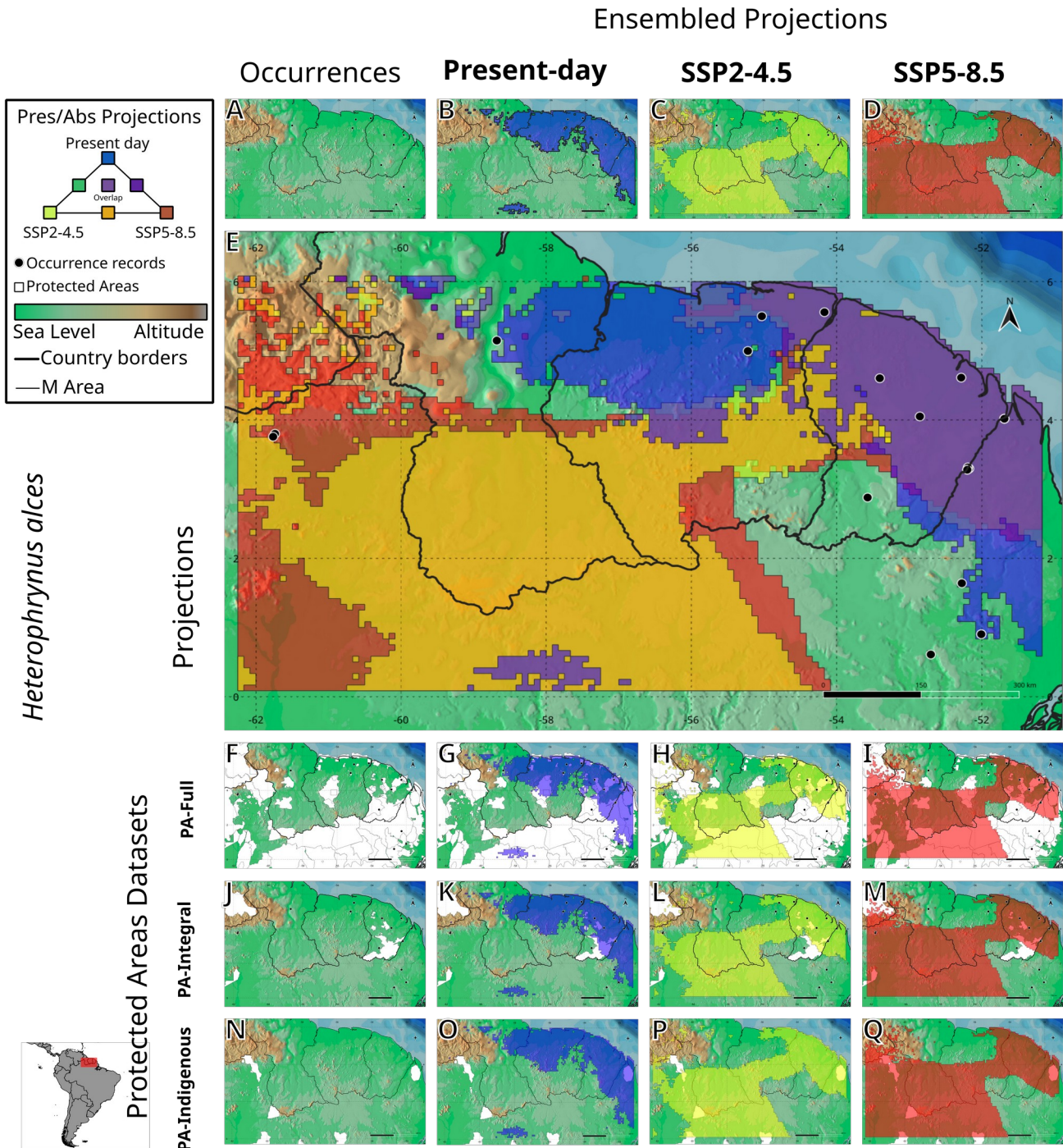


Fig. 19: *H. alces* Ensembled Presence/Absence maps for the three climatic scenarios and their overlap with the Protected Areas Datasets. **A:** occurrence records. **B:** present-day presence/absence ensembled projections. **C:** presence/absence ensembled projections under SSP2-4.5 scenario. **D:** presence/absence ensembled projections under SSP5-8.5 scenario. **E:** A-C overlaid in a single map. **F:** Full protected areas dataset overlaid with occurrence records. **G:** Full protected areas dataset overlaid with B. **H:** Full protected areas dataset overlaid with C. **I:** Full protected areas dataset overlaid with D. **J:** Integral Protection Areas dataset overlaid with occurrence records. **K:** Integral Protection Areas dataset overlaid with B. **L:** Integral Protection Areas dataset overlaid with C. **M:** Integral Protection Areas dataset overlaid with D. **N:** Indigenous Areas dataset overlaid with occurrence records. **O:** Indigenous Areas dataset overlaid with B. **P:** Indigenous Areas dataset overlaid with C. **Q:** Indigenous Areas dataset overlaid with D.

208 3.3 – *Heterophrynus armiger* Pocock, 1902

209 The final *H. armiger* model was constructed using an M built from a 200km radius around the
 210 occurrence records (amounting to 8470 cells), and BRT and MaxEnt algorithms were ensemble.
 211 Suitability projections are presented in Fig. 20. Ensembled P/A projections and their overlap with the
 212 PA-datasets are presented in Fig. 21.

213 Present day ensemble projections indicate climatic suitability for the species in west Ecuador,
 214 where it is currently found. Both other tested scenarios show a similar suitability map, suggesting that
 215 this regions' climate is expected to remain largely similar to present-day, even under high emission
 216 scenarios.

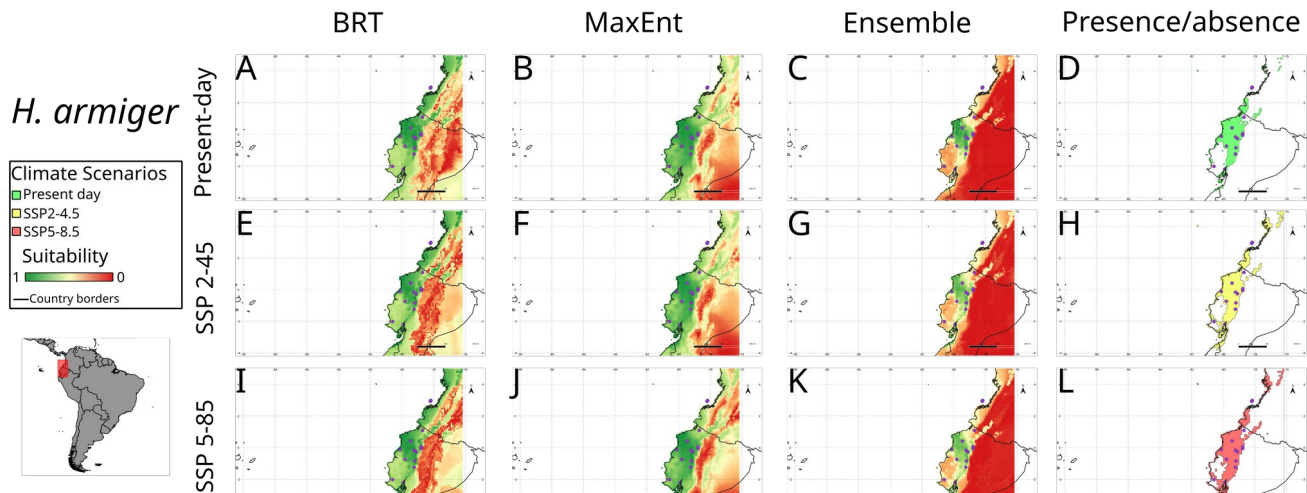


Fig. 20: *H. armiger* model and ensemble outputs for the three climate scenarios. Purple dots represent occurrence records.

217 This is the species with the least amount of suitable area falling under any type of Protected
 218 Area under Present Projections. Integral Protection areas under any climate scenario do not amount
 219 to one percent of suitable area. Fortunately, projections show that suitable area will not shift or shrink
 220 in G, so even though this species is not currently protected by Protection Areas, our projections
 221 indicate that climate change will not affect the species by a lot.

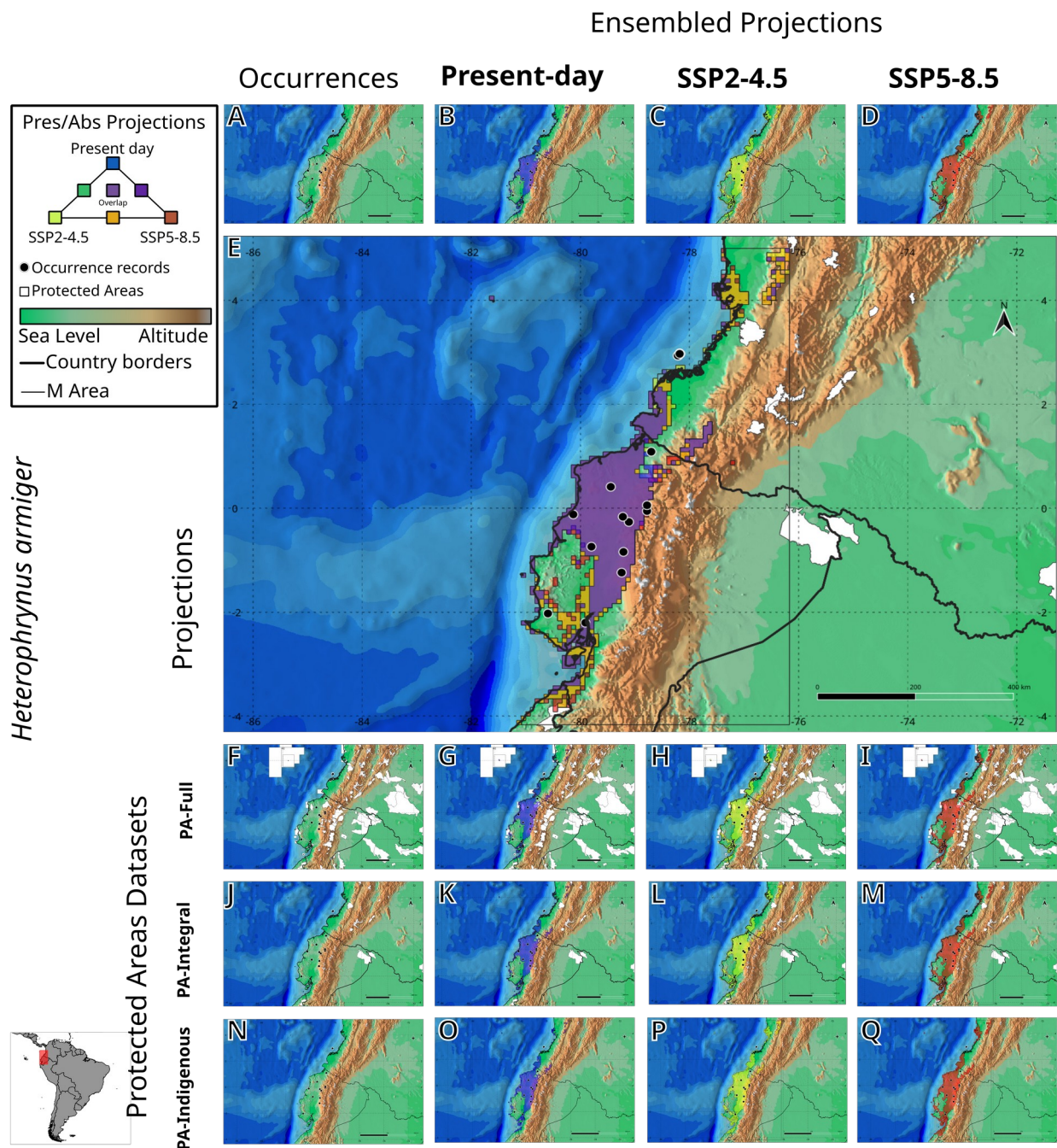


Fig. 21: *H. armiger* Ensembled Presence/Absence maps for the three climatic scenarios and their overlap with the Protected Areas Datasets. **A:** occurrence records. **B:** present-day presence/absence ensemble projections. **C:** presence/absence ensemble projections under SSP2-4.5 scenario. **D:** presence/absence ensemble projections under SSP5-8.5 scenario. **E:** A-C overlayed in a single map. **F:** Full protected areas dataset overlayed with occurrence records. **G:** Full protected areas dataset overlayed with B. **H:** Full protected areas dataset overlayed with C. **I:** Full protected areas dataset overlayed with D. **J:** Integral Protection Areas dataset overlayed with occurrence records. **K:** Integral Protection Areas dataset overlayed with B. **L:** Integral Protection Areas dataset overlayed with C. **M:** Integral Protection Areas dataset overlayed with D. **N:** Indigenous Areas dataset overlayed with occurrence records. **O:** Indigenous Areas dataset overlayed with B. **P:** Indigenous Areas dataset overlayed with C. **Q:** Indigenous Areas dataset overlayed with D.

223 3.4 – *Heterophrynus batesii* Butler, 1873

224 The final *H. batesii* model was constructed using an M built from a 400km radius around the
 225 occurrence records (amounting to 127,395 cells), and BRT and MaxEnt algorithms were used in
 226 ensembling. Suitability projections are presented in Fig. 22. Ensembled P/A projections and their
 227 overlap with the PA-datasets are presented in Fig. 23.

228 Present day ensembled projections (Figs. 22-D and 23-B) indicate climatic suitability in the
 229 central and western parts of the Amazon Basin, advancing well into the Northern Andes to the West,
 230 with suitable areas in most of Colombia. The projection also shows an unconnected suitable area
 231 where today *H. alces* is present in Guyana, Suriname and the French Guiana. Moreover, both SSP2-
 232 4.5 and SSP5-8.5 show the connection toward the coast through Suriname, same as the *H. alces*
 233 projections (Fig. 23 C-D). Moreover, the Northern tip of Bolivia seems to present a suitable climate
 234 that is present in both present-day and SSP2-4.5 scenarios, but the area is deemed unsuitable in the
 235 SSP5-8.5 scenario, and suitability remains only over the border with Brazil. Overall, the species'
 236 suitability maps highly agree on the three scenarios, suggesting that climate change could have little
 237 impact on the taxon. Of course there can be several sources of error in the models and this finding
 238 should be taken with a grain of salt.

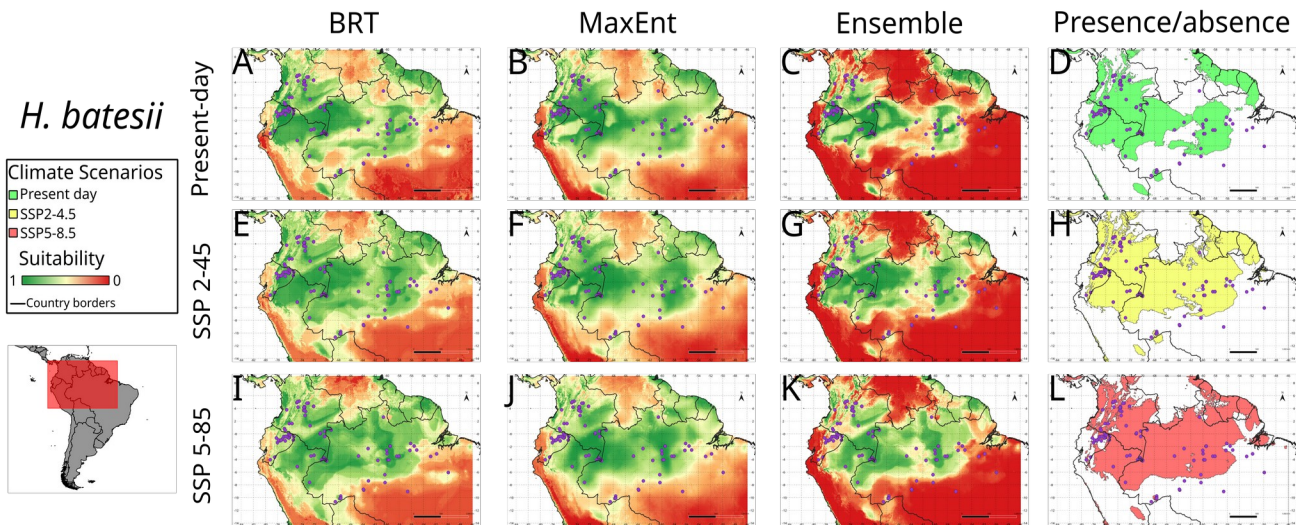


Fig. 22: *H. batesii* model and ensemble outputs for the three climate scenarios. Purple dots represent occurrence records.

239 Like *H. alces*, almost half of predicted suitable area lies within the PA-Full dataset in the three
 240 climatic scenarios. Also like *H. alces* however, PA-Integral only covers around 3.5-4% of the
 241 predicted suitable area, even less than PA-Indigenous which covers 4.5-5% of the area depending on
 242 the scenario. This means that in a high emission scenario (SSP5-8.5), indigenous land can help protect
 243 over a million hectares of suitable area more than current Integral Protection Areas.
 244

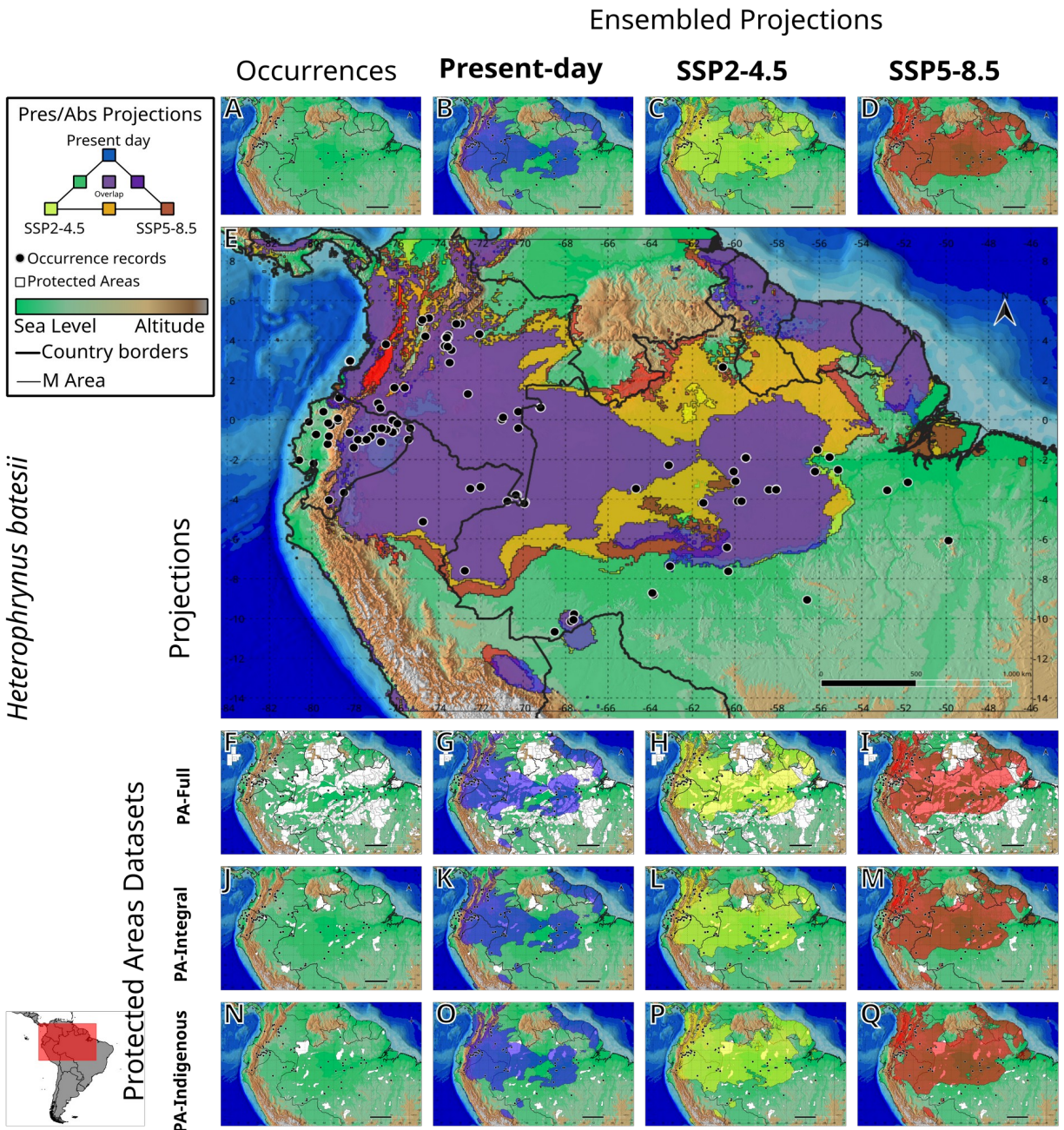


Fig. 23: *H. batesii* Ensembled Presence/Absence maps for the three climatic scenarios and their overlap with the Protected Areas Datasets. **A**: occurrence records. **B**: present-day presence/absence ensembled projections. **C**: presence/absence ensembled projections under SSP2-4.5 scenario. **D**: presence/absence ensembled projections under SSP5-8.5 scenario. **E**: A-C overlaid in a single map. **F**: Full protected areas dataset overlaid with occurrence records. **G**: Full protected areas dataset overlaid with B. **H**: Full protected areas dataset overlaid with C. **I**: Full protected areas dataset overlaid with D. **J**: Integral Protection Areas dataset overlaid with occurrence records. **K**: Integral Protection Areas dataset overlaid with B. **L**: Integral Protection Areas dataset overlaid with C. **M**: Integral Protection Areas dataset overlaid with D. **N**: Indigenous Areas dataset overlaid with occurrence records. **O**: Indigenous Areas dataset overlaid with B. **P**: Indigenous Areas dataset overlaid with C. **Q**: Indigenous Areas dataset overlaid with D.

246 3.5 – *Heterophrynus boterorum* Giupponi & Kury, 2013

247 The final *H. boterorum* model was constructed using an M built from a 200km radius around
 248 the occurrence records (amounting to 4800 cells), and BRT and MaxEnt algorithms were use in
 249 ensembling. Suitability projections are presented in Fig. 24. Ensembled P/A projections and their
 250 overlap with the PA-datasets are presented in Fig. 25.

251 Present day ensembled projections show suitability restricted to the Andean valleys of
 252 Colombia. Suitability largely remains the same under the SSP2-4.5 and SSP5-8.5 climate scenarios,
 253 with one notable exception in the Chaparral/Tuluni area, where the species is present today, and where
 254 suitability is lost under both emission scenarios. This is the southernmost population of the species,
 255 and it is isolated from other populations by large mountain chains on all sides. This means not only
 256 that the population in this area could be endangered, but also that genetic diversity may be at risk. The
 257 same suitability loss and observations apply to the population in Ibagué.

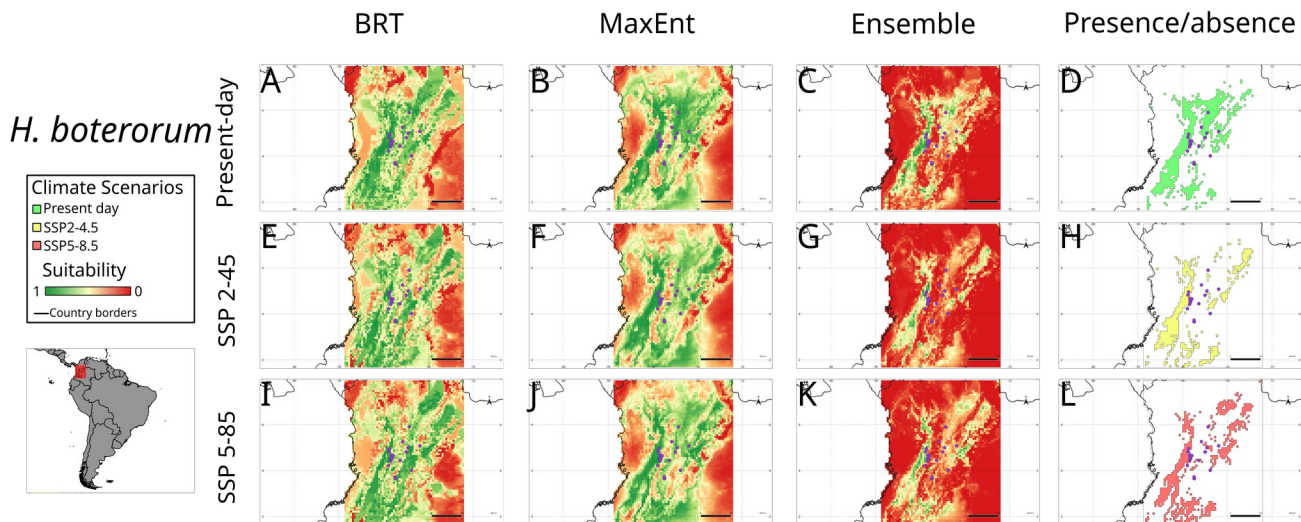


Fig. 24: *H. boterorum* model and ensemble outputs for the three climate scenarios. Purple dots represent occurrence records.

258 Merely 8.6% of present day predicted suitable areas lie within the PA-Full dataset. The high
 259 emission scenario SSP5-8.5 has a smaller suitable area than Present-day, but 10% of this area lies
 260 within PA-Full, a third of which is composed by Integral Protection Areas. The SSP2-4.5 scenario has
 261 both the smallest predicted suitable area and the smallest percentage of Protection Area coverage.
 262

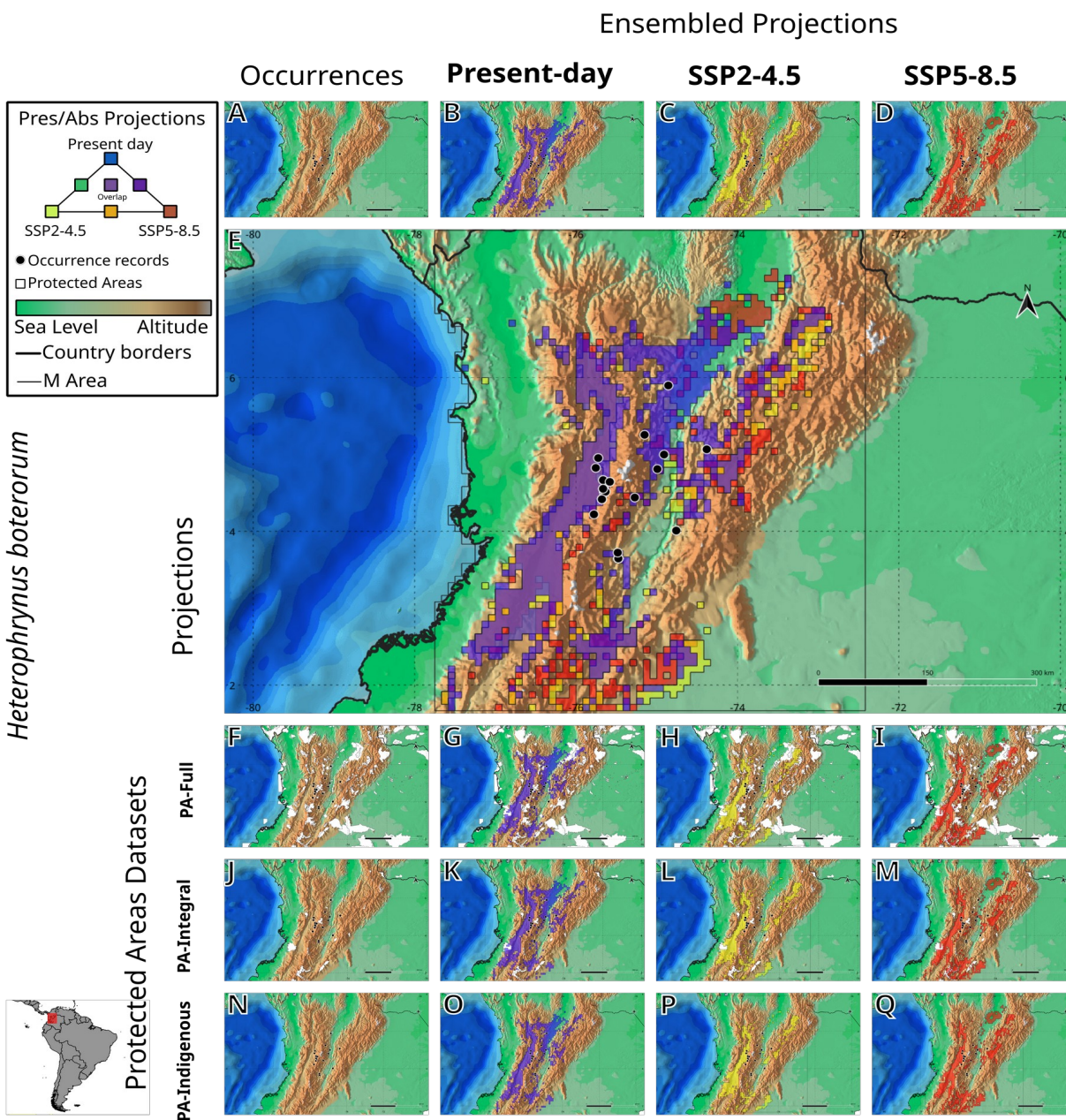


Fig. 25: *H. boterorum* Ensembled Presence/Absence maps for the three climatic scenarios and their overlap with the Protected Areas Datasets. **A:** occurrence records. **B:** present-day presence/absence ensembled projections. **C:** presence/absence ensembled projections under SSP2-4.5 scenario. **D:** presence/absence ensembled projections under SSP5-8.5 scenario. **E:** A-C overlaid in a single map. **F:** Full protected areas dataset overlaid with occurrence records. **G:** Full protected areas dataset overlaid with B. **H:** Full protected areas dataset overlaid with C. **I:** Full protected areas dataset overlaid with D. **J:** Integral Protection Areas dataset overlaid with B. **K:** Integral Protection Areas dataset overlaid with C. **L:** Integral Protection Areas dataset overlaid with D. **M:** Integral Protection Areas dataset overlaid with D. **N:** Indigenous Areas dataset overlaid with occurrence records. **O:** Indigenous Areas dataset overlaid with B. **P:** Indigenous Areas dataset overlaid with C. **Q:** Indigenous Areas dataset overlaid with D.

264 3.6 – *Heterophrynus cervinus* Pocock, 1894

265 The final *H. cervinus* model was constructed using an M built from a 200km radius around the
 266 occurrence records (amounting to 10920 cells), and BRT and SVM algorithms were used in
 267 ensembling. Suitability projections are presented in Fig. 26. Ensembled P/A projections and their
 268 overlap with the PA-datasets are presented in Fig. 27.

269 Present day ensembled projections show habitat suitability in Ecuador, mainly East of the
 270 mountains and into the Amazon Basin, as well as in Colombian valleys. Both SSP2-4.5 and SSP5-8.5
 271 show a retraction in suitable areas, with one exception in the area consisting of two Colombian
 272 National Parks, Parque Nacional Cueva de los Guacharos and Parque Nacional Natural de Puracé,
 273 where suitability remains somewhat stable. Other areas, especially East of the Andes in Ecuador,
 274 where most occurrence records are and which is the largest contiguous area predicted to be suitable in
 275 the present, largely lose suitability in both analyzed scenarios.

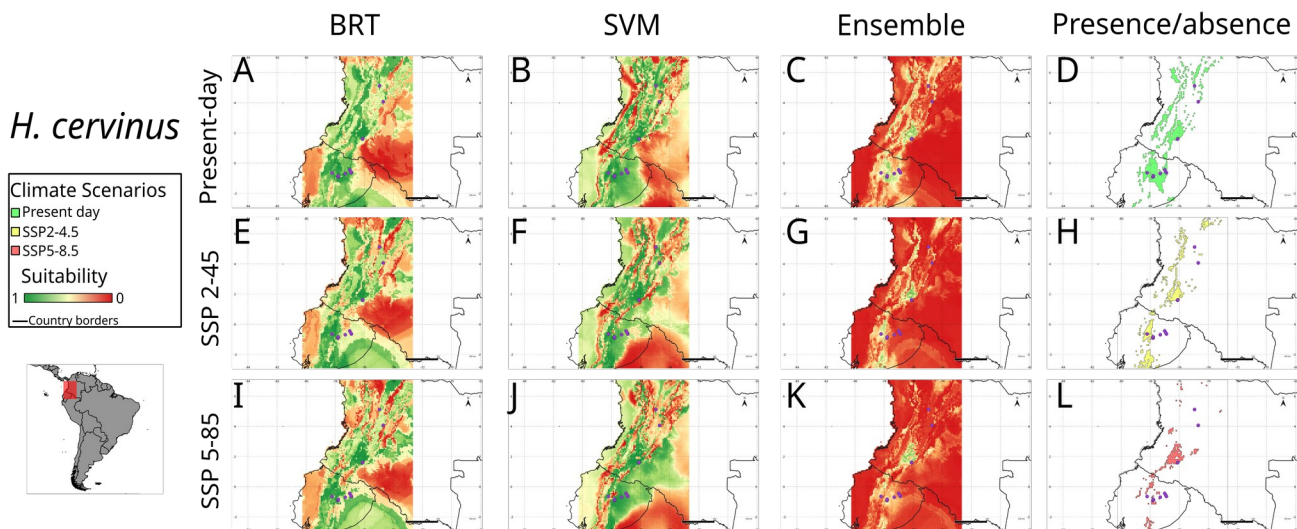


Fig. 26: *H. cervinus* model and ensemble outputs for the three climate scenarios. Purple dots represent occurrence records.

276 Present-day projection shows 20% of predicted suitable area being covered by PA-Full.
 277 Scenarios SSP2-4.5 and SSP5-8.5 project a little over half and a little under a third of original
 278 predicted suitable area, respectively. Both of these last two scenarios have a quarter of the area
 279 overlapping with PA-Full. Integral protection areas cover 3.5% of present and SSP2-4.5 projections,
 280 and 10% of SSP5-8.5 scenario. This percentage is deceptive however, as it does not mean that the
 281 species will be more protected in a high emission scenario: predicted suitable area overlap with PA-
 282 Integral under present day is 0.26 Mha, the same value as SSP5-8.5 scenario.

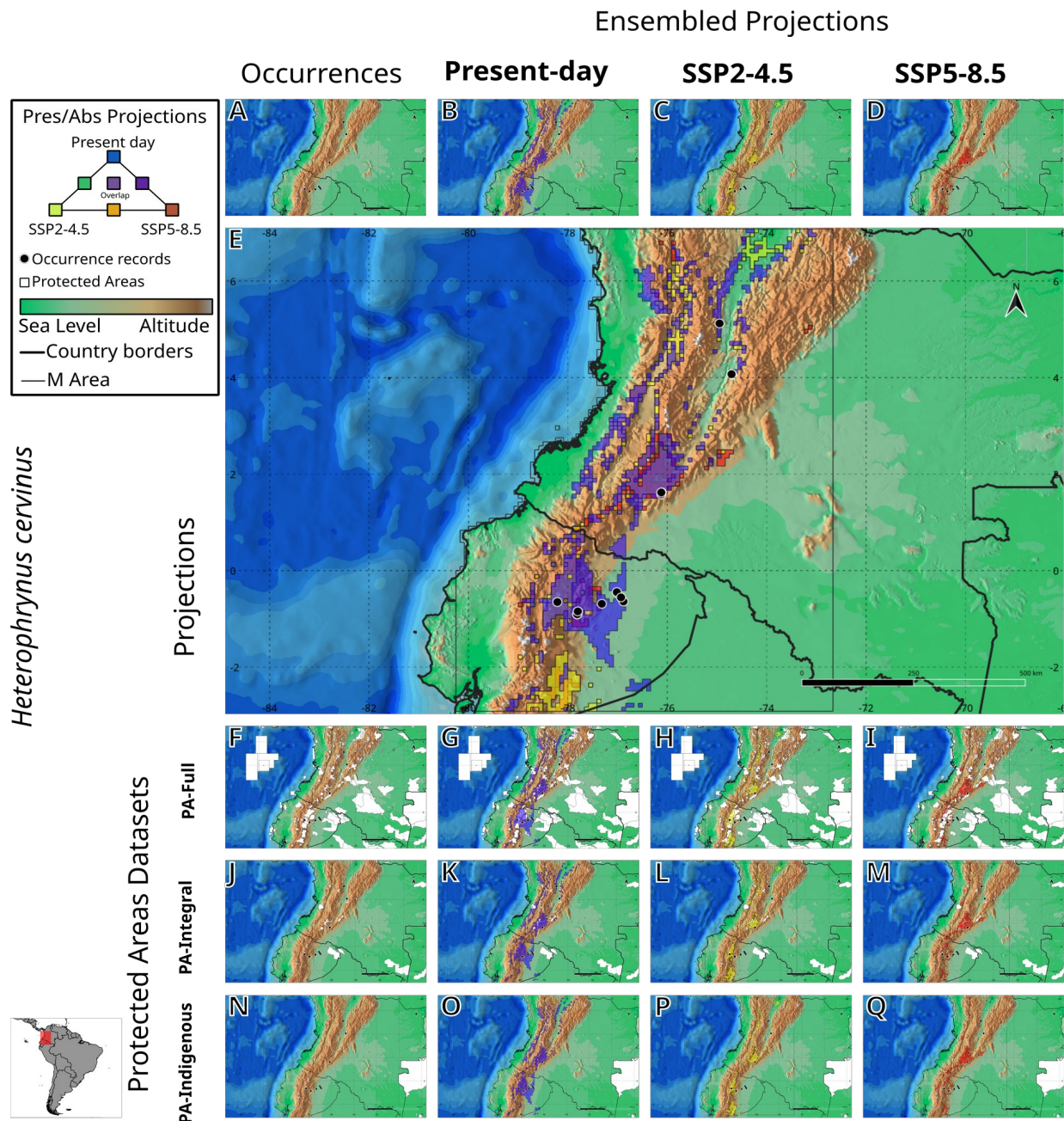


Fig. 27: *H. cervinus* Ensembled Presence/Absence maps for the three climatic scenarios and their overlap with the Protected Areas Datasets. **A**: occurrence records. **B**: present-day presence/absence ensembled projections. **C**: presence/absence ensembled projections under SSP2-4.5 scenario. **D**: presence/absence ensembled projections under SSP5-8.5 scenario. **E**: A-C overlaid in a single map. **F**: Full protected areas dataset overlaid with occurrence records. **G**: Full protected areas dataset overlaid with B. **H**: Full protected areas dataset overlaid with C. **I**: Full protected areas dataset overlaid with D. **J**: Integral Protection Areas dataset overlaid with occurrence records. **K**: Integral Protection Areas dataset overlaid with B. **L**: Integral Protection Areas dataset overlaid with C. **M**: Integral Protection Areas dataset overlaid with D. **N**: Indigenous Areas dataset overlaid with occurrence records. **O**: Indigenous Areas dataset overlaid with B. **P**: Indigenous Areas dataset overlaid with C. **Q**: Indigenous Areas dataset overlaid with D.

284 3.7 – *Heterophrynus cheiracanthus* Gervais, 1842

285 The final *H. cheiracanthus* model was constructed using an M built from a 200km radius
 286 around the occurrence records (amounting to 15036 cells), and BRT and SVM algorithms were used
 287 in ensembling. Suitability projections are presented in Fig. 28. Ensembled P/A projections and their
 288 overlap with the PA-datasets are presented in Fig. 29.

289 Present day ensembled projections show large, almost contiguous coastal areas as suitable for
 290 the species, mainly in Venezuela. Outside of Venezuela, some areas are deemed suitable in Guyana
 291 and Colombia. In Venezuela, a complex present-day scenario is found: habitat suitability follows the
 292 mountain chains from the West, up to the coastal hills around Valencia and Caracas, as well as the
 293 altitude areas East of Barcelona. The suitability map spans over several National Parks: Parque
 294 Nacional Juan Pablo Peñaloza, Parque Nacional Tapo-Caparo, Parque Nacional Sierra La Culata,
 295 Parque Nacional Tirgua, Parque Nacional Cerro Saroche, Parque Nacional Morrocoy, Parque
 296 Nacional Henri Pitter and Parque Nacional Guatopo. Suitable areas are also present in many of the
 297 islands off the coast of Venezuela, from Aruba to Barbados, where the species hasn't been recorded.
 298 SSP2-4.5 scenario shows an overall loss in suitable area, specially in the hills West of Barcelona and
 299 in the lower areas of Northern Venezuela, around El Congal. SSP5-8.5 scenario follows the same
 300 trend, and few areas remain under this scenario, mainly in the region around Caracas and in the
 301 western mountains in Sierra Nevada and Sierra La Culata National Parks.

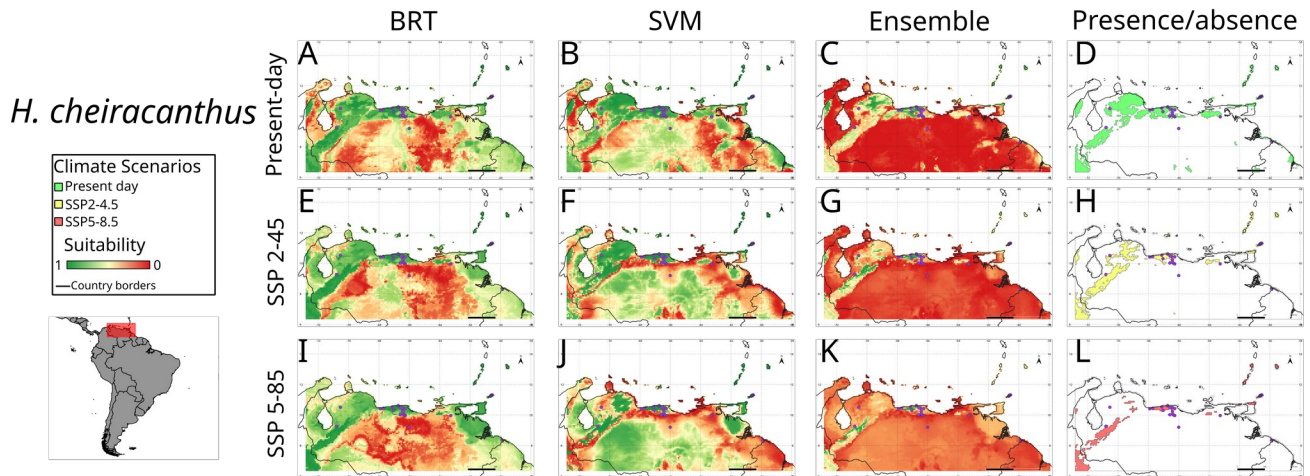


Fig. 28: *H. cheiracanthus* model and ensemble outputs for the three climate scenarios. Purple dots represent occurrence records.

302 The present-day ensembled projection shows 10 Mha of suitable area for the species, and
 303 much like *H. cervinus* this value shrinks by half under SSP2-4.5 scenario and by two thirds under the
 304 high emission scenario. This is the species with the highest percentage of present-day predicted
 305 suitable area under protection found in this study, as almost 70% of this area lies within PA-Full (Fig.
 306 29-G). Integral protection however lies around 0.5 Mha for the three climatic scenarios.

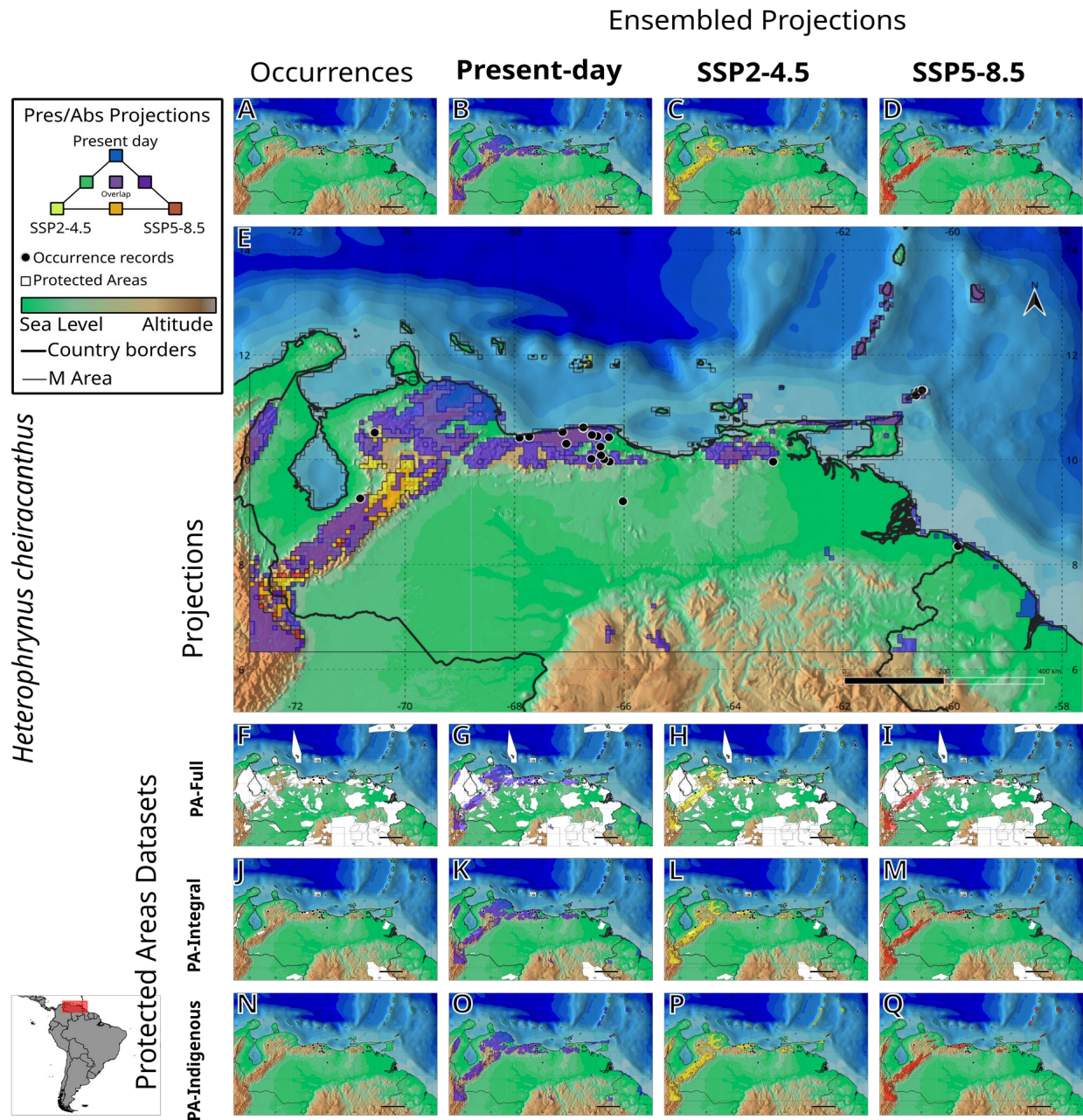


Fig. 29: *H. cheiracanthus* Ensembled Presence/Absence maps for the three climatic scenarios and their overlap with the Protected Areas Datasets. **A:** occurrence records. **B:** present-day presence/absence ensembled projections. **C:** presence/absence ensembled projections under SSP2-4.5 scenario. **D:** presence/absence ensembled projections under SSP5-8.5 scenario. **E:** A-C overlaid in a single map. **F:** Full protected areas dataset overlaid with occurrence records. **G:** Full protected areas dataset overlaid with B. **H:** Full protected areas dataset overlaid with C. **I:** Full protected areas dataset overlaid with D. **J:** Integral Protection Areas dataset overlaid with occurrence records. **K:** Integral Protection Areas dataset overlaid with B. **L:** Integral Protection Areas dataset overlaid with C. **M:** Integral Protection Areas dataset overlaid with D. **N:** Indigenous Areas dataset overlaid with occurrence records. **O:** Indigenous Areas dataset overlaid with B. **P:** Indigenous Areas dataset overlaid with C. **Q:** Indigenous Areas dataset overlaid with D.

308 *3.8 – Heterophrynus elaphus* Pocock, 1903

309 The final *H. elaphus* model was constructed using an M built from a 200km radius around the
 310 occurrence records (amounting to 27745 cells), and BRT and SVM algorithms were used in
 311 ensembling. Suitability projections are presented in Fig. 30. Ensembled P/A projections and their
 312 overlap with the PA-datasets are presented in Fig. 31.

313 Present day ensembled projections show suitable areas for the species in central Peru, East of
 314 the Andes, with suitability extending southward into Bolivia. SSP2-4.5 scenario shows a stable
 315 scenario in which suitability area is maintained, and SSP5-8.5 suggests an increase in suitable area for
 316 the species in all directions, possibly due to the high altitude areas in the Andean Mountains shifting
 317 towards a hotter and more humid climate.

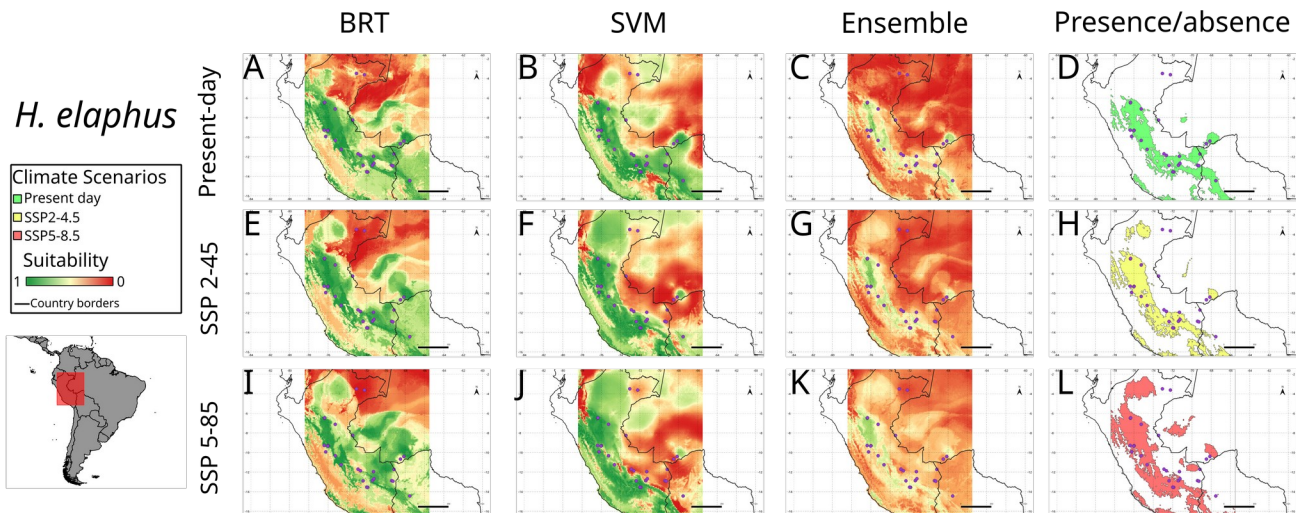


Fig. 30: *H. elaphus* model and ensemble outputs for the three climate scenarios. Purple dots represent occurrence records.

318 With the increase in suitable area follows an increase in suitable Integral-Protection area. The
 319 predicted suitable area overlap with the PA-Full dataset decreases however, most notably on Manu
 320 National Park, on Bahuaja – Sonene National Park and on Tambopata National Reserve, all areas
 321 where the species has been recorded and where our predictions show will lose suitability under both
 322 tested scenarios. The PA-Indigenous dataset contributes to little protection under any scenario.

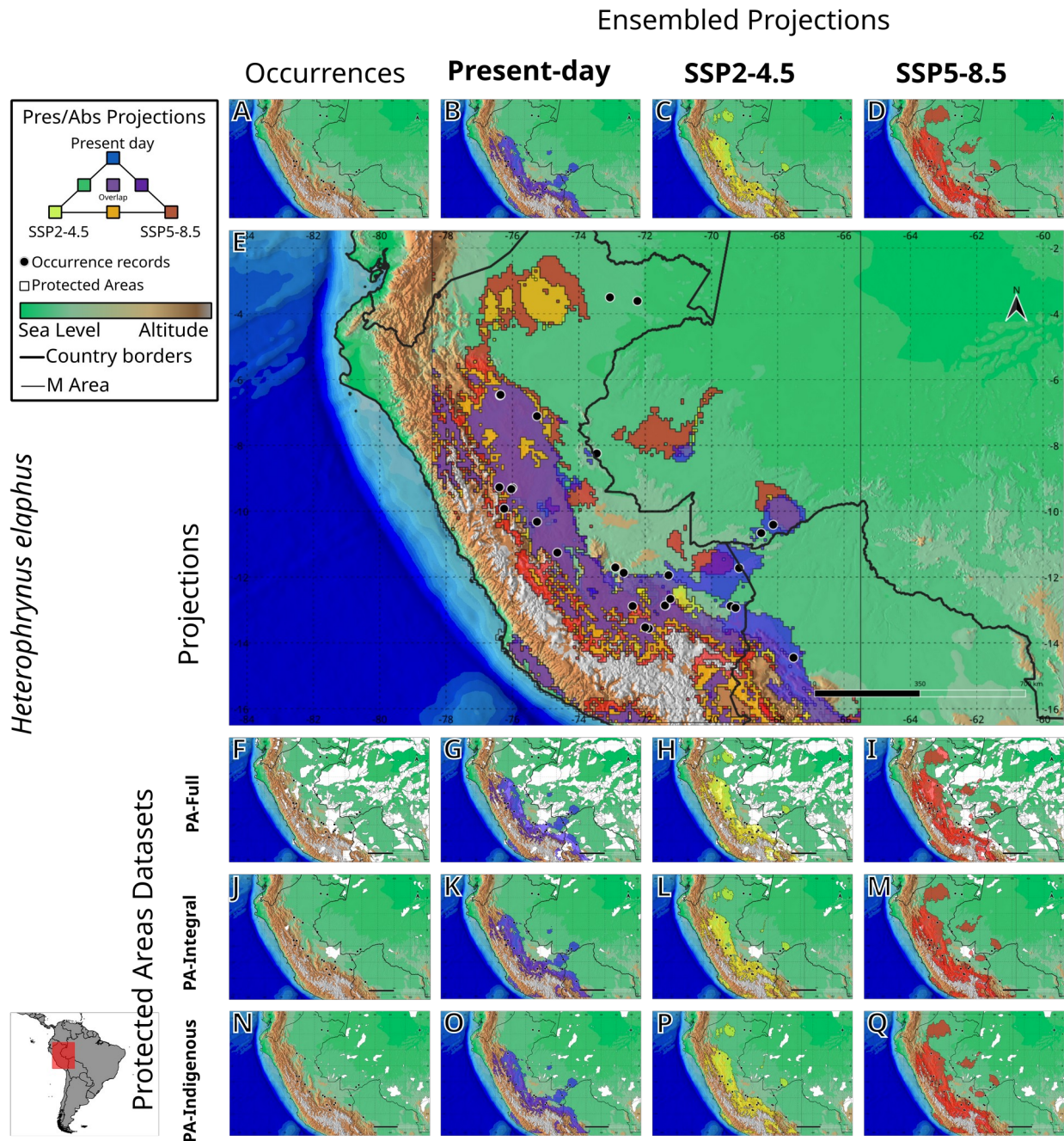


Fig. 31: *H. elaphus* Ensembled Presence/Absence maps for the three climatic scenarios and their overlap with the Protected Areas Datasets. **A:** occurrence records. **B:** present-day presence/absence ensembled projections. **C:** presence/absence ensembled projections under SSP2-4.5 scenario. **D:** presence/absence ensembled projections under SSP5-8.5 scenario. **E:** A-C overlaid in a single map. **F:** Full protected areas dataset overlaid with occurrence records. **G:** Full protected areas dataset overlaid with B. **H:** Full protected areas dataset overlaid with C. **I:** Full protected areas dataset overlaid with D. **J:** Integral Protection Areas dataset overlaid with occurrence records. **K:** Integral Protection Areas dataset overlaid with B. **L:** Integral Protection Areas dataset overlaid with C. **M:** Integral Protection Areas dataset overlaid with D. **N:** Indigenous Areas dataset overlaid with occurrence records. **O:** Indigenous Areas dataset overlaid with B. **P:** Indigenous Areas dataset overlaid with C. **Q:** Indigenous Areas dataset overlaid with D.

324 3.9 – *Heterophrynus longicornis* Butler 1873

325 The final *H. longicornis* model was constructed using an M built from a 200km radius around
 326 the occurrence records (amounting to 123624 cells), and BRT and SVM algorithms were used in
 327 ensembling. Suitability projections are presented in Fig. 32. Ensembled P/A projections and their
 328 overlap with the PA-datasets are presented in Fig. 33.

329 Present day ensembled projections show few regions being suitable for the species, mostly in
 330 the western part of the Amazon Rainforest even though it is highly sampled throughout the Amazon
 331 Basin, with records even in the Brazilian Cerrado and Caatinga Biomes. The last two are highly
 332 different from the Amazon Rainforest, the Cerrado being a tropical savanna and the Caatinga being a
 333 predominantly arid biome. *H. longicornis* occurs in these biomes in refugia, altitude marshes, caves
 334 and karstic areas, which can be a problem for models particularly at the broad scale we used
 335 (Carvalho et al. 2011). These populations are perhaps reminiscent of past distributions, when the
 336 Amazon and Atlantic Rainforests dominated most of what is now central and eastern Brazil (Sobral-
 337 Souza et al. 2015). As discussed before, the two algorithms used show many highly suitable areas in
 338 the central Amazon, but as the algorithms are divergent in predictions, the ensembled
 339 Presence/Absence maps do not represent many of such areas (Fig. 33 C, D and G).

340 The ensembled maps are biased and dictated by artifacts (Fig. 32 C, G and K), and their
 341 overlap with the PA datasets are uninformative. Both future climate scenario models retained almost
 342 no suitable area for the species (Fig. 32 H and L), amounting to virtually no overlap with Protected
 343 Areas (Fig. 33 H and I).

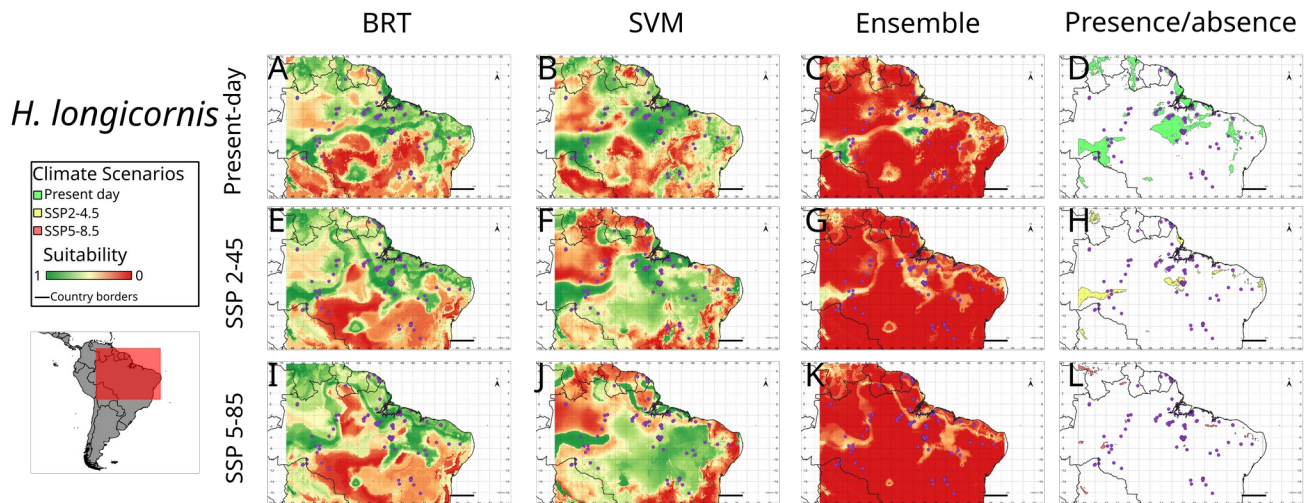


Fig. 32: *H. longicornis* model and ensemble outputs for the three climate scenarios. Purple dots represent occurrence records.

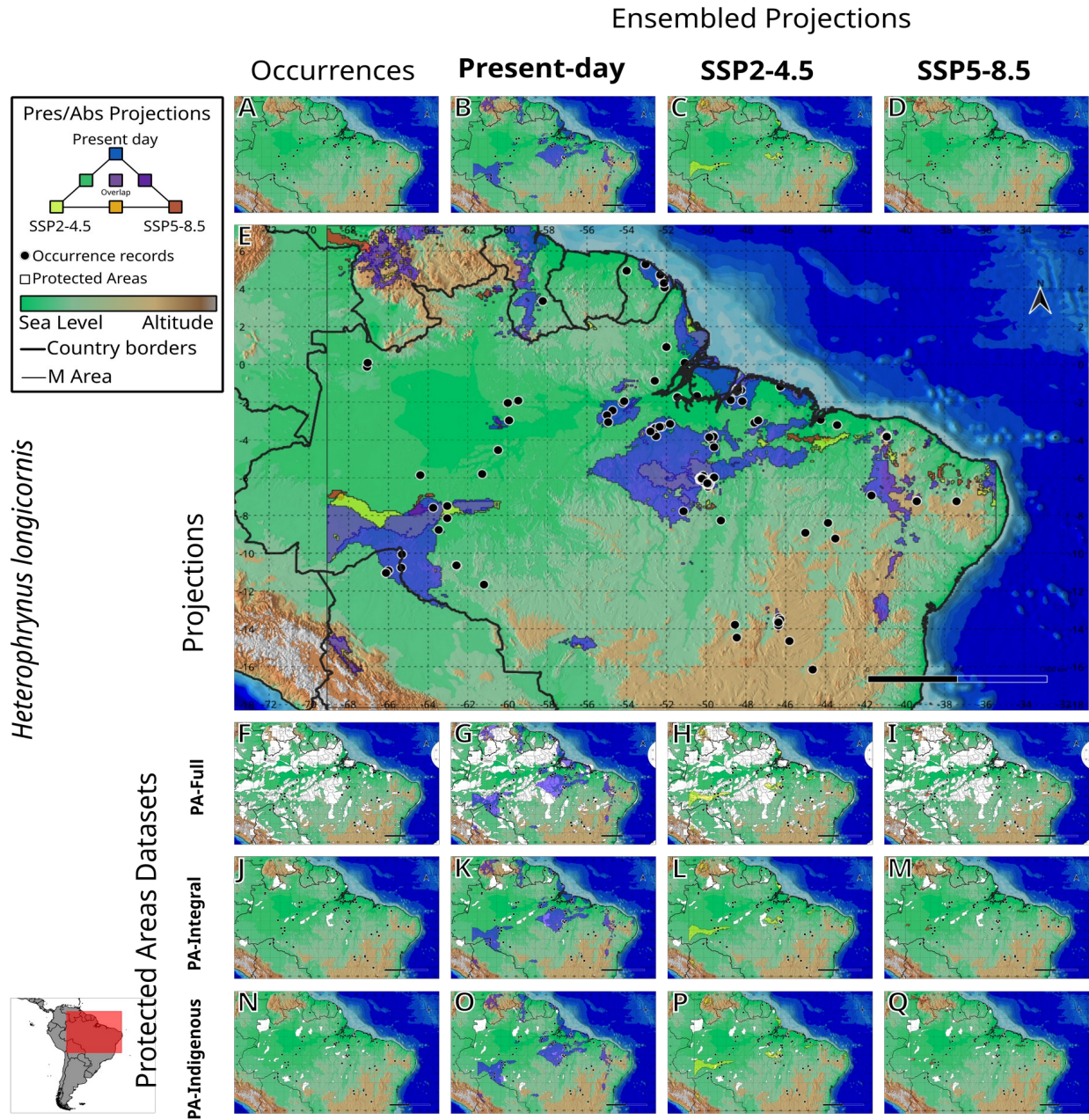


Fig. 33: *H. longicornis* Ensembled Presence/Absence maps for the three climatic scenarios and their overlap with the Protected Areas Datasets. **A:** occurrence records. **B:** present-day presence/absence ensembled projections. **C:** presence/absence ensembled projections under SSP2-4.5 scenario. **D:** presence/absence ensembled projections under SSP5-8.5 scenario. **E:** A-C overlaid in a single map. **F:** Full protected areas dataset overlaid with occurrence records. **G:** Full protected areas dataset overlaid with B. **H:** Full protected areas dataset overlaid with C. **I:** Full protected areas dataset overlaid with D. **J:** Integral Protection Areas dataset overlaid with occurrence records. **K:** Integral Protection Areas dataset overlaid with B. **L:** Integral Protection Areas dataset overlaid with C. **M:** Integral Protection Areas dataset overlaid with D. **N:** Indigenous Areas dataset overlaid with occurrence records. **O:** Indigenous Areas dataset overlaid with B. **P:** Indigenous Areas dataset overlaid with C. **Q:** Indigenous Areas dataset overlaid with D.

345 3.10 – *Heterophrynus vesanicus* Mello-Leitão 1931

346 The final *H. vesanicus* model was constructed using an M built from a 200km radius around
 347 the occurrence records (amounting to 27495 cells), and BRT and SVM algorithms were used in
 348 ensembling. Suitability projections are presented in Fig. 34. Ensembled P/A projections and their
 349 overlap with the PA-datasets are presented in Fig. 35.

350 Present day ensembled model projections show few suitable areas, but as in the last case it can
 351 be seen that both algorithms predicted highly suitable areas in the Brazilian Cerrado and even some
 352 connection to the Atlantic Rainforest to the East. However, there is a clear sampling bias here, as most
 353 of the species' records fall in the Serra da Bodoquena region (18 out of 35), a karstic area where the
 354 vegetation resembles more the Atlantic Rainforest than its surrounding Cerrado (Cardoso da Silva et
 355 al. 2004), and most of these records are from caves. Moreover, other records are placed in the
 356 highlands and plateaus that surround the Pantanal Wetland Basin, but the species hasn't been recorded
 357 in the Basin itself, and although the ensemble doesn't show it as being suitable, each algorithm
 358 predicts the region to be suitable in the present.

359 Future climate scenarios diverge significantly from one another, as BRT projections show a
 360 maintenance of suitability and even an increase in suitable area, and SVM shows an extremely
 361 different prediction where present day suitable area is almost entirely lost and there is a shift towards
 362 the East toward the Atlantic Rainforest and to the North towards the Cerrado and the Amazon. The
 363 only areas that both algorithms agree are presented in the ensemble map, that shows most of the
 364 Brazilian state of Mato Grosso do Sul as suitable in present day climate, Pantanal excluded. Both
 365 future climate ensemble projections show a loss of suitability in the karstic area of Serra da
 366 Bodoquena, presenting a shift in suitability towards the states of São Paulo to the East, and toward
 367 Paraná to the South, following present-day Atlantic Rainforest domains.

368 Like the former species, as algorithms projections diverge few suitable areas can be assessed
 369 in ensemble maps, but the areas that can be poorly protected, even under the scope of PA-Full.
 370 Integral Protection areas cover one percent of suitable area in all scenarios. Indigenous Areas cover
 371 less than third of a percent of predicted suitable area in all scenarios. Moreover, as the two algorithms
 372 show opposite suitability exactly where the species has been mostly sampled, we are not able to truly
 373 trust any of these conclusions.

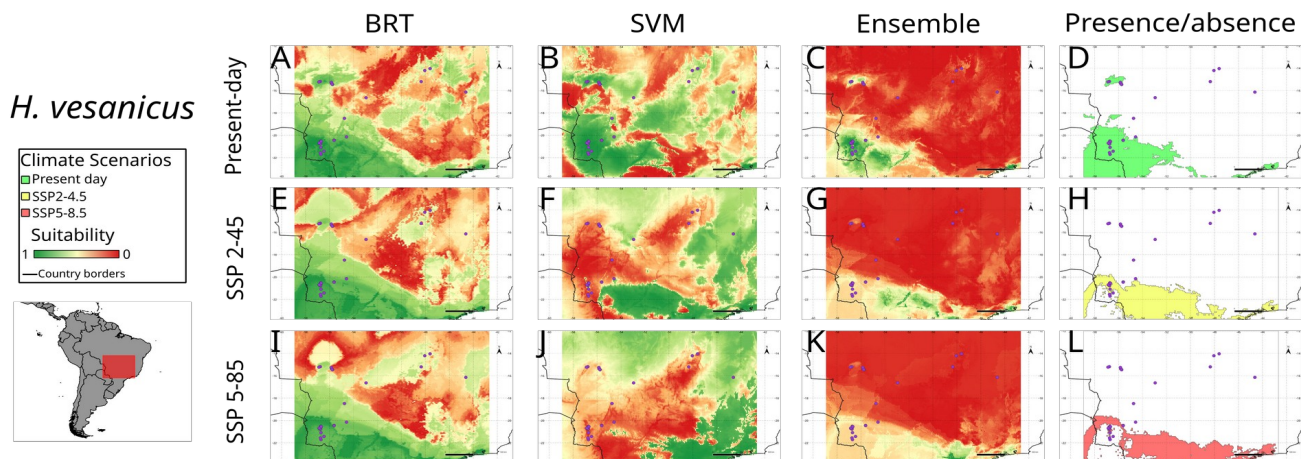


Fig. 34: *H. vesanicus* model and ensemble outputs for the three climate scenarios. Purple dots represent occurrence records.

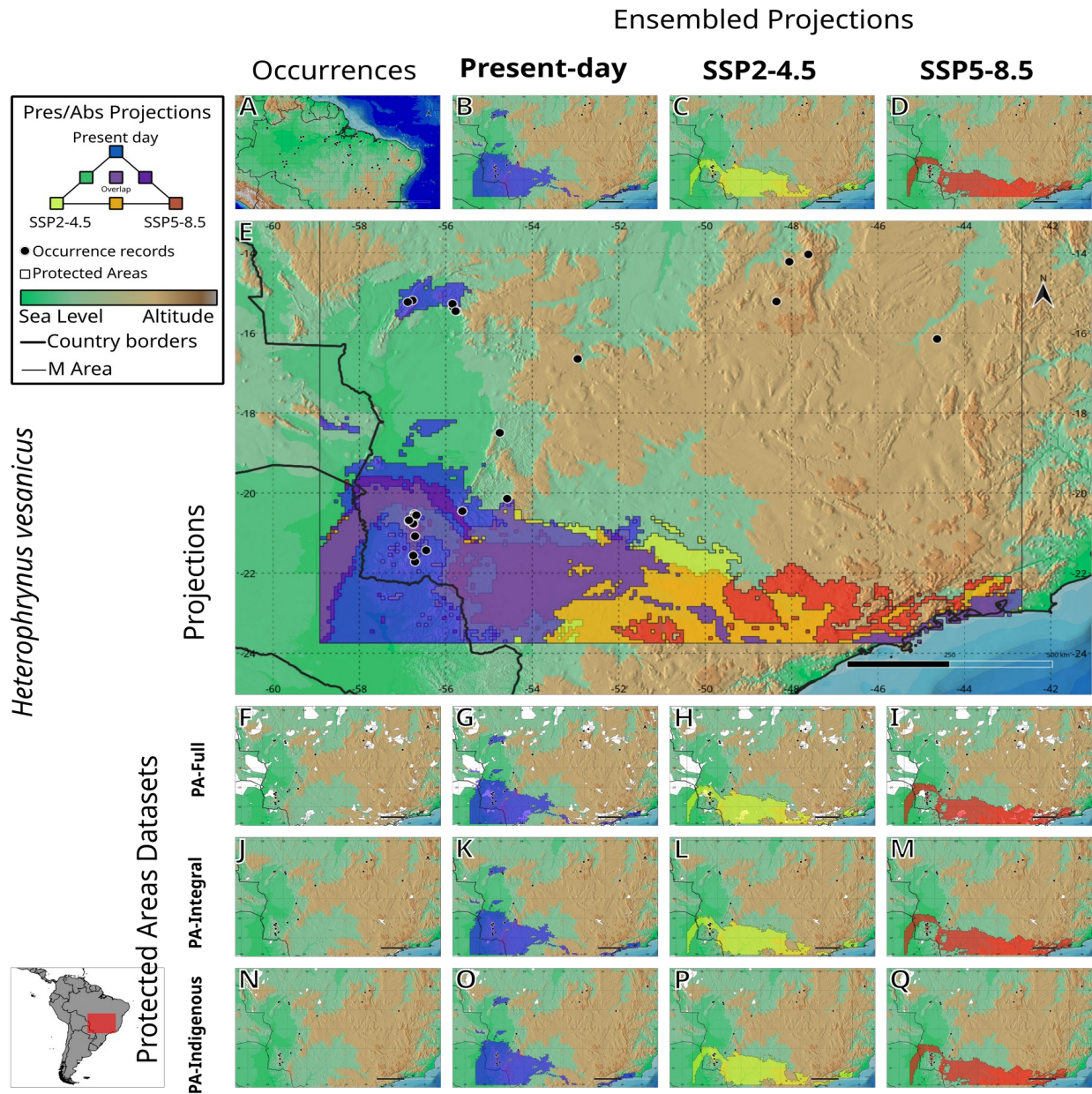


Fig. 35: H. vesanicus Ensembled Presence/Absence maps for the three climatic scenarios and their overlap with the Protected Areas Datasets. **A:** occurrence records. **B:** present-day presence/absence ensembled projections. **C:** presence/absence ensembled projections under SSP2-4.5 scenario. **D:** presence/absence ensembled projections under SSP5-8.5 scenario. **E:** A-C overlaid in a single map. **F:** Full protected areas dataset overlaid with occurrence records. **G:** Full protected areas dataset overlaid with B. **H:** Full protected areas dataset overlaid with C. **I:** Full protected areas dataset overlaid with D. **J:** Integral Protection Areas dataset overlaid with occurrence records. **K:** Integral Protection Areas dataset overlaid with B. **L:** Integral Protection Areas dataset overlaid with C. **M:** Integral Protection Areas dataset overlaid with D. **N:** Indigenous Areas dataset overlaid with occurrence records. **O:** Indigenous Areas dataset overlaid with B. **P:** Indigenous Areas dataset overlaid with C. **Q:** Indigenous Areas dataset overlaid with D.

375 In summary, our results show that some species will lose total suitable area, namely *H. boterorum*, *H.*
 376 *cervinus* and *H. cheiracanthus*, while others will have its suitable area increase under both future
 377 emission scenarios (*H. alces*, *H. armiger*, *H. batesii* and *H. elaphus*). For the remaining two species
 378 (*H. longicornis* and *H. vesanicus*) ensembled models were inconclusive mainly due to our ensembling
 379 approach. Roughly a third of all species' collective suitable area in this study fall within some kind of
 380 Protected Area under any of the tested climate scenarios, on average.

381 Moreover, from the PA-Full overlap analysis we verify that species *H. boterorum*, *H. cervinus*,
 382 *H. cheiracanthus* and *H. vesanicus* will lose suitability in Protected Areas, while *H. alces*, *H. armiger*,
 383 *H. batesii* and *H. elaphus* will have an increase in suitable area inside Protected Areas.

384 From the PA-Integral overlap perspective, our results indicate that species are to lose or gain
 385 suitable area depending on the climate scenario: *H. alces* and *H. boterorum* will lose suitable area
 386 inside Integral Protection areas under SSP2-4.5 scenario, but will gain it under the SSP5-8.5 scenario.
 387 The opposite is true for *H. cheiracanthus*, that will lose suitable area inside PA-Integral under an
 388 SSP5-8.5 scenario, but gain area under an SSP2-4.5 scenario. Species *H. cervinus* will lose suitable
 389 area inside PA-Integral under an SSP2-4.5 scenario, but the area will remain stable under an SSP5-8.5
 390 scenario. *H. vesanicus* will simply lose suitable area inside PA-Integral, and *H. elaphus* will have it
 391 increased, under any scenario.

392 Finally, from the PA-Indigenous overlap analysis only a few species' suitable areas fell inside
 393 the dataset. Species *H. alces*, *H. batesii* and *H. elaphus* will see an increase in suitable area inside
 394 Indigenous Land or Territory, and the opposite is true for *H. vesanicus*.

395 On an average of all eight species (*H. longicornis* disregarded), PA-Full overlaps with 31.55%
 396 of present-day suitable area, 32.07% of SSP2-4.5 suitable area and 33.16% of SSP5-8.5 suitable area.
 397 PA-Integral overlaps with merely 2.66% of present-day suitable area, 2.87% of SSP2-4.5 suitable area
 398 and 4.58% of SSP5-8.5 suitable area. For species that have its suitable area overlapping with PA-
 399 Indigenous (i.e. *H. alces*, *H. batesii*, *H. elaphus* and *H. vesanicus*), these areas cover on average
 400 2.54% of present-day suitable area, 2.81% of SSP2-4.5 suitable area and 2.90% of SSP5-8.5 suitable
 401 area. These figures suggest that on average, Indigenous Land or Territory cover roughly the same area
 402 as Integral Protection Areas for our tested species both in present-day projections and in an SSP2-4.5
 403 projections, but Integral Protection Areas seem to cover more relative area under an SSP5-8.5
 404 scenario. Currently, Indigenous Land and Territory accounts for more protection area as Integral
 405 Protection Areas (IUCN Categories Ia, Ib and II) only for *H. batesii*, and this will remain true under
 406 both of the tested SSP scenarios.

407 4.0 – Discussion

408 Our work provides another example of taxa for which ITs have a great potential in conserving
 409 diversity. Current demarcated ITs play as big as a role in the conservation of our studied whip-spider
 410 species as Integral Protection Areas under almost all tested climatic scenarios for almost all species.
 411 Moreover, being one of the least diverse arachnid groups, data on whip-spiders are usually scarce and
 412 there is almost no knowledge on these taxa's population size, biology, ecology, and their sensibility to
 413 neither anthropogenic nor climate-change related threats. As with most invertebrates, this lack of data
 414 translates into a complete vacuum of information regarding their protection status and their
 415 susceptibility to extinction under man-made threats, and conservation of these species is not typically
 416 tackled or mentioned in the literature.

417 There are currently only two whip-spider species listed in the IUCN Red List (IUCN 2021),
 418 neither from the whip-spider Family in this study. This is concerning because our models suggest that
 419 for at least one of the species (*H. cheiracanthus*), habitat suitability will decrease to a half or a third of
 420 present-day suitable area under an SSP2-4.5 or SSP5-8.5 scenarios respectively, and to the best of our
 421 knowledge there are no conservation efforts focused on whip-spiders in South America. Moreover,
 422 even though some species will even see an increase in suitable area under the tested scenarios (namely
 423 *H. alces*, *H. armiger*, *H. batesii* and *H. elaphus*), these suitable areas will only stay roughly in the
 424 same place as present-day suitable area for three of them (*H. armiger*, *H. batesii*, and *H. elaphus*). All
 425 other species will see a shrinking and/or shifting in present-day suitable area where these species
 426 currently occur.

427 Adding to the concern mentioned on the last paragraph, our models are based on climate only,
 428 and they are completely blind to habitat degradation, fragmentation and/or destruction, which is a
 429 major threat especially in the Amazon, that has seen increasing levels of deforestation in recent years
 430 (Silva et al. 2022, Deutsch & Fletcher 2022), and even indigenous peoples and their lands are
 431 themselves under current threat given the current Brazilian Administration's environmental policies
 432 (Atahyde et al. 2022). Moreover, this is yet another reason why ITs can play a major role in the
 433 conservation of whip-spiders, as deforestation is significantly smaller in these areas than in other
 434 types of PA (Nepstad et al. 2006, Begotti & Peres 2019), and intact forests are more common in ITs
 435 than anywhere else (Fa et al. 2020). Some studies have found that amazonian ITs can even retain a
 436 higher level of diversity than other PAs (Fernández-Llamarazes et al. 2021, Sanabria & Achuri 2021)
 437 in some cases, or at least the same level in others (Prada & Xavante 2021).

438 One unexpected pattern that arose in two independent models (*H. alces* and *H. batesii*) under
 439 both future scenarios is the appearance of a suitable area corridor through Guyana and Suriname
 440 towards the Brazilian states of Pará and Roraima. These findings are reminiscent to the work of
 441 Sobral-Souza et al. (2015), in which the authors modeled past connections between the Amazon and
 442 Atlantic Rainforests, where a similar corridor towards the coast appeared in the Last Glacial
 443 Maximum (LGM, ca. 21Kya). Their study classifies this area as suitable for both the Northern
 444 Atlantic Forest and the Western Amazon in that time period. Yet, one of the species only occurs North
 445 of the "corridor" (*H. alces*) while the other to the South and West of it (*H. batesii*), which makes the
 446 convergence in the models even more intriguing. Our models were not designed to further explore this
 447 pattern. Regardless, the area seems to be of an immense importance under future climate scenarios as
 448 it could become a bridge and/or harbor refugia for species which suitable area are shrinking both to
 449 the North and to the South. We also note that the area where the connection appears hosts relatively
 450 few Protected Areas when comparing to its surroundings in Northern Brazil and Venezuela (Fig. 24-
 451 F), none of which are of Integral Protection or an IT (Figs. 24-J and -N respectively). Moreover,
 452 *Heterophrynus* diversity seem to be greater in the Western Amazon, at least given the currently
 453 recognized species, which could be explained by the cradles-and-graves biogeographical hypothesis
 454 (Rangel et al. 2008), but our models were not designed to test whether this is the case.

455 Given that our models were truncated (i.e. they did not extrapolate suitability beyond the
 456 training range) we were surprised to find that our models show the suitability range for *H. batesii*
 457 increase, even in the highest carbon-fueled-development scenario (SSP5-8.5), in which the areas
 458 where the species occurs are supposed to be both hotter (2.8 to >5°C) and drier by the end of the
 459 century (Almazroui et al. 2021). One of the reasons for this could be the use of the single GCM
 460 MIROC6, which diverges from the mean of ensembled GCMs in all regions of South America
 461 (Almazroui et al. 2021).

462 5.0 – Conclusions

463 The little known and widespread genus *Heterophrynus* have been focus of small ecological and
464 taxonomic studies. This is the first time the group is treated in its entirety and this work provides
465 information that potentially will guide future collecting and conservation efforts. The first main result
466 of this work is the production of suitability maps for *Heterophrynus* species, a novelty for the Family.
467 These maps allowed us to compile possible trends in the distribution of the species, and will give
468 researchers a list of areas with the potential presence of new populations, and perhaps even new
469 species.

470 This work also presents further evidence of the current and future roles of ITs in preserving
471 biodiversity in South America. Presently recognized Protected Areas cover almost half of the Amazon,
472 and ITs nearly a quarter of it. However, IT networks in the Amazon have been demonstrated to be of
473 immense importance in flying mammal conservation (Fernández-Llamazares et al. 2021), even greater
474 than regular PAs. We think more evidence needs to be gathered on the importance of ITs for
475 biodiversity conservation, as Indigenous Peoples and ITs have been suffering increasing pressure,
476 invasions and outright attacks, and their protection has not been guaranteed because of socio-political
477 trends in South America over the last few years. We state that increasing the effective protection of
478 Indigenous Peoples from miners, loggers and agribusiness interests, and further implementing and
479 recognizing new ITs can be one of the most cost-effective conservation strategies at hand if the South
480 American developing countries are to uphold the Conservation Strategies of the Paris Agreement
481 (Garnett et al. 2018).

482 Finally, we list some limitations of our work we deem important and direct future research in
483 the area of ENM for possible solutions. First, the use of a single GCM as previously mentioned should
484 be avoided when possible (Almazroui et al. 2021), as well as the use of a single climatic dataset
485 (WorldClim; Morales-Barbero & Vega-Álvarez 2018). Second, many of the species had relatively few
486 occurrence records over wide areas (see Pearson et al. 2006 for steps in assessing small model
487 performance). Third, ensembling by the PA method has its downsides, but we chose this method over
488 weighted by any statistic as the most commonly used are AUC and TSS, and these statistics mean
489 little to nothing in presence-background or presence-absence models (Jiménez & Soberón 2020).
490 Fourth, the taxa we chose are known to occur in caves and other types of refugia, and we used cave
491 entrance coordinates in these cases, which is problematic at best in ecological niche modeling (see
492 Mammola et al. 2018 for steps that can be taken to minimize these problems). Fifth, more algorithms
493 could have been tested, especially ‘simpler’ ones as DOMAIN or BIOCLIM for reference (Konowalik
494 & Nosol 2021). Sixth and finally, a systematization of the tested M sizes would be desirable in any
495 future studies. It is worth mentioning that pends further investigation whether the WDPA dataset is
496 complete with all the ITs that the Rede Amazônica de Informação Socioambiental Georreferenciada
497 dataset (RAISG 2019) contains, which might be of better use in Amazonian areas.

498

1 **General Conclusion**

2 This study explored the feasibility and restraints in building ENMs for a terrestrial arthropod in South
3 America. We showed the limitations of BioClim especially in the Amazon Basin, as well as the
4 dissimilarity between its outputs and other climatic datasets. Our results suggest that RF and MARS
5 overfit models and GLM, GLMNet and MaxLike underfit models given tested settings, regardless of
6 the species, geographical context or model size. Moreover, our approach further demonstrates the
7 shortcomings of AUC and TSS statistics as an evaluation method of presence-absence and presence-
8 background ENMs. Our study also demonstrates that selecting M should be done by fitting a few
9 models *a priori* and selecting the desired size based on the intended purpose of model use (e.g. does
10 one need to exhaust all suitable area or are more localized patterns the focus).

11 We built, projected and ensembled models for *Heterophrynus* species under two end-of-century
12 SSP scenarios, from which we assessed suitable area overlap with Protected Areas. Our results show
13 that suitable area gain, loss, or shift varies widely between species, as well as protection area overlap.
14 We show that currently, most of the protection comes from IUCN categories III-VI areas, and that
15 Indigenous Land or Territories cover roughly the same suitable area as IUCN categories Ia, Ib and II
16 areas overall.

17 Future research should, therefore, apply new advances in ENM's algorithms and expand on this
18 study by adding more distribution points strengthening analysis. We also expect that our findings
19 guide decision makers in defining new conservation areas and increasing protection of existing ones.

Cited Literature

- 20 Ackerly, D. D. (2003). Community assembly, niche conservatism, and adaptive evolution in changing
 21 environments. *International Journal of Plant Sciences*, 164(S3), S165-S184.
- 22 Almazroui, M., Ashfaq, M., Islam, M. N., Rashid, I. U., Kamil, S., Abid, M. A., ... & Sylla, M. B.
 23 (2021). Assessment of CMIP6 performance and projected temperature and precipitation changes over
 24 South America. *Earth Systems and Environment*, 5(2), 155-183.
- 25 Araújo, M. B., Anderson, R. P., Márcia Barbosa, A., Beale, C. M., Dormann, C. F., Early, R., ... &
 26 Rahbek, C. (2019). Standards for distribution models in biodiversity assessments. *Science Advances*,
 27 5(1), eaat4858.
- 28 de Armas, L. F., Contreras, R. T., & García, D. M. A. (2015). Nueva especie de "*Heterophrynus*"
 29 (Amblypygi: Phrynidæ) del Caribe colombiano. *Revista Ibérica de Aracnología*, (26), 69-73.
- 30 Athayde, S., Fonseca, A., Araújo, S. M., Gallardo, A. L., Moretto, E. M., & Sánchez, L. E. (2022).
 31 The far-reaching dangers of rolling back environmental licensing and impact assessment legislation in
 32 Brazil. *Environmental Impact Assessment Review*, 94, 106742.
- 33 Barbet-Massin, M., Jiguet, F., Albert, C. H., & Thuiller, W. (2012). Selecting pseudo-absences for
 34 species distribution models: how, where and how many?. *Methods in Ecology and Evolution*, 3(2),
 35 327-338.
- 36 Barlow, J., Gardner, T. A., Lees, A. C., Parry, L., & Peres, C. A. (2012). How pristine are tropical
 37 forests? An ecological perspective on the pre-Columbian human footprint in Amazonia and
 38 implications for contemporary conservation. *Biological Conservation*, 151(1), 45-49.
- 39 Barve, N., Barve, V., Jiménez-Valverde, A., Lira-Noriega, A., Maher, S. P., Peterson, A. T., ... &
 40 Villalobos, F. (2011). The crucial role of the accessible area in ecological niche modeling and species
 41 distribution modeling. *Ecological Modelling*, 222(11), 1810-1819.
- 42 Begotti, R. A., & Peres, C. A. (2019). Brazil's indigenous lands under threat. *Science*, 363(6427), 592-
 43 592.
- 44 Breiner, F. T., Guisan, A., Bergamini, A., & Nobis, M. P. (2015). Overcoming limitations of modelling
 45 rare species by using ensembles of small models. *Methods in Ecology and Evolution*, 6(10), 1210-
 46 1218.
- 47 Breiner, F. T., Nobis, M. P., Bergamini, A., & Guisan, A. (2018). Optimizing ensembles of small
 48 models for predicting the distribution of species with few occurrences. *Methods in Ecology and*
 49 *Evolution*, 9(4), 802-808.
- 50 Brown, J. L., Hill, D. J., Dolan, A. M., Carnaval, A. C., & Haywood, A. M. (2018). PaleoClim, high
 51 spatial resolution paleoclimate surfaces for global land areas. *Scientific data*, 5(1), 1-9.
- 52 Burns, P., Clark, M., Salas, L., Hancock, S., Leland, D., Jantz, P., ... & Goetz, S. J. (2020).
 53 Incorporating canopy structure from simulated GEDI lidar into bird species distribution models.
 54 *Environmental Research Letters*, 15(9), 095002.
- 55 Campbell, L. P., Luther, C., Moo-Llanes, D., Ramsey, J. M., Danis-Lozano, R., & Peterson, A. T.
 56 (2015). Climate change influences on global distributions of dengue and chikungunya virus vectors.
 57 *Philosophical Transactions of the Royal Society B: Biological Sciences*, 370(1665), 20140135.
- 58 Cardoso da Silva, J. M., Cardoso de Sousa, M., & Castelletti, C. H. (2004). Areas of endemism for
 59 passerine birds in the Atlantic forest, South America. *Global Ecology and Biogeography*, 13(1), 85-
 60 92.

- 61 Carvalho, L. S., Oliveira-Marques, F. N., & Silva, P. R. (2011). Arachnida, Amblypygi, *Heterophrynus*
62 *longicornis* (Butler, 1873): Distribution extension for the state of Piauí northeastern Brazil. *Check*
63 *List*, 7(3), 267-269.
- 64 Carvalho, W. D., Mustin, K., Hilário, R. R., Vasconcelos, I. M., Eilers, V., & Fearnside, P. M. (2019).
65 Deforestation control in the Brazilian Amazon: A conservation struggle being lost as agreements and
66 regulations are subverted and bypassed. *Perspectives in Ecology and Conservation*, 17(3), 122-130.
- 67 Castellanos, A. A., Huntley, J. W., Voelker, G., & Lawing, A. M. (2019). Environmental filtering
68 improves ecological niche models across multiple scales. *Methods in Ecology and Evolution*, 10(4),
69 481-492.
- 70 Chapman, A. D., & Wieczorek, J. R. (2020) Georeferencing Best Practices. Copenhagen. *GBIF*
71 *Secretariat*. <https://doi.org/10.15468/doc-gg7h-s853>
- 72 Chiriví-Joya, D. A. Sistematic review of subfamily Phryninae (Arachnida: Amblypygi) (Doctoral
73 dissertation, Universidade de São Paulo).
- 74 Chiriví-Joya, D. (2021). Four new species of *Phrynus*, Lamarck (Arachnida: Amblypygi) from
75 Mexico. *Zootaxa*, 4948(2), zootaxa-4948.
- 76 Clark, J. A., & May, R. M. (2002). Taxonomic bias in conservation research. *Science*, 297(5579), 191-
77 192.
- 78 Cordeiro, L. M., Borghezán, R., & Trajano, E. (2014). Subterranean biodiversity in the Serra da
79 Bodoquena karst area, Paraguay river basin, Mato Grosso do Sul, Southwestern Brazil. *Biota*
80 *Neotropica*, 14.
- 81 de Armas, L. F. (2015). Una especie nueva de *Heterophrynus* Pocock, 1894 (Amblypygi: Phrynidae)
82 del suroeste de Colombia. *Revista Ibérica de Aracnología*, 27, 95-8.
- 83 de Armas, L. F., Contreras, R. T., & García, D. M. A. (2015). Nueva especie de "*Heterophrynus*"
84 (Amblypygi: Phrynidae) del Caribe colombiano. *Revista Ibérica de Aracnología*, (26), 69-73.
- 85 Deblauwe, V., Droissart, V., Bose, R., Sonké, B., Blach-Overgaard, A., Svenning, J. C., ... &
86 Couvreur, T. L. P. (2016). Remotely sensed temperature and precipitation data improve species
87 distribution modelling in the tropics. *Global Ecology and Biogeography*, 25(4), 443-454.
- 88 Deutsch, S., & Fletcher, R. (2022). The 'Bolsonaro bridge': Violence, visibility, and the 2019 Amazon
89 fires. *Environmental Science & Policy*, 132, 60-68.
- 90 Di Cola, V., Broennimann, O., Petitpierre, B., Breiner, F. T., d'Amen, M., Randin, C., ... & Guisan, A.
91 (2017). ecospat: an R package to support spatial analyses and modeling of species niches and
92 distributions. *Ecography*, 40(6), 774-787.
- 93 Elton, C. S. (1927). *Animal Ecology*. Sedgwick & Jackson Ltd., London. 207 pp. SR. S. M iller. 1952.
94 The ecological survey of animal communities, with a practical system of classifying habitats by
95 structural characters. *Journal of Ecology*, 42, 460-496.
- 96 Eyring, V., Bony, S., Meehl, G. A., Senior, C. A., Stevens, B., Stouffer, R. J., & Taylor, K. E. (2016).
97 Overview of the Coupled Model Intercomparison Project Phase 6 (CMIP6) experimental design and
98 organization. *Geoscientific Model Development*, 9(5), 1937-1958.
- 99 Fa, J. E., Watson, J. E., Leiper, I., Potapov, P., Evans, T. D., Burgess, N. D., ... & Garnett, S. T. (2020).
100 Importance of Indigenous Peoples' lands for the conservation of Intact Forest Landscapes. *Frontiers*
101 *in Ecology and the Environment*, 18(3), 135-140.
- 102 Farrell, S. L., Collier, B. A., Skow, K. L., Long, A. M., Campomizzi, A. J., Morrison, M. L., ... &
103 Wilkins, R. N. (2013). Using LiDAR-derived vegetation metrics for high-resolution, species
104 distribution models for conservation planning. *Ecosphere*, 4(3), 1-18.

- 105 Feng, X., Park, D. S., Walker, C., Peterson, A. T., Merow, C., & Papeş, M. (2019). A checklist for
 106 maximizing reproducibility of ecological niche models. *Nature Ecology & Evolution*, 3(10), 1382-
 107 1395.
- 108 Fernández-Llamazares, Á., López-Baucells, A., Velazco, P. M., Gyawali, A., Rocha, R., Terraube, J.,
 109 & Cabeza, M. (2021). The importance of Indigenous Territories for conserving bat diversity across the
 110 Amazon biome. *Perspectives in Ecology and Conservation*, 19(1), 10-20.
- 111 Ficetola, G. F., Canedoli, C., & Stoch, F. (2019). The Racovitza impediment and the hidden
 112 biodiversity of unexplored environments. *Conservation Biology*, 33(1), 214-216.
- 113 Fick, S. E., & Hijmans, R. J. (2017). WorldClim 2: new 1-km spatial resolution climate surfaces for
 114 global land areas. *International journal of climatology*, 37(12), 4302-4315.
- 115 García, D. M. Á., de Armas² & Jorge, L. F., & Pérez, D. (2015). Una especie nueva de *Heterophrynus*
 116 (*Amblypygi*: Phrynidæ) del nordeste de Colombia. *Revista Ibérica de Aracnología*, (27), 45-49.
- 117 Gastón, A., García-Viñas, J. I., Bravo-Fernández, A. J., López-Leiva, C., Oliet, J. A., Roig, S., &
 118 Serrada, R. (2014). Species distribution models applied to plant species selection in forest restoration:
 119 are model predictions comparable to expert opinion?. *New forests*, 45(5), 641-653.
- 120 Gause, G. F. (1934). The struggle for existence. Baltimore. *Williams and Wilkins*. 163 p.
- 121 Giupponi, A. P., & Kury, A. B. (2013). Two new species of *Heterophrynus* Pocock, 1894 from
 122 Colombia with distribution notes and a new synonymy (Arachnida: Amblypygi: Phrynidæ). *Zootaxa*,
 123 3647(2), 329-342.
- 124 Grinnell, J. (1914). Barriers to distribution as regards birds and mammals. *The American Naturalist*,
 125 48(568), 248-254.
- 126 Grinnell, J. (1917). The niche-relationships of the California Thrasher. *The Auk*, 34(4), 427-433.
- 127 Guillera-Aroita, G., Lahoz-Monfort, J. J., Elith, J., Gordon, A., Kujala, H., Lentini, P. E., ... & Wintle,
 128 B. A. (2015). Is my species distribution model fit for purpose? Matching data and models to
 129 applications. *Global Ecology and Biogeography*, 24(3), 276-292.
- 130 Guisan, A., & Thuiller, W. (2005). Predicting species distribution: offering more than simple habitat
 131 models. *Ecology letters*, 8(9), 993-1009.
- 132 Wickham, H. (2016). ggplot2: Elegant Graphics for Data Analysis. *Springer-Verlag* New York. ISBN
 133 978-3-319-24277-4, <https://ggplot2.tidyverse.org>.
- 134 Harvey, M. S. (2002). The neglected cousins: what do we know about the smaller arachnid orders?.
 135 *The Journal of Arachnology*, 30(2), 357-372.
- 136 Hijmans, R. J., Cameron, S. E., Parra, J. L., Jones, P. G., & Jarvis, A. (2005). Very high resolution
 137 interpolated climate surfaces for global land areas. *International Journal of Climatology: A Journal of*
 138 *the Royal Meteorological Society*, 25(15), 1965-1978.
- 139 Hijmans, R. (2022). *_raster: Geographic Data Analysis and Modeling_*. R package version 3.5-15,
 140 <<https://CRAN.R-project.org/package=raster>>
- 141 Hijmans R. J., Phillips S, Leathwick J, Elith J (2021). *_dismo: Species Distribution Modeling_*. R
 142 package version 1.3-5, <<https://CRAN.R-project.org/package=dismo>>.
- 143 Hirzel, A. H., Le Lay, G., Helfer, V., Randin, C., & Guisan, A. (2006). Evaluating the ability of habitat
 144 suitability models to predict species presences. *Ecological Modelling*, 199(2), 142-152.
- 145 Hole, D. G., Willis, S. G., Pain, D. J., Fishpool, L. D., Butchart, S. H., Collingham, Y. C., ... &
 146 Huntley, B. (2009). Projected impacts of climate change on a continent-wide protected area network.
 147 *Ecology Letters*, 12(5), 420-431.
- 148 Hutchinson, G. E. (1957). Concluding Remarks. *Cold Spring Harbor Symposia on Quantitative*
 149 *Biology*. 22, 415-427

- 150 Hutchinson, G. E. (1978) An Introduction to Population Biology. Yale. *University Press, New Haven*.
 151 271 p.
- 152 IUCN. 2021. The IUCN Red List of Threatened Species. Version 2021-3. <https://www.iucnredlist.org>.
 153 Accessed on [08 April 2022].
- 154 Jackson, S. T., & Overpeck, J. T. (2000). Responses of plant populations and communities to
 155 environmental changes of the late Quaternary. *Paleobiology*, 26(S4), 194-220.
- 156 Jiménez, L., & Soberón, J. (2020). Leaving the area under the receiving operating characteristic curve
 157 behind: An evaluation method for species distribution modelling applications based on presence-only
 158 data. *Methods in Ecology and Evolution*, 11(12), 1571-1586.
- 159 Jiménez-Valverde, A., & Lobo, J. M. (2007). Threshold criteria for conversion of probability of
 160 species presence to either–or presence–absence. *Acta oecologica*, 31(3), 361-369.
- 161 Karger, D. N., Conrad, O., Böhner, J., Kawohl, T., Kreft, H., Soria-Auza, R. W., ... & Kessler, M.
 162 (2017). Climatologies at high resolution for the earth's land surface areas. *Scientific Data*, 4(1), 1-20.
- 163 Konowalik, K., & Nosol, A. (2021). Evaluation metrics and validation of presence-only species
 164 distribution models based on distributional maps with varying coverage. *Scientific Reports*, 11(1), 1-
 165 15.
- 166 Ladle, R. J., & Velandar, K. (2003). Fishing behavior in a giant whip spider. *The Journal of*
 167 *Arachnology*, 31(1), 154-156.
- 168 Leather, S. R. (2009). Taxonomic chauvinism threatens the future of entomology. *Biologist*, 56(1), 10-
 169 13.
- 170 Lehmann, T., & Friedrich, S. (2018). DNA barcoding the smaller arachnid orders from ACP
 171 Panguana, Amazonian Peru. *Spixiana*, 41(2), 169-172.
- 172 Lima-Ribeiro, M. S., Varela, S., González-Hernández, J., de Oliveira, G., Diniz-Filho, J. A. F., &
 173 Terribile, L. C. (2015). EcoClimate: a database of climate data from multiple models for past, present,
 174 and future for macroecologists and biogeographers. *Biodiversity Informatics*, 10.
- 175 Liu, C., Wolter, C., Xian, W., & Jeschke, J. M. (2020). Most invasive species largely conserve their
 176 climatic niche. *Proceedings of the National Academy of Sciences*, 117(38), 23643-23651.
- 177 Lobo, J. M., Jiménez-Valverde, A., & Real, R. (2008). AUC: a misleading measure of the performance
 178 of predictive distribution models. *Global ecology and Biogeography*, 17(2), 145-151.
- 179 Lobo, J. M., Jiménez-Valverde, A., & Hortal, J. (2010). The uncertain nature of absences and their
 180 importance in species distribution modelling. *Ecography*, 33(1), 103-114.
- 181 Mammides, C. (2019). European Union's conservation efforts are taxonomically biased. *Biodiversity*
 182 *and Conservation*, 28(5), 1291-1296.
- 183 Mammola, S., Goodacre, S. L., & Isaia, M. (2018). Climate change may drive cave spiders to
 184 extinction. *Ecography*, 41(1), 233-243.
- 185 Mammola, S., Riccardi, N., Prié, V., Correia, R., Cardoso, P., Lopes-Lima, M., & Sousa, R. (2020).
 186 Towards a taxonomically unbiased European Union biodiversity strategy for 2030. *Proceedings of the*
 187 *Royal Society B*, 287(1940), 20202166.
- 188 Mammola, S., Pétilion, J., Hacala, A., Monsimet, J., Marti, S. L., Cardoso, P., & Lafage, D. (2021).
 189 Challenges and opportunities of species distribution modelling of terrestrial arthropod predators.
 190 *Diversity and Distributions*, 27(12), 2596-2614.
- 191 Merow, C., LaFleur, N., Silander Jr, J. A., Wilson, A. M., & Rubega, M. (2011). Developing dynamic
 192 mechanistic species distribution models: predicting bird-mediated spread of invasive plants across
 193 northeastern North America. *The American Naturalist*, 178(1), 30-43.

- 194 Mi, C., Huettmann, F., Guo, Y., Han, X., & Wen, L. (2017). Why choose Random Forest to predict
 195 rare species distribution with few samples in large undersampled areas? Three Asian crane species
 196 models provide supporting evidence. *PeerJ*, 5, e2849.
- 197 Miranda, G. S., Giupponi, A. P. L., Scharff, N., Prendini, L. (2020). Phylogeny and biogeography of
 198 the pantropical whip spider family Charinidae (Arachnida, Amblypygi). *Zoological Journal of the*
 199 *Linnean Society*. 194(1), 136-180.
- 200 Morales-Barbero, J., & Vega-Álvarez, J. (2019). Input matters matter: Bioclimatic consistency to map
 201 more reliable species distribution models. *Methods in Ecology and Evolution*, 10(2), 212-224.
- 202 Naimi, B., & Araújo, M. B. (2016). sdm: a reproducible and extensible R platform for species
 203 distribution modelling. *Ecography*, 39(4), 368-375.
- 204 Nepstad, D., Schwartzman, S., Bamberger, B., Santilli, M., Ray, D., Schlesinger, P., ... & Rolla, A.
 205 (2006). Inhibition of Amazon deforestation and fire by parks and indigenous lands. *Conservation*
 206 *Biology*, 20(1), 65-73.
- 207 Nepstad, D., Soares-Filho, B. S., Merry, F., Lima, A., Moutinho, P., Carter, J., ... & Stella, O. (2009).
 208 The end of deforestation in the Brazilian Amazon. *Science*, 326(5958), 1350-1351.
- 209 Oliveira, U., Paglia, A. P., Brescovit, A. D., de Carvalho, C. J., Silva, D. P., Rezende, D. T., ... &
 210 Santos, A. J. (2016). The strong influence of collection bias on biodiversity knowledge shortfalls of
 211 Brazilian terrestrial biodiversity. *Diversity and Distributions*, 22(12), 1232-1244.
- 212 Vásquez Palacios, S., Chiriví Joya, D. A., García Hernández, A. L., Mantilla-Meluk, H., & Torres
 213 Carrera, J. D. (2019). Morphological variation in *Heterophrynus boterorum* (Arachnida: Amblypygi:
 214 Phrynidae). *Biota colombiana*, 20(2), 32-45.
- 215 Pearson, R. G., Raxworthy, C. J., Nakamura, M., & Townsend Peterson, A. (2007). Predicting species
 216 distributions from small numbers of occurrence records: a test case using cryptic geckos in
 217 Madagascar. *Journal of Biogeography*, 34(1), 102-117.
- 218 Peterson, A. T., & Soberón, J. (2012). Species distribution modeling and ecological niche modeling:
 219 getting the concepts right. *Natureza & Conservação*, 10(2), 102-107.
- 220 Porto, T. J., & Peixoto, P. E. C. (2013). Experimental evidence of habitat selection and territoriality in
 221 the Amazonian whip spider *Heterophrynus longicornis* (Arachnida, Amblypygi). *Journal of Ethology*,
 222 31(3), 299-304.
- 223 Prous, X., Pietrobon, T., Ribeiro, M. S., & Zampaulo, R. D. A. (2017). Bat necrophagy by a whip-
 224 spider (Arachnida, Amblypygi, Phrynidae) in a cave in the eastern Brazilian Amazon. *Acta*
 225 *Amazonica*, 47, 365-368.
- 226 Qiao, H., Soberón, J., & Peterson, A. T. (2015). No silver bullets in correlative ecological niche
 227 modelling: insights from testing among many potential algorithms for niche estimation. *Methods in*
 228 *Ecology and Evolution*, 6(10), 1126-1136.
- 229 Qiao, H., Peterson, A. T., Ji, L., & Hu, J. (2017). Using data from related species to overcome spatial
 230 sampling bias and associated limitations in ecological niche modelling. *Methods in Ecology and*
 231 *Evolution*, 8(12), 1804-1812.
- 232 RAISG – Rede Amazônica de Informação Socioambiental,
 233 <https://www.amazoniasocioambiental.org/en/about/>, 2019 (Accessed 18 April 2022)
- 234 Rangel, T. F., Edwards, N. R., Holden, P. B., Diniz-Filho, J. A. F., Gosling, W. D., Coelho, M. T. P., ...
 235 & Colwell, R. K. (2018). Modeling the ecology and evolution of biodiversity: Biogeographical
 236 cradles, museums, and graves. *Science*, 361(6399), eaar5452.
- 237 Rapozo, P. (2021). Necropolitics, State of Exception, and Violence Against Indigenous People in the
 238 Amazon Region During the Bolsonaro Administration. *Brazilian Political Science Review*, 15.

- 239 Regos, A., Gagne, L., Alcaraz-Segura, D., Honrado, J. P., & Domínguez, J. (2019). Effects of species
 240 traits and environmental predictors on performance and transferability of ecological niche models.
 241 *Scientific Reports*, 9(1), 1-14.
- 242 Reveillion, F., Wattier, R., Montuire, S., Carvalho, L. S., & Bollache, L. (2020). Cryptic diversity
 243 within three South American whip spider species (Arachnida, Amblypygi). *Zoological Research*,
 244 41(5), 595.
- 245 Riahi, K., Van Vuuren, D. P., Kriegler, E., Edmonds, J., O'neill, B. C., Fujimori, S., ... & Tavoni, M.
 246 (2017). The shared socioeconomic pathways and their energy, land use, and greenhouse gas emissions
 247 implications: an overview. *Global Environmental Change*, 42, 153-168.
- 248 Ricketts, T. H., Soares-Filho, B., da Fonseca, G. A., Nepstad, D., Pfaff, A., Petsonk, A., ... &
 249 Victurine, R. (2010). Indigenous lands, protected areas, and slowing climate change. *PLoS Biology*,
 250 8(3), e1000331.
- 251 Rios, N. E., & Bart, H. L. (2010). GEOLocate (Version 3.22) computer software. *Tulane University*
 252 *Museum of Natural History*, Belle Chasse, LA.
- 253 Rivera, J. A., & Arnould, G. (2020). Evaluation of the ability of CMIP6 models to simulate
 254 precipitation over Southwestern South America: Climatic features and long-term trends (1901–2014).
 255 *Atmospheric Research*, 241, 104953.
- 256 Sacek, V. (2014). Drainage reversal of the Amazon River due to the coupling of surface and
 257 lithospheric processes. *Earth and Planetary Science Letters*, 401, 301-312.
- 258 Sanabria, C., & Achury, R. (2022). Amazonian indigenous territories as reservoirs of biodiversity: The
 259 army ants of Santa Sofia (Amazonas–Colombia). *Caldasia*, 44(2).
- 260 Sarquis, J. A., Cristaldi, M. A., Arzamendia, V., Bellini, G., & Giraud, A. R. (2018). Species
 261 distribution models and empirical test: Comparing predictions with well-understood geographical
 262 distribution of *Bothrops alternatus* in Argentina. *Ecology and Evolution*, 8(21), 10497-10509.
- 263 Saupe, E. E., Barve, V., Myers, C. E., Soberón, J., Barve, N., Hensz, C. M., ... & Lira-Noriega, A.
 264 (2012). Variation in niche and distribution model performance: the need for a priori assessment of key
 265 causal factors. *Ecological Modelling*, 237, 11-22.
- 266 Schleicher, J., Peres, C. A., Amano, T., Lactayo, W., & Leader-Williams, N. (2017). Conservation
 267 performance of different conservation governance regimes in the Peruvian Amazon. *Scientific*
 268 *Reports*, 7(1), 1-10.
- 269 Seiter, M., & Gredler, R. (2020). Review of the reproductive behavior and spermatophore morphology
 270 in the whip spider genus *Heterophrynus* Pocock, 1894 (Arachnida, Amblypygi), with description of
 271 new data and a new species. *Zoologischer Anzeiger*, 287, 1-13.
- 272 Seiter, M., Reyes Lerma, A. C., Král, J., Sember, A., Divišová, K., Palacios, J. G. V., ... & Prendini, L.
 273 (2020). Cryptic diversity in the whip spider genus *Paraphrynus* (Amblypygi: Phrynididae): Integrating
 274 morphology, karyotype and DNA. *Arthropod Syst. Phylogeny*, 78, 265-285.
- 275 Sillero, N., & Barbosa, A. M. (2021). Common mistakes in ecological niche models. *International*
 276 *Journal of Geographical Information Science*, 35(2), 213-226.
- 277 Sillero, N. (2011). What does ecological modelling model? A proposed classification of ecological
 278 niche models based on their underlying methods. *Ecological Modelling*, 222(8), 1343-1346.
- 279 da Costa Silva, R. G., da Silva, V. V., de Mello-Théry, N. A., & Lima, L. A. P. (2021). New Frontier of
 280 Expansion and Protected Areas in the State of Amazonas. *Mercator-Revista de Geografia da UFC*,
 281 20(2).

- 282 Silva Junior, C. H., Pessoa, A., Carvalho, N. S., Reis, J. B., Anderson, L. O., & Aragao, L. E. (2021).
 283 The Brazilian Amazon deforestation rate in 2020 is the greatest of the decade. *Nature Ecology &*
 284 *Evolution*, 5(2), 144-145.
- 285 Sinakevitch, I., Long, S. M., & Gronenberg, W. (2021). The central nervous system of whip spiders
 286 (Amblypygi): large mushroom bodies receive olfactory and visual input. *Journal of Comparative*
 287 *Neurology*, 529(7), 1642-1658.
- 288 Smith, A. B., Godsoe, W., Rodríguez-Sánchez, F., Wang, H. H., & Warren, D. (2019). Niche
 289 estimation above and below the species level. *Trends in Ecology & Evolution*, 34(3), 260-273.
- 290 Soberón, J., & Arroyo-Peña, B. (2017). Are fundamental niches larger than the realized? Testing a 50-
 291 year-old prediction by Hutchinson. *Plos One*, 12(4), e0175138.
- 292 Peterson, A. T., & Soberón, J. (2005). Interpretation of models of fundamental ecological niches and
 293 species distribution areas. *Biodiversity Informatics*, 2, 1-10.
- 294 Soberón, J., & Townsend Peterson, A. (2011). Ecological niche shifts and environmental space
 295 anisotropy: a cautionary note. *Revista Mexicana de Biodiversidad*, 82(4), 1348-1355.
- 296 Soberón, J., & Townsend Peterson, A. (2011). Ecological niche shifts and environmental space
 297 anisotropy: a cautionary note. *Revista Mexicana de Biodiversidad*, 82(4), 1348-1355.
- 298 Sobral-Souza, T., Lima-Ribeiro, M. S., & Solferini, V. N. (2015). Biogeography of Neotropical
 299 Rainforests: past connections between Amazon and Atlantic Forest detected by ecological niche
 300 modeling. *Evolutionary Ecology*, 29(5), 643-655.
- 301 Steen, V. A., Tingley, M. W., Paton, P. W., & Elphick, C. S. (2021). Spatial thinning and class
 302 balancing: Key choices lead to variation in the performance of species distribution models with citizen
 303 science data. *Methods in Ecology and Evolution*, 12(2), 216-226.
- 304 Stork, N. E. (2018). How many species of insects and other terrestrial arthropods are there on Earth?.
 305 *Annual Review of Entomology*, 63, 31-45.
- 306 Taucare-Ríos, A., Nentwig, W., Bizama, G., & Bustamante, R. O. (2018). Matching global and
 307 regional distribution models of the recluse spider *Loxosceles rufescens*: to what extent do these reflect
 308 niche conservatism?. *Medical and Veterinary Entomology*, 32(4), 490-496.
- 309 Title, P. O., & Bemmels, J. B. (2018). ENVIREM: an expanded set of bioclimatic and topographic
 310 variables increases flexibility and improves performance of ecological niche modeling. *Ecography*,
 311 41(2), 291-307.
- 312 Tollefson, J. (2015). Battle for the Amazon. *Nature*, 520(7545), 20-24.
- 313 UNEP-WCMC, I. U. C. N. (2021). Protected planet: the world database on protected areas (WDPA)
 314 and world database on other effective area-based conservation measures (WD-OECM). UNEP-
 315 WCMC and IUCN, Cambridge, UK. *UNEP-WCMC and IUCN*, Cambridge, UK.
 316 www.protectedplanet.net. Accessed Oct. 2021
- 317 Van Vuuren, D. P., Edmonds, J., Kainuma, M., Riahi, K., Thomson, A., Hibbard, K., ... & Rose, S. K.
 318 (2011). The representative concentration pathways: an overview. *Climatic Change*, 109(1), 5-31.
- 319 C Vega, G., Pertierra, L. R., & Olalla-Tárraga, M. Á. (2017). MERRAclim, a high-resolution global
 320 dataset of remotely sensed bioclimatic variables for ecological modelling. *Scientific Data*, 4(1), 1-12.
- 321 Velásquez-Tibatá, J., Olaya-Rodríguez, M. H., López-Lozano, D., Gutiérrez, C., González, I., &
 322 Londoño-Murcia, M. C. (2019). BioModelos: A collaborative online system to map species
 323 distributions. *PloS One*, 14(3), e0214522.
- 324 Veloz, S. D. (2009). Spatially autocorrelated sampling falsely inflates measures of accuracy for
 325 presence-only niche models. *Journal of Biogeography*, 36(12), 2290-2299.

- 326 Viquez, C., Chirivi, D., Moreno-González, J. A., & Christensen, J. A. (2014). *Heterophrynus armiger*
327 Pocock, 1902 (Amblypygi: Phrynidae): First record from Colombia, with notes on its historic
328 distribution records and natural history. *Check List*, 10(2), 457-460.
- 329 Wallace, A. R. (1858). Note on the theory of permanent and geographical varieties. *Zoologist*,
330 16(185–186), 5887-5888.
- 331 Waltari, E., Schroeder, R., McDonald, K., Anderson, R. P., & Carnaval, A. (2014). Bioclimatic
332 variables derived from remote sensing: Assessment and application for species distribution modelling.
333 *Methods in Ecology and Evolution*, 5(10), 1033-1042.
- 334 Warren, D. L. (2012). In defense of ‘niche modeling’. *Trends in ecology & evolution*, 27(9), 497-500.
- 335 Werneck, F. P. (2011). The diversification of eastern South American open vegetation biomes:
336 historical biogeography and perspectives. *Quaternary Science Reviews*, 30(13-14), 1630-1648.
- 337 Weygoldt, P. (1977). Coexistence of two species of whip spiders (genus *Heterophrynus*) in the
338 neotropical rain forest (Arachnida, Amblypygi). *Oecologia*, 27(4), 363-370.
- 339 Weygoldt, P. (2000). Whip spiders. Stenstrup. *Apollo Books*. 163p.
- 340 Jaffé, R., Nunes, S., Dos Santos, J. F., Gastauer, M., Giannini, T. C., Nascimento Jr, W., ... & Fletcher,
341 R. J. (2021). Forecasting deforestation in the Brazilian Amazon to prioritize conservation efforts.
342 *Environmental Research Letters*, 16(8), 084034.
- 343 Zhang, L., Huettmann, F., Liu, S., Sun, P., Yu, Z., Zhang, X., & Mi, C. (2019). Classification and
344 regression with random forests as a standard method for presence-only data SDMs: A future
345 conservation example using China tree species. *Ecological Informatics*, 52, 46-56.
- Zizka, A., Silvestro, D., Andermann, T., Azevedo, J., Duarte Ritter, C., Edler, D., ... & Antonelli, A.
(2019). CoordinateCleaner: Standardized cleaning of occurrence records from biological collection
databases. *Methods in Ecology and Evolution*, 10(5), 744-751.